Journal of Medicinal Chemistry

Article

Synthesis and Biological Evaluation of Calothrixins B and their Deoxygenated Analogues

Bose Muthu Ramalingam, Nachiappan Dhatchana Moorthy, Somenath Roy Chowdhury, Thiyagarajan Mageshwaran, Elangovan Vellaichamy, Sourav Saha, Karthikeyan Ganesan, B. Navin Rajesh, Saleem Iqbal, Hemanta Kumar Majumder, Krishnasamy Gunasekaran, Ramamoorthy Siva, and Arasambattu Kannan Mohanakrishnan

J. Med. Chem., **Just Accepted Manuscript** • DOI: 10.1021/acs.jmedchem.7b01797 • Publication Date (Web): 09 Jan 2018

Just Accepted

ACS Publications

Journal of Medicinal Chemistry is published by the American Chemical Society. 1155 Sixteenth Street N.W., Washington, DC 20036

Synthesis and Biological Evaluation of Calothrixins B and their Deoxygenated Analogues

Authors List:

Bose Muthu Ramalingam,[1] Nachiappan Dhatchana Moorthy,[2,4] Somenath Roy Chowdhury,[3] Thiyagarajan Mageshwaran,[1] Elangovan Vellaichamy,[2] Sourav Saha,[3] Karthikeyan Ganesan,[4] B. Navin Rajesh,[4] Saleem Iqbal,[5] Hemanta K. Majumder,[3] Krishnasamy Gunasekaran,[5] Ramamoorthy Siva,[6] and Arasambattu K. Mohanakrishnan[1*]

[1] Department of Organic Chemistry, University of Madras, Guindy Campus, Chennai 600 025, India

[2] Department of Biochemistry, University of Madras, Guindy Campus, Chennai 600 025, India

[3] Division of Infectious Diseases & Immunology, Indian Institute of Chemical Biology, 4 Raja S. C. Mullick Road, Jadavpur, Kolkata 700032, India.

[4] Research and Development Centre, Orchid Pharma Ltd, Sholinganallur, Chennai 600 119, India

[5] CAS in Crystallography & Biophysics, University of Madras, Chennai 600 025, India

[6] School of Bio Sciences and Technology, VIT University, Vellore 632 014, India

Abstract

A series of calothrixin B (**2**) analogues bearing substituents at the 'E' ring and their corresponding deoxygenated quinocarbazoles lacking quinone unit were synthesized. The cytotoxicities of calothrixins **1**, **2**, **15b-p** and quinocarbazole analogues were investigated against nine cancer cell lines. The quinocarbazoles **21a** and **25a** inhibited the catalytic activity of human topoisomerase II. The plasmid DNA cleavage abilities of calothrixins **1**, **2**, **15b-p** identified compound **15h** causing DNA cleavage comparable to that of calothrixin A (**1**). Calothrixin A (**1**), 3-fluorocalothrixin **15h** and 4-fluoroquinocarbazole **21b** induced extensive DNA damage followed by apoptotic cell death. Spectral and plasmid unwinding studies demonstrated an intercalative mode of binding for quinocarbazoles. We identified two promising drug candidates, the 3-fluorocalothrixin B **15h** with low toxicity in animal model and its deoxygenated derivative 4-fluoroquinocarbazole **21b** as having potent cytotoxicity against NCI-H460 cell line with a GI_{50} of 1 nM.

Introduction

Quinones consist an important class of antitumor agents and are known to act as DNA intercalators, reductive alkylators of biomolecules and also as generators of reactive oxygen species.[1] The biological redox activity of these compounds is recognized to play a key role in their cytotoxicity.[2] However, the biological mode of action of quinones is highly dependent on their structural motif. The structurally complex quinones such as doxorubicin are known to exhibit cytotoxicity through polymodal action.[3] Among indole based quinone alkaloids, murrayaquinone A and mitomycin C are known to exhibit cytotoxicity.[4,5] Calothrixin A (**1**) and B **2** (Chart 1) are carbazole-1, 4-quinone alkaloids isolated from *Calothrix cyanobacteria* with unique indolo [3,2-*j*] phenanthridine framework.[6]

Chart 1. Calothrixin A (1), Calothrixin B (2) and its Analogues 3-6

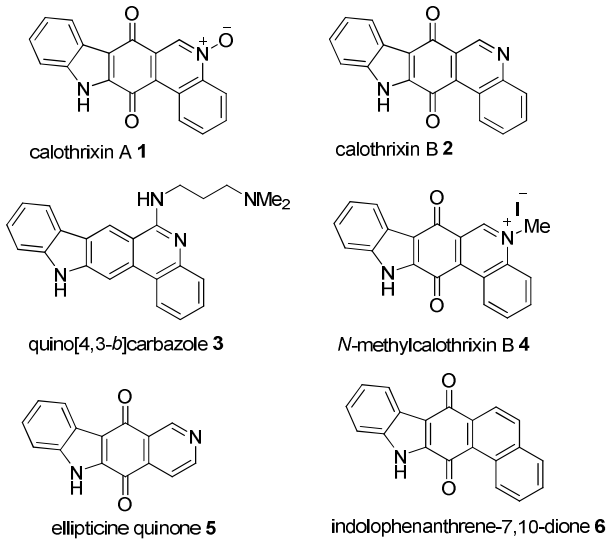

Calothrixins inhibit the growth of human HeLa cancer cells and chloroquine resistant strain of *Plasmodium falciparum* within the nanomolar range.[6] They inhibit the bacterial RNA polymerase[7] and also poisons the DNA topoisomerase I.[8] In addition, calothrixin A (**1**) is also known to induce the intracellular formation of reactive oxygen species.[9]

Quinocarbazole **3** (Chart 1) was first synthesized from this laboratory via thermal electrocyclization of 1-phenylsulfonyl-2,3-divinylindole as a key step.[10] Five years later, oxidized form of quinocarbazole, i.e. calothrixin A (**1**) and B (**2**) were isolated by Rickards and coworkers.[6] To date, twenty different syntheses for calothrixin have been reported. In 2000, Kelly et al reported the first synthesis of calothrixin B (**2**) involving double lithiation strategy from *N*,*N*-diethyl-quinoline-4-carboxamide and *N*-MOM-protected indole-3-carboxaldehyde.[11] Chai and coworkers reported a simple and concise route to calothrixin B (**2**) *via* Friedel-Crafts acylation followed by lithiation mediated cyclization.[12] Hibino and coworkers employed an allene-mediated electrocyclization as a key step for calothrixin B (**2**).[13] The same group also achieved the biomimetic synthesis of calothrixin B (**2**).[14] Syntheses of calothrixin were also established using hetero Diels-Alder reaction[15] as well as radical cyclization protocols.[16]

Moody and coworkers reported the biomimetic synthesis of calothrixin from indolo[2,3-*a*]carbazole.[17] Synthesis of calothrixin B (**2**) was achieved by Abe et al[18] as well as Kumar et al,[19] involving Pd-catalyzed tandem cyclization/cross coupling reactions. The Pd-mediated cross coupling strategies for indolophenanthridine system were also achieved independently by Kusurkar et al[20] as well as Nagarajan and coworkers.[21]A linear synthesis of calothrixin B and its analogues were achieved from this laboratory involving thermal electrocyclization of 2-nitroarylvinyl-3-phenylsulfonylvinyl indoles.[22] Total synthesis of calothrixins A (**1**) and B (**2**) was achieved via $Mn(OAc)_3$-mediated oxidative radical reaction of cyclohexenone with amino-phenanthridinedione.[23] Mal and coworkers outlined a short synthesis of calothrixin B unit via anionic annulation of furoindolone with 4-bromoquinoline.[24] Dethe and coworkers reported a concise total synthesis of calothrixin B using LTA-mediated rearrangement as the key step.[25]

Despite, several synthetic routes explored for calothrixins, there are only few reports on cytotoxicity and antimalarial activity of these compounds. An assembly of three pharmacophores in calothrixins namely indole, quinone and quinoline spanning five rings (A-E) provides a unique possibility for structural modification so as to produce analogues of calothrixin with better cytotoxic profile. Earlier attempts to study the contribution of different structural features of calothrixins towards anti-cancer potency indicate that the introduction of MOM group on the indole nitrogen (N-MOM-calothrixin B)[26] or methyl group to the D-ring nitrogen (N-methycalothrixin B)[8] decrease the cytotoxic potency in HeLa and CEM leukemic cell lines, respectively. The removal of D-ring nitrogen atom (indolophenanthrene-7,13-dione)[27] or both the E and D rings (2-methylcarbazoledione)[27] of calothrixin B (**2**) decreased anti-proliferative potency in HeLa cells with the exception of ellipticine quinone which lack the E-ring is equally potent as calothrixin B (**2**).[27] The quinones containing bi- and tricylic systems (murrayaquinone, 2-methylcarbazoledione, and isoquinoline-5,8-dione) are less active than the pentacyclic calothrixin B (**2**) in HeLa cells but not in case of murine P388 macrophage cancer cells.[27]

To date, the anti-cancer SAR studies carried out with calothrixin analogues highlight the involvement of ring structure (A-E) and importance of indole or D-ring nitrogen atom on the inhibitory action, mainly in HeLa cells. However, the contribution of the quinone unit to the cytotoxicity of calothrixin in cancer cells is not studied. Most importantly, the spectrum of anti-cancer activity of calothrixins in other cancer cell lines is not reported. The ring structure of calothrixins might favor DNA intercalation which can result in cellular cytotoxicity, however less is known about its interaction with DNA. The precise mechanism on the effect of calothrixins on cell cycle is not clear. When administered at low concentration (0.1 μM) to p53

proficient CEM leukemic cells, calothrixin B (**2**) but not calothrixin A (**1**) caused arrest of cells in G1-phase. Whereas higher concentration of calothrixin A (**1**) and *N*-methyl calothrixin B caused G2-M arrest although in a reversible manner.[8] The calothrixins A (**1**), B (**2**) and *N*-methyl calothrixin B are shown to stabilize cleavable complexes of topo I-DNA, though at one fifth of the potency of camptothecin.[8] Along with the cell cycle arrest at G2-M phase, calothrixin A (**1**) was observed to generate reactive oxygen species (ROS) and induce cell death through apoptosis in Jurkat cell line.[9] Recently, Velu and coworkers reviewed the synthesis and biological evaluation of calothrixin B (**2**).[28]

In the present study, we planned to address the above mentioned lacunae and to get further insight on the biological effects of calothrixins. Another objective is to delineate the role of quinone moiety towards cellular cytotoxicity by synthesizing quinocarbazole analogues which lack the quinone unit of calothrixin. The quinocarbazole ring system is of interest because of its close relationship with ellipticine, a well-known anti-cancer alkaloid.[29] The presence of quinone functionality in calothrixins may lead to the generation of toxicological intermediates in cellular milieu which may result in variety of harmful effects *in vivo*, including acute cytotoxicity, immuno and genotoxicity.[30] On the other hand, the quinone lacking pyridocarbazole namely the ellipticine being structurally related to calothrixin possess fewer adverse effects.[31] Thus the role of quinone in mediating the adverse effects of calothrixin was investigated in an acute toxicological study in mice following oral administration of promising calothrixin analogue. A schematic view of overall research work carried out is represented in the form of a flow chart (Fig. 1).

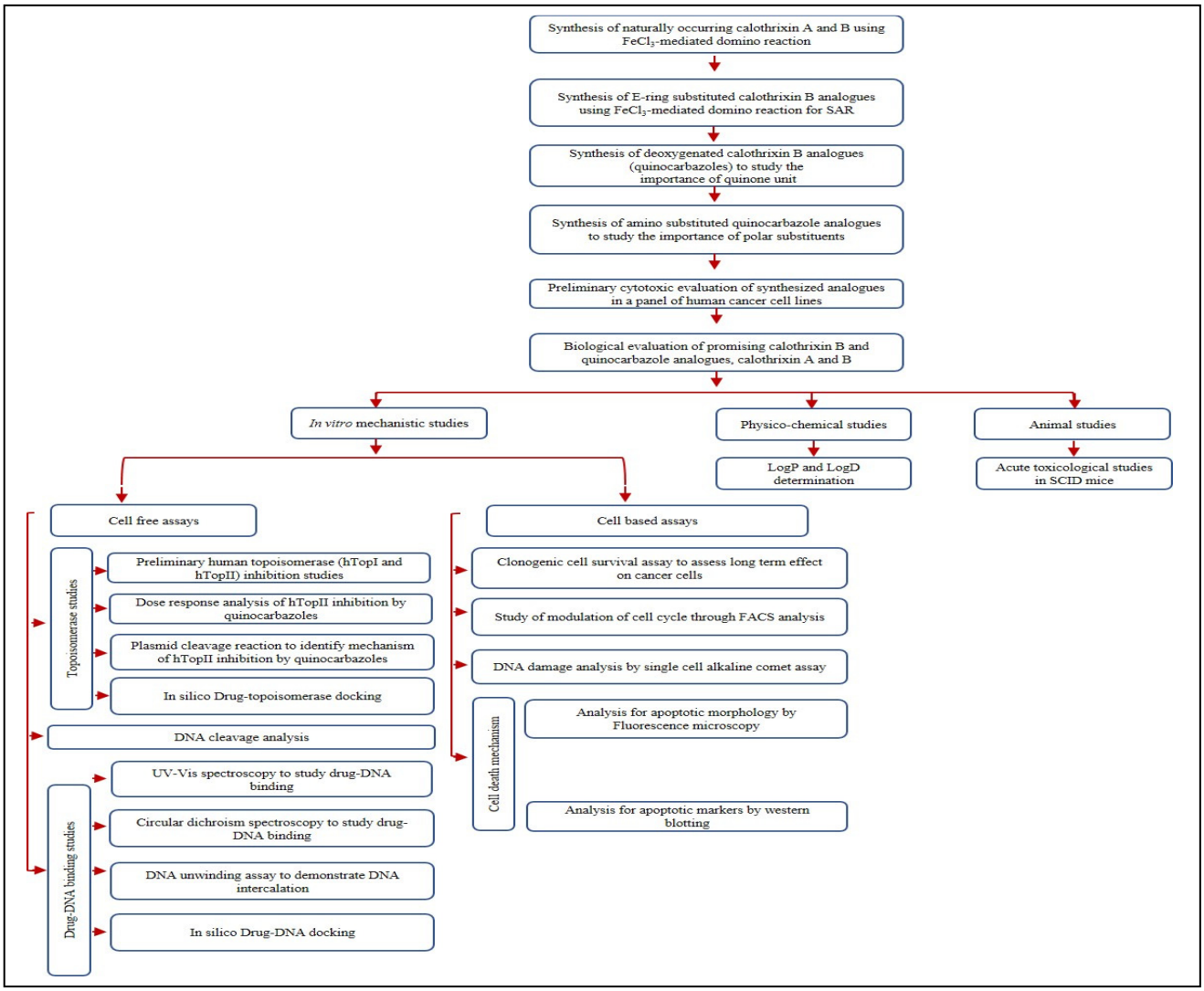

Fig. 1. Schematic representation of synthetic and biological studies carried on calothrixin and its analogues

Results and Discussion

Synthesis

Recently, a facile synthesis of calothrixin B and its analogues were achieved from this lab involving $FeCl_3$-mediated domino reaction of enamines.[32] Among the various methodologies reported for calothrixin,[11-25] this method[32] provides calothrixin B and its analogues in very good overall yields involving minimum number of steps. Hence, we decided to explore the synthesis

of diverse calothrixin analogues for biological screening using this $FeCl_3$-mediated domino reaction strategy.

Scheme 1[a]

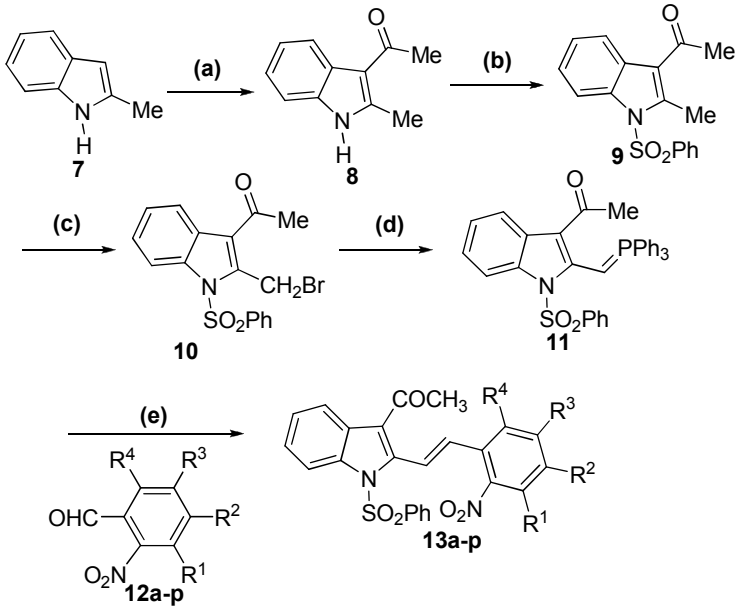

13	R^1	R^2	R^3	R^4	yield (%)
a	H	H	H	H	92
b	OMe	H	H	H	85
c	H	H	OMe	H	92
d	H	OMe	OMe	H	88
e	H	$-OCH_2O-$		H	90
f	H	Br	H	H	90
g	H	Cl	H	H	94
h	H	F	H	H	93
i	H	H	Br	H	90
j	H	H	Cl	H	91
k	H	H	H	Cl	80
l	Cl	H	H	H	89
m	H	F	Br	H	89
n	H	F	Cl	H	90
o	H	Cl	Cl	H	93
p	Cl	H	Cl	H	90

[a]Reagents and conditions : (a) DMA, $POCl_3$; (b) $PhSO_2Cl$, PTC, Benzene, 50% NaOH, rt,1 h; (c) NBS, AIBN, CCl_4, reflux, 3 h; (d) PPh_3, THF, reflux, 2 h followed by K_2CO_3, DCM rt, 12 h; (e) 12a-p, DCM/DCE, reflux, 6-12 h.

Our synthetic work began with acetylation of 2-methylindole **7** under Vilsmeier condition. The resulting 3-acetylindole **8** upon protection of indole nitrogen by employing PTC conditions

furnished the required 1-phenylsulfonyl-2-methyl-3-acetylindole **9**. Subsequently, an allylic bromination at 2-methyl position of **9** using NBS and a catalytic amount of AIBN in CCl_4 at reflux led to the corresponding 2-bromomethylindole **10**. Next, the 2-bromomethylindole **10** was then smoothly transformed into phosphorous ylide **11** as a stable yellow solid. The ylide **11** underwent a facile Wittig reaction with 2-nitroarylaldehydes **12a-p** under refluxing conditions in DCM/1,2-DCE to afford the respective 2-nitroarylvinylindoles **13a-p** in 80-94% yields (Scheme 1).

Scheme 2[a]

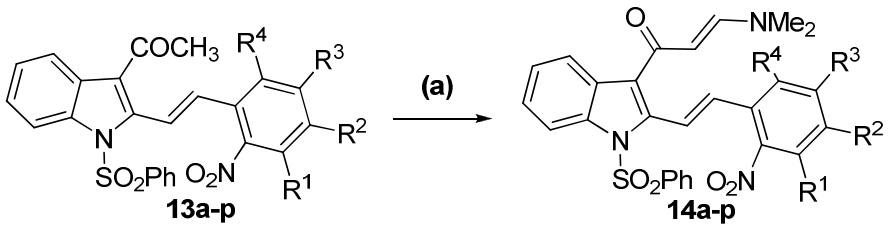

14	R^1	R^2	R^3	R^4	yield (%)
a	H	H	H	H	89[a]
b	OMe	H	H	H	85[a]
c	H	H	OMe	H	90[a]
d	H	OMe	OMe	H	97[b]
e	H	$-OCH_2O-$		H	85[a]
f	H	Br	H	H	96[b]
g	H	Cl	H	H	92[a]
h	H	F	H	H	91[a]
i	H	H	Br	H	92[a]
j	H	H	Cl	H	96[b]
k	H	H	H	Cl	88[a]
l	Cl	H	H	H	91[a]
m	H	F	Br	H	89[a]
n	H	F	Cl	H	88[a]
o	H	Cl	Cl	H	88[a]
p	Cl	H	Cl	H	86[a]

[a]isolated yield, [b]Crude yield of enamine

[a]Reagents and conditions : (a) DMF.DMA, glycocyamine (50 mol %), 100 °C, 3-5 h.

The 3-acetyl-2-nitroarylvinylindoles **13a-p** upon heating with dimethylformamide dimethyl acetal (DMF.DMA) in the presence of 50 mol% glycocyamine at 100 ^{o}C for 3-5 h produced push-pull type enamines **14a-p** (Scheme 2). Most of these enamines were isolated and well characterized by ^{1}H and ^{13}C NMR spectral studies. However, it should be noted that some of the enamines **14d**, **14f** and **14j** were used as such for next step without any further characterization.

The enamines **14a-p** upon refluxing with 3 equiv of anhydrous $FeCl_3$ in DMF underwent electrocyclization, reductive cyclization and oxidation followed by cleavage of phenylsulfonyl group to afford calothrixin B **2** and its analogues **15b-p** in 45-67% yields (Scheme 3).

Scheme 3[a]

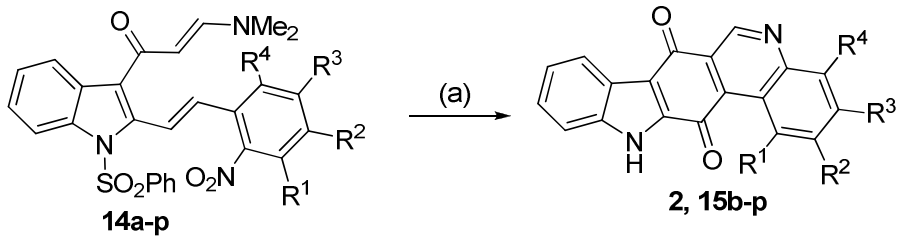

Compound	R^1	R^2	R^3	R^4	yield (%)
2	H	H	H	H	65
15b	H	H	H	OMe	45
15c	H	OMe	H	H	65
15d	H	OMe	OMe	H	57
15e	H	-OCH$_2$O-		H	60
15f	H	H	Br	H	64
15g	H	H	Cl	H	67
15h	H	H	F	H	64
15i	H	Br	H	H	65
15j	H	Cl	H	H	62
15k	Cl	H	H	H	65
15l	H	H	H	Cl	52
15m	H	Br	F	H	63
15n	H	Cl	F	H	62
15o	H	Cl	Cl	H	65
15p	H	Cl	H	Cl	65

[a]Reagents and conditions : (a) 3 equiv $FeCl_3$, DMF, reflux, 3 h.

As expected calothrixin B **2** upon oxidation using *m*-CPBA in DCM at reflux furnished calothrixin A **1**. However, all our attempts to transform representative calothrixin B analogues into their respective calothrixin A analogues using reported conditions[11,18] were found to be unsuccessful (Scheme 4). The reason for failure to oxidize the calothrixin B analogues (**15c**, **15d**, **15g** and **15h**) containing electron releasing as well as electron withdrawing substituents is highly surprising. For some unclarified reasons, these calothrixin B analogues were found to be highly resistant for oxidation.

Scheme 4[a]

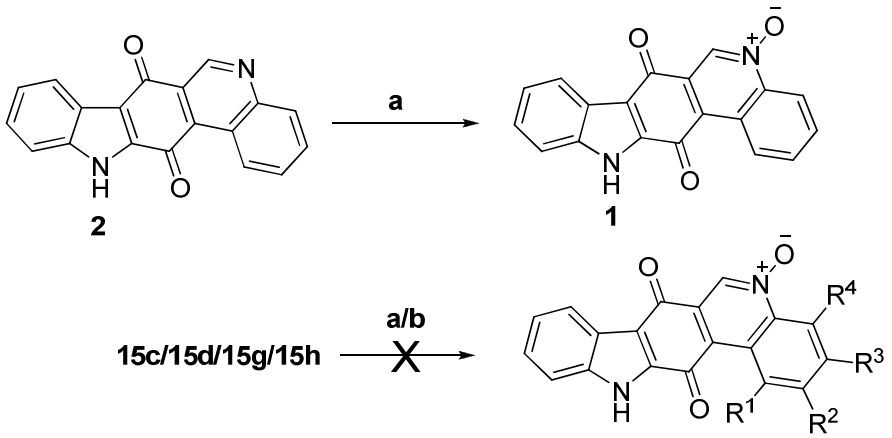

[a]Reagents and conditions : (a) *m*-CPBA, DCM, reflux, 18 h. (b) oxone, acetone, K_2CO_3, rt

In order to understand the importance of quinone unit on structure activity relationship of calothrixin B, synthesis of benzoellipticine analogues were planned. Accordingly, the known phosphonate ester **16** was reacted with 2-nitroarylaldehydes **12a/12h/12g** using K_2CO_3 as a base in DMF at room temperature for 12 h to afford 2,3-divinylindoles **17a-c**. Refluxing, a xylene solution of 2,3-divinylindoles **17a-c** in the presence of 10% Pd/C underwent smooth electrocyclization followed by aromatization to furnish the respective 2-nitroarylcarbazoles **18a-c**. After several attempts, the chemo-selective reduction of ester group without affecting the nitro group was carried out by DIBAL-H. Thus, the reduction of carbazoles **18a-c** with DIBAL-

H (20% in toluene) in dry DCM at 0 °C afforded the elusive benzylic alcohols **19a-c**. Transformation of benzylic alcohols **19a-c** into corresponding aldehydes **20a-c** was performed using PCC in dry DCM. Subsequent reductive cyclization of carbazole-3-carbaldehydes **20a-c** using Ra-Ni in THF at room temperature for 3 h followed by hydrolysis using 50% NaOH afforded quinocarbazoles **21a-c** in good yields.

Scheme 5[a]

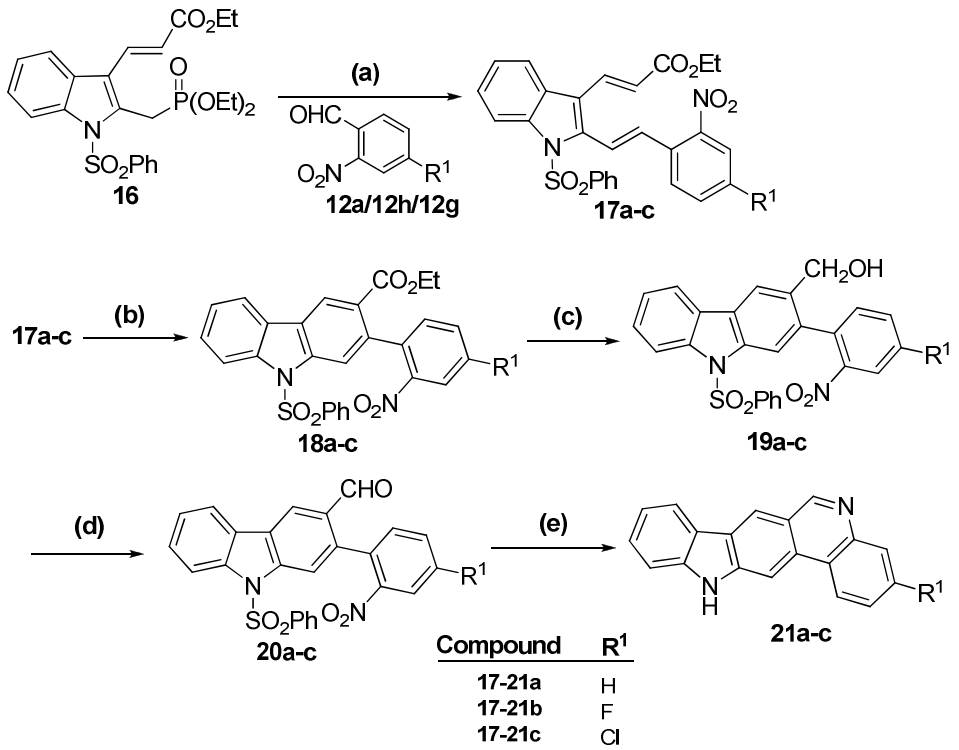

[a]Reagents and conditions : (a) K_2CO_3, DMF, rt, 12 h, 85-88%; (b) 10% Pd-C, xylenes, reflux, 24 h, 80-85%;(c) DIBAL-H, DCM, 0 °C, 30 min; (d) PCC, celite, DCM, rt, 2 h, 77-80% (2 steps); (e) i) Ra-Ni, THF, rt, 3 h; ii) 50% NaOH, DMSO, rt, 6 h, 71-76% (2 steps)

Next, synthesis of the similar structural motiff of quinocarbazole having a methyl group at 4-position of carbazole was planned. As expected, reduction of ester unit of known carbazole **22a/22b**[33] using DIBAL-H (20% in toluene) followed by the oxidation of crude carbazole-3-methanol **23a/23b** using PCC in dry DCM furnished corresponding aldehyde **24a/24b**.

Reductive cyclization of carbazole aldehydes **24a/24b** employing Ra-Ni followed by cleavage of the phenylsulfonyl unit using 50% NaOH afforded quinocarbazole **25a/25b.**

Scheme 6[a]

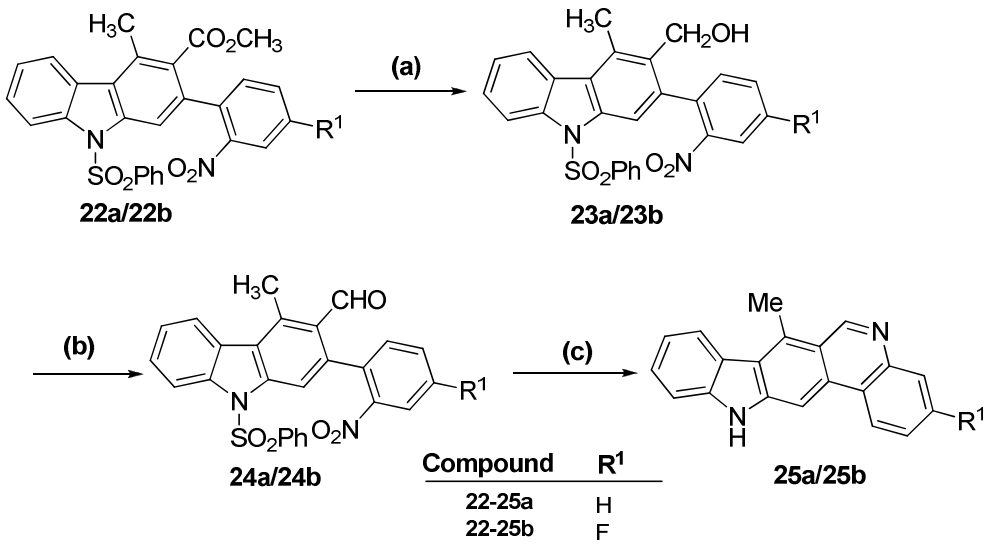

[a]Reagents and conditions : (a) DIBAL-H, DCM, 0 °C, 30 min; (b) PCC, celite, DCM, rt, 2 h, 73-75% (2 steps);(c) i) Ra-Ni, THF, rt, 3 h; ii) 50% NaOH, DMSO, rt, 6 h. 72-75% (2 steps)

Using the similar sequence of reactions, isomeric quinocarbazole **29** was smoothly prepared from the corresponding 3-2'-nitrophenylcarbazole **26**.[34]

Scheme 7[a]

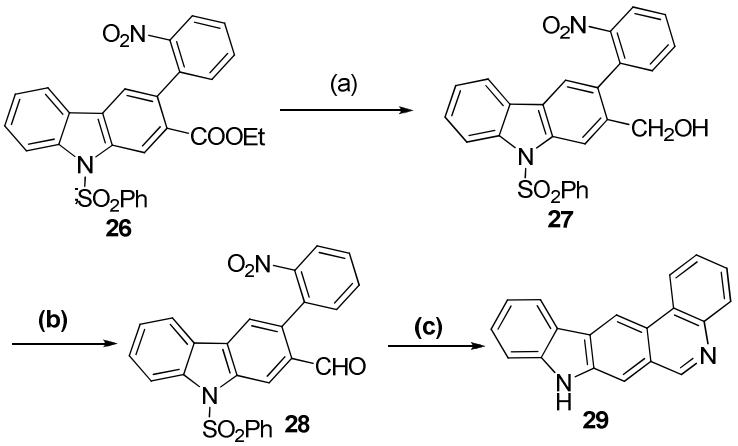

[a]Reagents and conditions : (a) DIBAL-H, DCM, 0 °C, 30 min; (b) PCC, celite, DCM, rt, 2 h, 76% (two steps); (c) i) Ra-Ni, THF, rt, 3 h; ii) 50% NaOH, DMSO, rt, 6 h, 75% (two steps).

Towards enhancing the solubility of quinocarbazole, an incorporation of hydrophilic substituent, amino group was planned (Scheme 8). Accordingly, Wittig reaction of aldehyde **30** with (cyanomethylene)triphenylphosphorane in xylenes at reflux afforded vinyl compound **31**. Benzylic bromination of **31** using NBS and a catalytic AIBN in CCl_4 at reflux for 45 min afforded bromo compound **32**. Subsequent reaction of the bromo compound **32** with PPh_3 followed by Wittig reaction of resulting phosphonium salt with 2-nitroaryl aldehydes **12a/12h/12g** using K_2CO_3 as a base in DCM at room temperature for 8 h led to divinyl compounds **33a-c**.

Scheme 8[a]

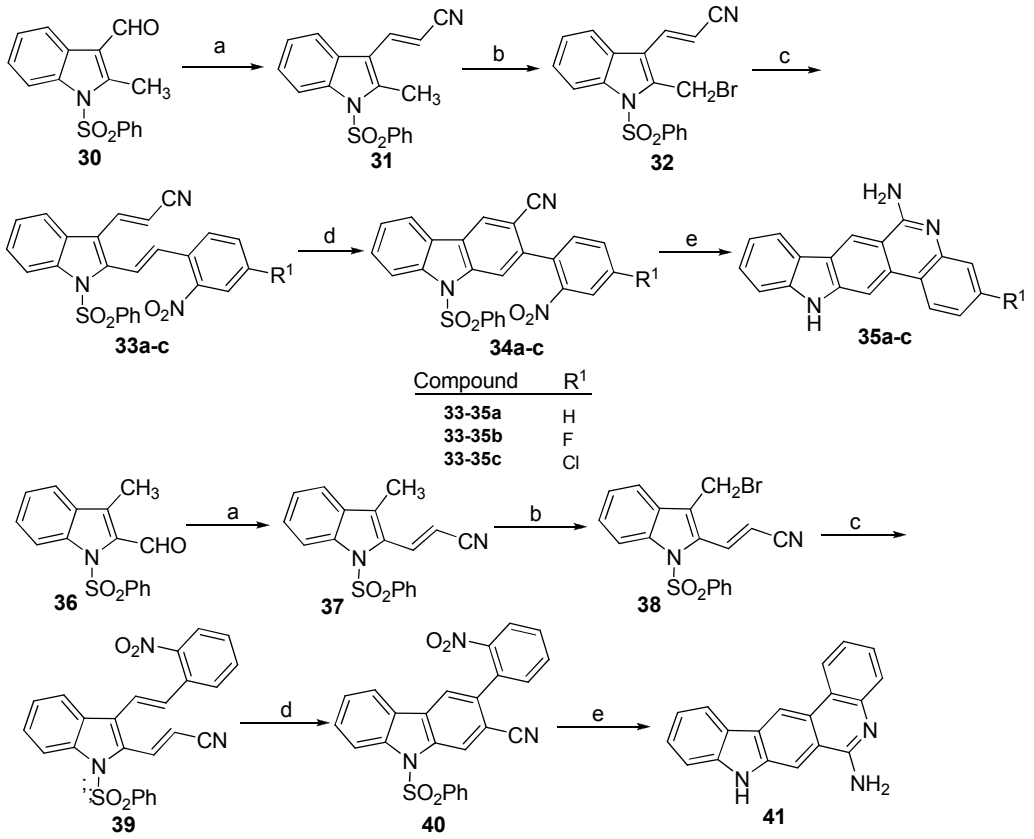

[a]Reagents and conditions : (a) Ph_3P=CHCN, xylenes, reflux, 8 h, 84-86%;(b) NBS, AIBN, CCl_4, reflux, 45 min, 89-91%; (c) PPh_3, THF, reflux, 3 h, followed by K_2CO_3, DCM rt, 8 h, 74-83%; (d) 10% Pd-C, xylenes, reflux, 24 h, 81-85%; (e) i) Ra-Ni, THF, reflux, 30 min; ii) 50% NaOH, DMSO, rt, 3 h, 74-78% (two steps).

Thermal electrocyclization of the divinyl indoles **33a-c** using 10% Pd/C in xylenes at reflux furnished 3-cyanocarbazoles **34a-c.** The reductive cyclization of the 3-cyanocarbazoles **34a-c** using Ra-Ni followed by cleavage of phenylsulfonyl group led to the expected 1-aminoquinocarbazoles **35a-c**. By using the similar sequence of reactions, 3-methyl-2-indole aldehyde **26** was smoothly transformed into an isomeric 1-aminoquinocarbazole **41** (Scheme 8). Next, reductive cyclization of carbazole ester **18a** with Ra-Ni followed by hydrolysis using 50% NaOH afforded amide compound **42**. The amide **42** upon refluxing with $POCl_3$ furnished 1-chloroquinocarbazole **43,** which upon refluxing with 3-(*N*,*N*-dimethylamino)-l-propylamine furnished quinocarbazole **44** (Scheme 9).

Scheme 9[a]

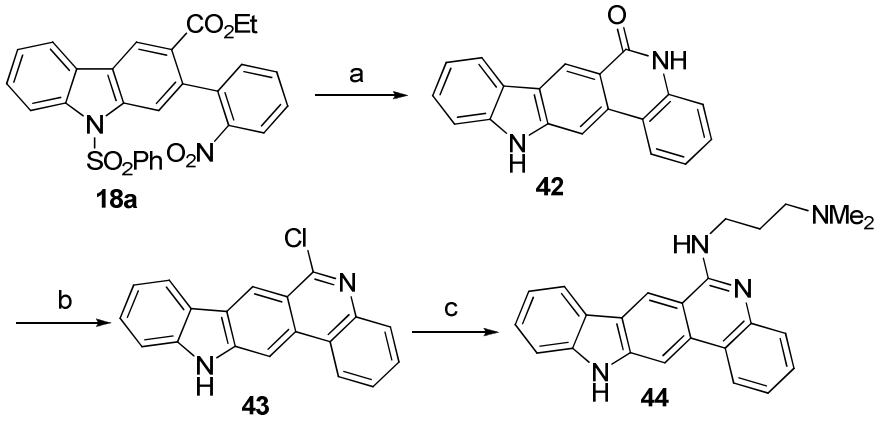

[a]Reagents and conditions : (a) i) Ra-Ni, THF, reflux, 4 h; ii) 50% NaOH, DMSO, rt, 12 h, 78% (two steps); (b) $POCl_3$, reflux, 24 h, 79%; (c) $NH_2(CH_2)_3NMe_2$, reflux, 20 h, 75%.

Finally, the known 1-phenylsulfonyl napthocarbazole **45**[35] upon hydrolysis using 50% NaOH afforded 12*H*-naphtho[1,2-*b*]carbazole **46**.

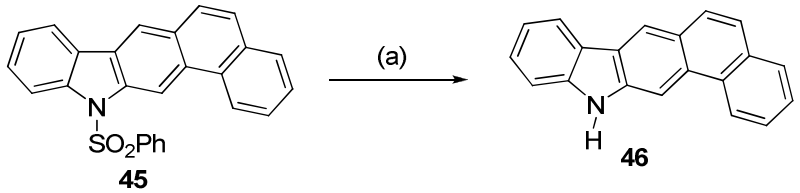

[a]Reagents and conditions : (a) 50% NaOH, DMSO, rt, 6 h, 84%

Cell Proliferation Inhibitory Activities of calothrixins B and quinocarbazole analogues

In order to gain information about the structure-activity relationships of the different calothrixin B and quinocarbazole analogues, chemosensitivity studies were performed and GI_{50} values were determined against nine different human cancer cell lines of diverse tumour origin. The *in vitro* GI_{50} (growth inhibition) values of calothrixins against individual cell lines are presented in **Table 1**, which also includes values of parent calothrixin A (**1**), calothrixin B (**2**) and the cytotoxic quinoline alkaloid, camptothecin.

It should be noted that for the first time, antiproliferative potential of calothrixins **1**, **2** and **15b-p** were evaluated against various cancer cell lines. As observed earlier,[6] calothrixin A (**1**) displayed comparatively better inhibitory effects than calothrixin B (**2**) against all the different cell lines tested. The calothrixin **15b** having a methoxy substituent at 4-position more or less maintains the growth inhibitory potential with exception of Jurkat, SiHa, HCT116 p53-/- and NCI-H460 cell lines. However, the presence of a 2-methoxy substituent on calothrixin B **15c** diminishes growth inhibitory effect in most of the cell lines except HCT116. The calothrixins **15d** and **15e** containing dimethoxy and methylenedioxy substituent at the 2- and 3-positions displayed negligible inhibitory effects in majority of the cell lines evaluated. However, these compounds showed greatest selectivity with GI_{50} values of 0.36 μM and 0.11 μM, respectively, against MCF-7 cancer cell line.

The presence of electron withdrawing halogen atoms at 3-position of calothrixin B (**2**) maintains or even improve the GI_{50} values. For 3-halo substituted calothrixins **15f-h**, the observed GI_{50} values are in the order of F > Cl ≥ Br. Compared to the parent compound **2**, the presence of chlorine/bromine at the 2-position of calothrixin B **15i/15j** enhances the GI_{50} values in many cell lines. It should be noted that the presence of a chlorine or bromine atom at

Table 1. *In vitro* cytotoxicity data for calothrixins **1**, **2** and **15b-p** against nine human tumor cell lines

	GI_{50} Average ± S.D. (μM)[a]																	
Compound	**Jurkat**		**HeLa**		**SiHa**		**MCF7**		**HCT116**		**HCT116 p53-/-**		**MDA-MB 231**		**U251**		**NCI-H460**	
1	0.07	± 0.01	0.08	± 0.00	0.05	± 0.05	0.03	± 0.0	0.11	± 0.05	0.08	± 0.01	0.04	± 0.01	0.08	± 0.01	0.22	± 0.02
2	>4		0.47	± 0.09	3.50	± 0.71	0.26	± 0.01	0.65	± 0.07	2.55	± 0.92	0.16	± 0.02	2.25	± 0.35	>4	
15b	>4		0.39	± 0.20	>4		0.60	± 0.42	0.33	± 0.06	>4		0.31	± 0.01	1.83	± 0.32	>4	
15c	>4		>4		>4		>4		0.63	± 0.11	>4		>4		>4		>4	
15d	>4		>4		>4		0.36	± 0.34	>4		>4		>4		>4		>4	
15e	>4		>4		>4		0.11	± 0.01	>4		>4		>4		>4		>4	
15f	1.50	± 0.57	0.21	± 0.13	>4		0.60	± 0.28	1.50	± 0.42	2.60	± 0.57	1.00	± 0.00	2.00	± 0.42	1.27	± 0.06
15g	3.55	± 0.64	0.07	± 0.02	1.60	± 0.57	0.53	± 0.38	1.50	± 0.28	2.60	± 0.71	0.36	± 0.04	2.83	± 0.29	1.40	± 0.14
15h	1.15	± 0.07	0.05	± 0.02	0.93	± 0.12	0.85	± 0.07	0.83	± 0.06	1.10	± 0.14	0.30	± 0.12	1.20	± 0.22	1.18	± 0.13
15i	1.50	± 0.71	0.29	± 0.05	1.40	± 0.14	0.22	± 0.05	0.70	± 0.00	1.13	± 0.15	0.27	± 0.05	0.60	± 0.14	1.10	± 0.14
15j	1.40	± 0.28	0.50	± 0.14	1.67	± 0.19	0.35	± 0.22	0.42	± 0.17	1.50	± 0.42	0.17	± 0.00	0.50	± 0.00	0.70	± 0.42
15k	>4		>4		>4		0.80	± 0.42	3.50	± 0.71	>4		>4		>4		>4	
15l	>4		>4		>4		>4		>4		>4		>4		>4		>4	
15m	>4		0.27	± 0.11	>4		0.66	± 0.76	>4		>4		0.4	± 0.14	>4		2.25	± 0.78
15n	>4		2.00	± 0.00	>4		1.35	± 0.35	>4		>4		>4		>4		>4	
15o	>4		1.80	± 0.00	>4		>4		>4		>4		1.80	± 0.28	>4		>4	
15p	2.60	± 0.57	0.50	± 0.00	1.80	± 0.00	0.50	± 0.00	1.20	± 0.14	2.00	± 0.00	0.2	± 0.00	1.50	± 0.28	0.73	±0.25
CPT	0.06	± 0.01	0.19	± 0.03	0.55	± 0.00	0.06	± 0.00	0.05	± 0.01	0.195	± 0.01	0.4	± 0.01	0.01	±0.0071	0.0057	±0.0029

[a] Values represents mean from at least two independent experiment

2-position has almost identical influence on its GI_{50} values. The 1-chlorocalothrixin B **15k** as well as 4-chlorocalothrixin B **15l** displayed reduced antiproliferative potential when compared to calothrixin B (**2**). In general, the mono-substitution of halogens at 3- or 2-positions of calothrixin B maintains or even improve the GI_{50} values whereas a similar substitution of halogens at 1- or 4-position is detrimental. Among the seven mono halo-substituted calothrixins **15f-l**, 3-fluorocalothrixin B **15h** showed higher GI_{50} value which is better than the parent calothrixin B (**2**) inhibition profile.

Addition of a second halogen atom (Br or Cl) at 2-position of highly active 3-fluoro calothrixin B **15h** greatly diminish the GI_{50} values. The resulting analogues **15m** and **15n** did not inhibit the growth of majority of cancer cell lines taken for the study with the exception of HeLa and MCF7. The presence of chlorine atoms at 2- and 3-positions of calothrixin B **15o** also reduced its antiproliferative potential. However, the presence of chlorine atoms at 2- and 4-positions (**15p**) more or less maintains the growth inhibition potency in comparison to the parent calothrixin B (**2**).

Calothrixin A (**1**) is more potent than calothrixin B (**2**) as well as its analogues **15b-p**. Calothrixin A (**1**) is equipotent in inhibiting the growth of all cell lines tested with the GI_{50} values ranging in sub-nanomolar concentration (30-220 nM). Among the analogues of calothrixin B **15b-p**, the 3-fluoro derivative **15h** is more potent followed by other 3- or 2-mono halo substituted calothrixin B analogues **15f, 15g**, **15i** and **15j**.

Next, the synthesized quinocarbazoles were evaluated for their cytotoxicity against different human cancer cell lines and their *in vitro* GI_{50} (growth inhibition) values against individual cell lines are presented in **Table 2**.

Table 2. *In vitro* cytotoxicity data for quinocarbazoles **21a-c**, **25a, b** and **29**, naphthocarbazole **31** against ten human tumor cell lines

	GI_{50} Average ± S.D. (μM)[a]																
Name	**Jurkat**		**HeLa**		**SiHa**	**MCF7**		**HCT116**		**MDA-MB 231**		**U251**	**NCI-H460**		**HEK293**		**A549**
21a	4.00	± 0.00	0.41	± 0.08	>4	>4	>4	11.5	± 0.07	>4		>4	5.5	± 0.70	>4		>4
21b	>4		0.02	± 0.01	>4	0.02	± 0.01	6	± 0.05	0.95	± 0.07	>4	0.0010	±0.0002	0.0052	±0.0021	>4
21c	>4		0.43	± 0.18	>4	>4	>4	28	± 0.23	>4		>4	10	± 0.00	>4		>4
25a	>4		0.36	± 0.06	>4	>4	>4	15	± 0.00	>4		>4	10.5	± 0.70	>4		>4
25b	>4		0.05	± 0.01	>4	0.27	± 0.02	30	± 0.12	>4		>4	0.04	± 0.04	>4		>4
29	>4		1.40	± 0.14	>4	>4		>50		>4		>4	10	± 0.05	>4		>4
46	>4		>4		>4	>4		>50		>4		>4	>50		>4		>4

[a] Values represents mean from at least two independent experiments

Table 3. *In vitro* cytotoxicity data for amino quinocarbazoles **35a-c, 41** and **44** against seven human tumor cell lines

	GI_{50} Average ± S.D. (μM)[a]													
Name	**HeLa**		**SiHa**		**MCF7**		**HCT116**		**MDA-MB 231**		**U251**		**NCI-H460**	
35a	0.80	± 0.14	1.05	± 0.07	1.00	± 0.14	1.00	± 0.09	1.00	± 0.1	1.05	± 0.09	1.00	± 0.05
35b	0.01	± 0.008	1.35	± 0.21	0.13	± 0.07	1.20	± 0.0	1.25	± 0.35	1.20	± 0.14	0.14	± 0.04
35c	0.53	± 0.10	1.10	± 0.00	0.95	± 0.07	1.00	± 0.0	0.90	± 0.28	1.20	± 0.00	1.05	± 0.07
41	1.40	± 0.14	1.30	± 0.28	1.00	± 0.00	1.05	± 0.07	1.10	± 0.00	0.65	± 0.21	1.05	± 0.12
44	1.10	± 0.00	1.15	± 0.07	2.75	± 0.35	1.75	± 0.35	1.00	± 0.14	1.35	± 0.21	1.50	± 0.70

[a] Values represents mean from at least two independent experiments

In the case of quinocarbazole **21a**, which lacks the quinone unit of calothrixin B there is a reduction in cytotoxic potential. However, introduction of the fluorine atom to the 4-position of **21a** resulted in quinocarbazole **21b** with greater enhancement of cytotoxicity with respect to HeLa, MCF7, MDA-MB-231 and NCI-H460 cells. With a GI_{50} value of 1 nM for NCI-H460 and 5 nM for transformed HEK293 cells, the compound **21b** appears to be the most active among the quinocarbazoles reported in this work. Also, **21b** is more active than the naturally occurring calothrixins or synthetic analogues of calothrixin B. However, the introduction of chlorine atom at the 4-position of **21a** produced only an inactive quinocarbazole **21c.** The introduction of electron releasing methyl group at 13-position (**21a→25a**) reduced its anti-proliferative potential. But with simultaneous introduction of fluorine and methyl groups at 4- and 13**-**positions (**21a→25b)** led to the marginal increase in cytotoxicity against three of the ten cell lines taken for the study. Unlike NCI-H460 cells, the other lung adenocarcinoma cell line A549 was insensitive to **21b.** Both the isomeric quinocarbazole **29** and naphthocarbazole **31** were inactive confirming that the presence of nitrogen atom and also its position are essential for the anticancer properties of quinocarbazoles. It is worth to mention that the introduction of fluorine atom to the 4-position of quinocarbazole imparts favorable cytototoxic potency to **21b** and **25b** which are otherwise less active (as in the case of **21a** and **25a**).

On the other hand, synthesized amino quinocarbazoles displayed significant cytotoxic profile with the GI_{50} values ranging between 0.01 μM to 2.75 μM (**Table 3**), which is far superior to the quinocarbazoles reported in this work (**Table 2**). Although, incremental benefit with respect to cytotoxicity is not seen among the differently substituted (Cl at 4th or dimethyl propyl amino at 1st position) amino quinocarbazoles, the presence of fluorine atom at the 4th position in **35b**

resulted in ten fold or greater increase in cytotoxicity in comparison to its parent compound **35a** in NCI-H460, MCF7 and HeLa cell lines.

Only minor differences in the growth inhibition pattern were observed between cell lines, where the p53 gene is functionally active (MCF7, HCT116, NCI-H460), mutated (Jurkat, MDA-MB 231 and U251), inactive (HeLa and SiHa due to Human Papilloma Viral (HPV) proteins) or absent (HCT116 p53-/-). This clearly indicates that the cellular cytotoxicity of calothrixins and its analogues/quinocarbazoles were not mediated by p53. Among the cell lines tested, HeLa (a HPV-18 positive cervical cancer cell line) is the more sensitive to calothrixin A (**1**), calothrixin B (**2**) and its analogues **15b-p** as well as quinocarbazoles or its amino derivatives. However, another HPV positive cell line (SiHa) was found to be less sensitive to calothrixin B and its analogues/quinocarbazoles in comparison to HeLa cells. Obviously, the extreme sensitivity of HeLa cells to the above calothrixin B analogues/quinocarbazoles is not attributed to HPV infection but rather by different mechanisms.

The cytotoxicity data indicate that the *p*-benzoquinone unit in calothrixin can be spared as the corresponding quinocarbazoles too exhibited antiproliferative activity and elimination of the quinoline nitrogen atom resulted in inactive analogues. Thus, the preliminary *in vitro* screening of the synthesized analogues indicated that the calothrixin B/quinocarbazole with a fluoro substituent to the E-ring of indolophenanthridine framework were highly potent against the cell lines tested (**Table 1 & 2**), and these analogues **15h, 21b** along with their parent compounds **2** and **21a** were taken for further functional studies.

Inhibition of clonogenic activity by E-ring fluoro analogue of calothrixin B/quinocarbazole

The cytotoxicity data highlighted the fact that E-ring fluoro analogues of calothrixin B/quinocarbazole were the most promising derivatives of the synthesized compounds tested in this work. Therefore, it was used in clonogenic cell survival assay to assess the long term effects of these analogues on colony forming properties of HCT116 and NCI-H460 cells and the results were compared to natural calothrixins, parent quinocarbazole **21a** and camptothecin. As shown in **Fig. 2**, the clonal growth was inhibited by calothrixin A (**1**), calothrixins B (**2**), **15h** and **21b** in a dose dependent manner in both the cell lines tested. The quinocarbazole **21a** does not abolish colony formation even at the highest concentration (5 μM) taken for the study. More importantly, the clonal potency of NCI-H460 cells were severely affected by treatment with as low as 1 nM of 4-fluoroquinocarbazole **21b** thus corroborating the findings from cytotoxicity assay (GI_{50} Value = 1 nM) and the other cell line HCT116 also shows extreme sensitivity to **21b** analogue where the clonogenic growth is inhibited above 0.1 μM although the GI_{50} value from SRB assay was high at 6 μM. However, the colonies in the **21b** treated plates of HCT116 cells were smaller when compared to the control colonies indicating arrest in the growth of surviving colonies. Consistent with their enhanced activity in preliminary cytotoxic studies, the E-ring fluoro analogues of calothrixin B/quinocarbazole effectively attenuated the clonogenic activity of HCT116 and NCI-H460 cells.

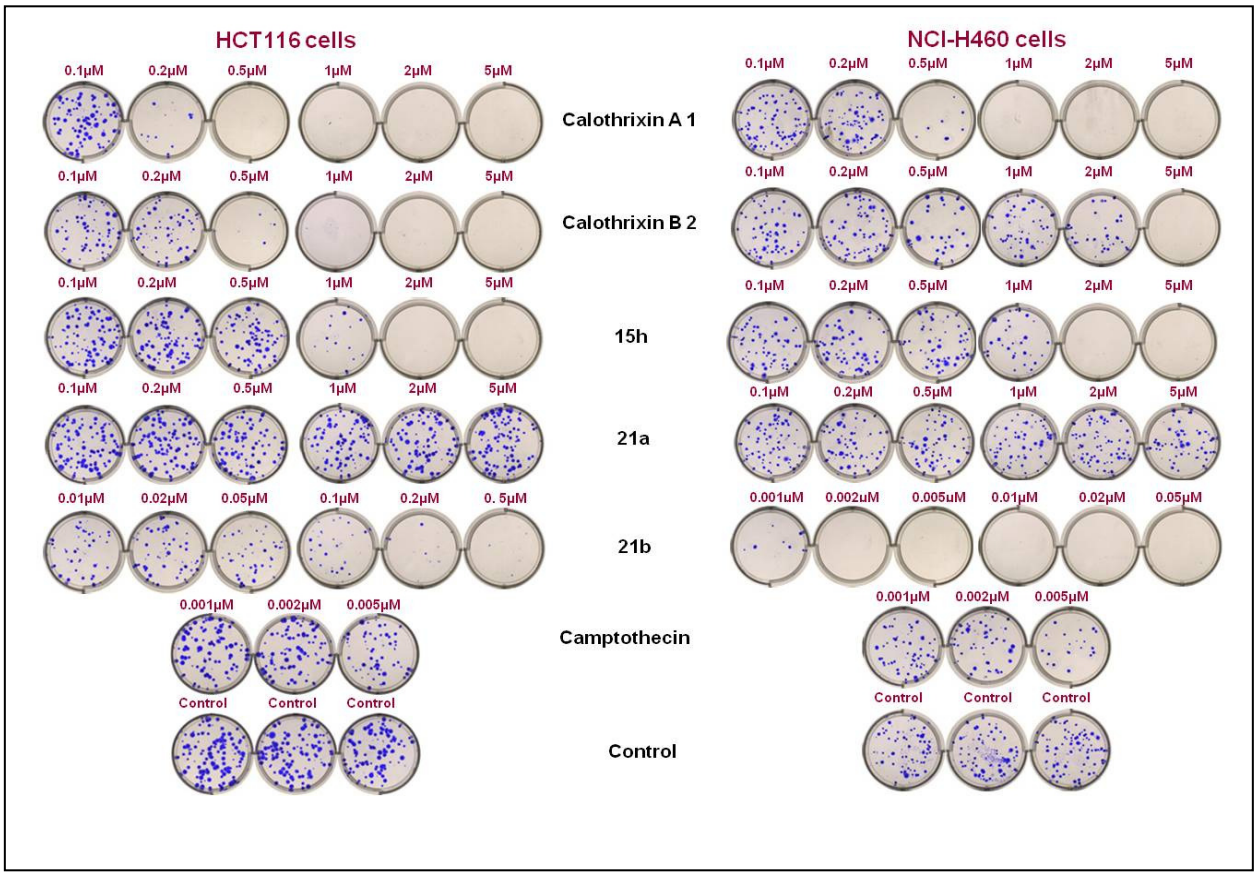

Fig. 2. Effects of calothrixin A**1**, B**2**, **15h** and Quinocarbazoles **21a**, **21b** on the clonogenic growth of colon adenocarcinoma (HCT116) and Lung adenocarcinoma (NCI-H460) cell lines.

Cells were seeded in a six well plate and after over-night adherence, treated with different concentrations (0.1 – 5 μM) of calothrixin A**1**, B**2**, **15h** and quinocarbazoles **21a**, **21b** (HCT116), 0.001 – 0.05 μM of quinocarbazole **21b** in case of NCI-H460 cells, for 48 h. After drug treatment, the cells were washed with Dulbecco's phosphate buffered saline and let grow up to 14 days in drug-free medium. Cell colonies were stained with crystal violet and photographed.

Calothrixins and quninocarbazoles exhibits differential cell cycle effects in HCT116 cells

With the aim of investigating the cellular effects that are induced by calothrixin/quinocarbazole analogues in terms of cell cycle modifications, a time-dependent evaluation of the cell cycle profile was performed by FACS in HCT116 cancer cells treated with these analogues (**Fig. 3**). The cell cycle analysis with 5 μM concentrations of calothrixins **1, 2, 15g** and **15h** for 20 h in HCT116 cells caused an accumulation of cells in G0/G1 phase and S-phase in case of **2** and **1**, **15h**, respectively. However, **21b** treatment to HCT116 cells caused accumulation of cells in G2/M phase, whereas **21a** treatment hardly caused any perturbation in

cell cycle. In order to determine the population of cells which are most affected by the calothrixins and maintenance of cell cycle arrest, nocodazole (a mitotic inhibitor which arrests all the cycling cells at G2/M phase) was added following treatment with calothrixins/quinocarbazoles. As seen in **Fig. 3**, calothrixin A (**1**) or 3-fluorocalothrixin B **15h** pre-treatment to HCT116 cells caused arrest of cells in S-phase which is maintained even after the addition of the nocodazole. Whereas calothrixin B (**2**) was unable to maintain the arrest of cells in G1 phase following nocodazole treatment, which pulled all the cells and arrests in G2/M phase. In a striking difference, addition of nocodazole to **21b** pre-treated cells reinforced accumulation of cells in G2/M phase of cell cycle. In other words, following treatment with nocodazole the cycling cells in G1-S phase adds on to the population of cells (G2/M) that were truly arrested by **21b**. The quinocarbazole **21a** behaved similar to that of its oxygenated congener, calothrixin B (**2**).

These results from cell cycle analysis clearly indicate that **15h** causes G1-S phase arrest whereas its corresponding quinocarbazole **21b** arrests cells at G2/M phase of cell cycle. It can be inferred that presence or absence of quinone functionality as in case of calothrixins or quinocarbazoles determines differential cell cycle effects by targeting diverse cellular target. The presence of fluorine atom at the 3-position of **15h** or 4-position of **21b** confers unique cell cycle signature with better cytotoxicity compared to their counterpart calothrixin B (**2**) or

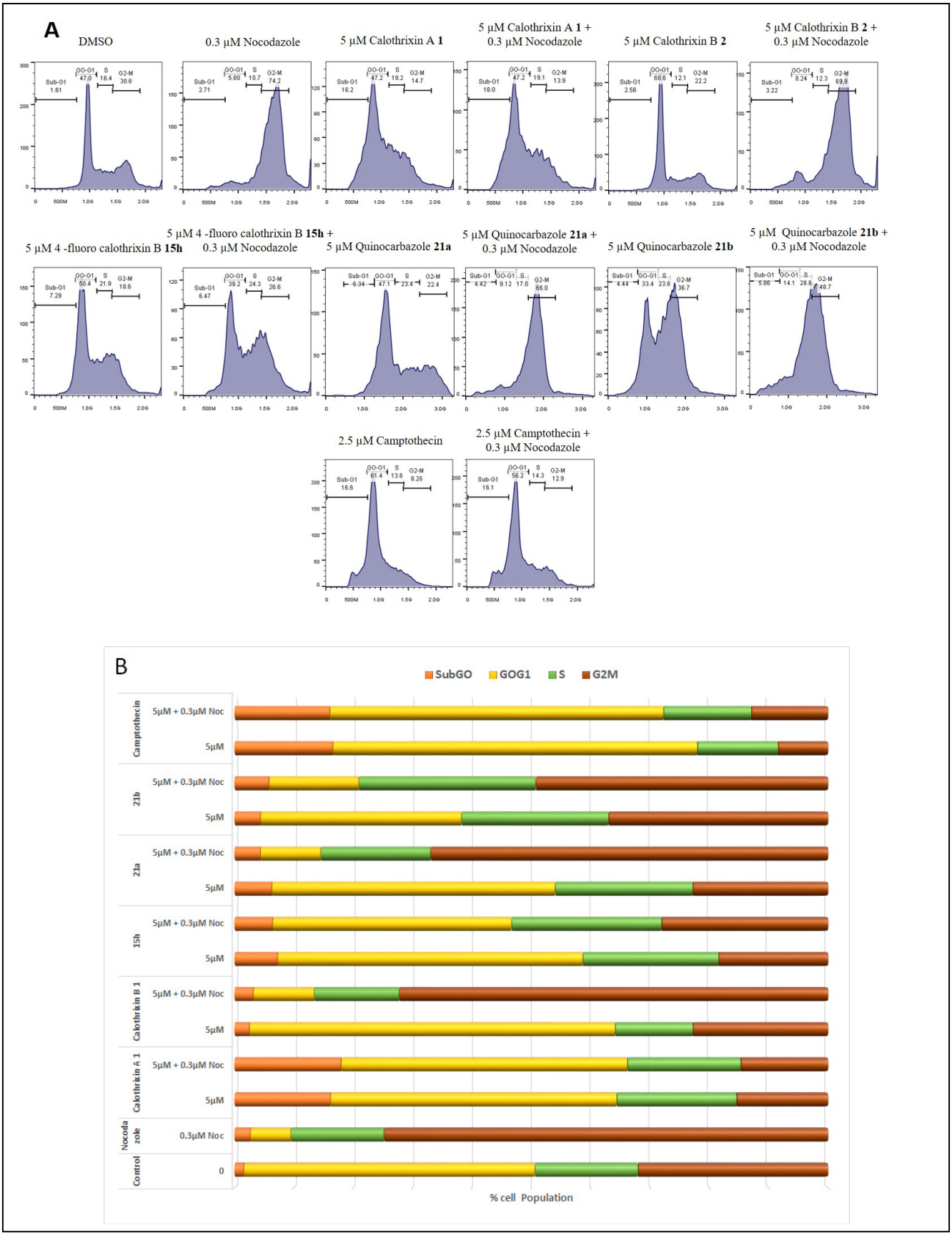
A
DMSO
0.3 µM Nocodazole
5 µM Calothrixin A 1
5 µM Calothrixin A 1 + 0.3 µM Nocodazole
5 µM Calothrixin B 2
5 µM Calothrixin B 2 + 0.3 µM Nocodazole
5 µM 4 -fluoro calothrixin B 15h
5 µM 4 -fluoro calothrixin B 15h + 0.3 µM Nocodazole
5 µM Quinocarbazole 21a
5 µM Quinocarbazole 21a + 0.3 µM Nocodazole
5 µM Quinocarbazole 21b
5 µM Quinocarbazole 21b + 0.3 µM Nocodazole
2.5 µM Camptothecin
2.5 µM Camptothecin + 0.3 µM Nocodazole
B
SubGO
GOG1
S
G2M
Camptothecin
21b
21a
15h
Calothrixin B 1
Calothrixin A 1
Nocodazole
Control
5µM + 0.3µM Noc
5µM
0.3µM Noc
0
% cell Population

Fig. 3. Cell cycle effects of calothrixin and its analogues. Cell cycle perturbation by calothrixins (**1**, **2**, and **15h**) or Quinocarbazoles (**21a** and **21b**) in the presence or absence of nocodazole. HCT116 cells were treated with 5 µM of calothrixin and its analogues for 20 h or 3 h pretreatment with 17 h in the presence of nocodazole (0.3 µM) followed by propidium iodide staining. Population of cells in different phases of cell cycle were analysed by flow cytometry. Figure is representative of other two experiments. (B) Percentages of HCT116 cells in the different phases of the cell cycle

quinocarbazole **21a**. Similar results were obtained from experiments with 1 µM treatment of calothrixins to HeLa cells followed by nocodazole treatment (**SI: Fig. 1**).

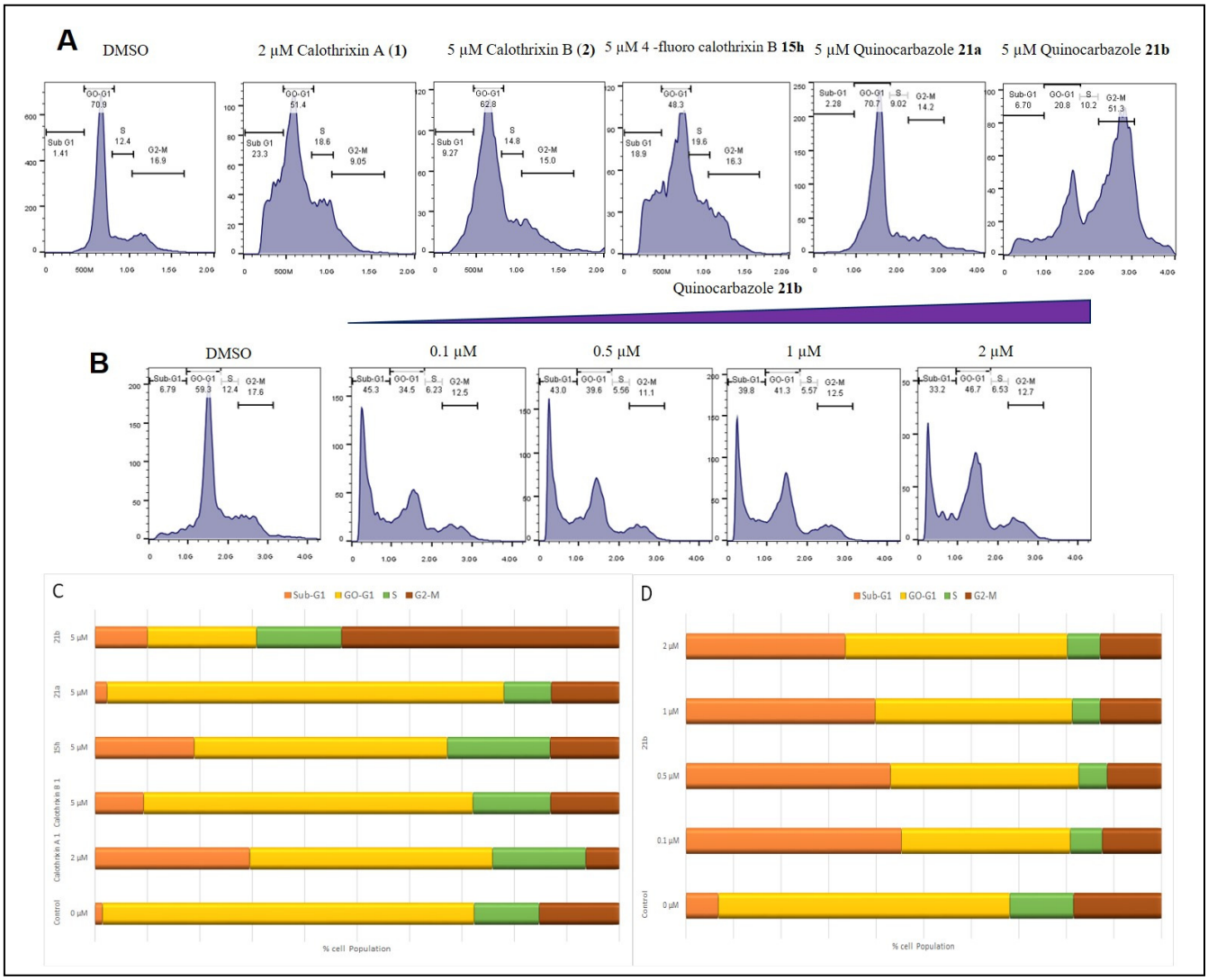

Fig. 4. (A) Cell cycle analysis of human colon HCT116 cells treated with the calothrixins (**1**, **2**, and **15h**) or quinocarbazoles (**21a** and **21b**) for 48 h. (B) Lung NCI-H460 cells treated with increasing concentrations of quinocarbazoles **21b** for 48 h. Figures are representative of other two experiments. (C&D) Percentages of HCT116 (A) or NCI-H460 (B) cells in the different phases of the cell cycle

Cell cycle analysis with HCT116 cells treated with calothrixin A (**1**) (2 μM), 3-fluorocalothrixin B **15h** (5 μM) for 48 h showed maintenance of G1-S phase arrest with concomitant increase in sub-G1 population (**Fig. 4** A, C). This indicates that these cells after DNA damage gets arrested in G1-S phase, followed by cell death at later time point (48 h) due to failure in the repair of damaged DNA and/or cellular stress. However, treatment with the parent calothrixin B (**2**) for 48 h showed G1 arrest with a marginal increase in sub-G1 population (cell death). Whereas quinocarbazole **21b** (5 μM) treatment to HCT116 cells for 48 h showed profound G2-M arrest, which was not seen with the parent quinocarbazole **21a.** In contrast, the quinocarbazole **21b** caused extensive cell death even with 0.1 μM treatment to NCI-H460 cells (**Fig. 4** B, D) with subsequent dose dependent accumulation of cells in G1 phase indicating altogether different mechanistic action of **21b** in this cell line.

Calothrixins as weak topo I inhibitor and quinocarbazoles as catalytic topo II inhibitor

To elucidate the possible mechanistic action of calothrixin B/quinocarbazole analogues, topo inhibition studies of these compounds are explored due to their structural similarities with the natural calothrixins/ellipticine which were reported to possess topoisomerase inhibitory activity.[8, 36] In general, topoisomerase I (hTopI) generates transient single stranded break and religates, thus relieving torsional stress, whereas topoisomerase II (hTopII) is able to cleave and religate double-stranded DNA, allowing strand passage. The calothrixin A (**1**), calothrixins B (**2**), 3-fluorocalothrixin B **15h** and quinocarbazole analogues **21a**, **21b** and **25a** were investigated for hTopI and hTopII inhibition using a relaxation assay by simultaneous incubation of supercoiled plasmid DNA, enzyme, and drug. The results from hTopI inhibition studies (**Fig. 5**) showed that the tested analogues did not have any significant effect even at the concentrations as high as 200 μM (**Fig. 5**, lanes 5 -10). Next, the hTopII inhibition capacity of

these selected calothrixin and quinocarbazole analogues were evaluated. The **Fig. 6** shows the relaxation of supercoiled pBS (SK+) plasmid DNA catalyzed by topo II (lane 2) and the effect of calothrixin A (**1**), calothrixins B (**2**), **15h** and quinocarbazole analogues (**21a**, **21b** & **25a**) at a concentration of 200 μM. The hTopII inhibition by 25 μM of etoposide was used as a positive control (**Fig. 6**, lane 4). Interestingly, among the quinone containing calothrixins, only calothrixin A (**1**) (**Fig. 6**, lane 5) showed effective inhibition of hTopII whereas in case of quinocarbazoles, only **21a** and **25a** showed complete inhibition (**Fig. 6**, lanes 8 and 10). Subsequent dose-dependent relaxation studies with these three analogues revealed that calothrixin A (**1**) could not inhibit the enzyme activity at a concentration <100 μM (data not shown). However, quinocarbazoles **21a** and **25a** exhibited almost 97% and 98% inhibitions, respectively, at 40 μM concentration (**Fig. 7, 8**). Their IC_{50} and IC_{90} values have been reported in **Table 4**. It is surprising to note that the 4-fluoroquinocarbazole analogue **21b** does not have the capacity to interfere with the relaxation activity of hTopII which is seen with its congener **21a**, although both these analogues intercalate with DNA.

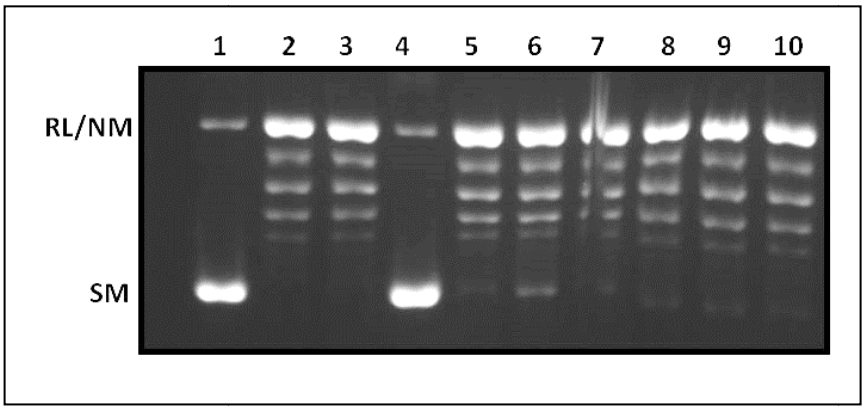

Fig. 5. Effects of calothrixin and quinocarbazole analogues on recombinant human topoisomerase I: Relaxation of negatively supercoiled pBS (SK+) DNA with purified hTopI at a molar ratio of 3:1 in simultaneous assay condition. Lane 1, 90 fmol of pBS (SK+) DNA; Lane 2, same as lane 1, but simultaneously incubated with 30 fmol of hTopI for 30 mins at 37 ^{o}C; Lane 3, same as lane 2 but in presence of 2% v/v DMSO; Lane 4, same as lane 2 but in presence of 25 μM camptothecin as positive control; Lanes 5-10, same as lane 2 but in presence of 200 μM concentration of calothrixin A **1**, calothrixins B **2**, **15h**, quinocarbazoles**21a**, **21b** and **25a**, respectively. Positions of supercoiled monomer (SM) and relaxed and nicked monomer (RL/NM) are indicated.All results depicted were performed three times and representative data are from one set of these experiments.

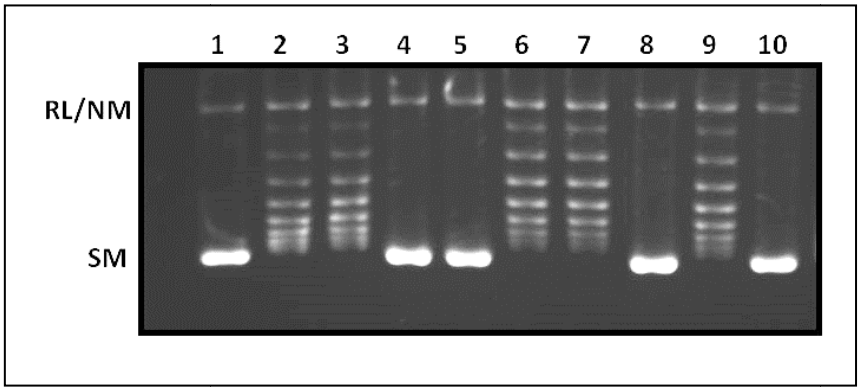

Fig. 6. Effects of calothrixin and quinocarbazole analogues on recombinant human topoisomerase II: Relaxation of negatively supercoiled pBS (SK+) DNA with purified hTopII at a molar ratio of 3:1 in simultaneous assay condition. Lane 1, 90 fmol of pBS (SK+) DNA; Lane 2, same as lane 1, but simultaneously incubated with 30 fmol of hTopII for 30 mins at 37 ^{o}C; Lane 3, same as lane 2 but in presence of 2% v/v DMSO; Lane 4, same as lane 2 but in presence of 25 µM etoposide as positive control; Lanes 5-10, same as lane 2 but in presence of 200 µM concentration of calothrixin A **1**, calothrixins B **2**, **15h**, quinocarbazoles **21a**, **21b** and **25a**, respectively. Positions of supercoiled monomer (SM) and relaxed and nicked monomer (RL/NM) are indicated. All results depicted were performed three times and representative data are from one set of these experiments.

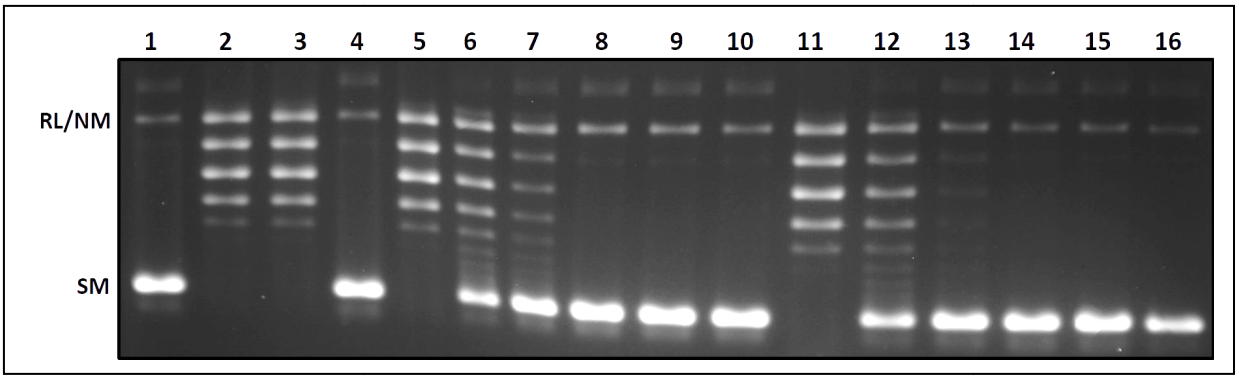

Fig. 7. Dose-dependent inhibition of recombinant human topoisomerase II by quinocarbazole analogues **21a** and **25a**: Relaxation of negatively supercoiled pBS (SK+) DNA with purified hTopII at a molar ratio of 3:1 in simultaneous assay condition. Lane 1, 90 fmol of pBS (SK+) DNA; Lane 2, same as lane 1, but simultaneously incubated with 30 fmol of hTopII for 30 mins at 37 ^{o}C; Lane 3, same as lane 2 but in presence of 2% v/v DMSO; Lane 4, same as lane 2 but in presence of 25 µM etoposide as positive control; Lanes 5-10, same as lane 2 but in presence of increasing concentrations (10, 20, 30, 40, 50, and 60 µM) of quinocarbazole **21a** and Lanes 11-16, same as lane 2 but in presence of increasing concentrations(10, 20, 30, 40, 50, and 60 µM) of quinocarbazole **25a**. Positions of supercoiled monomer (SM) and relaxed and nicked monomer (RL/NM) are indicated. All results depicted were performed three times and representative data are from one set of these experiments.

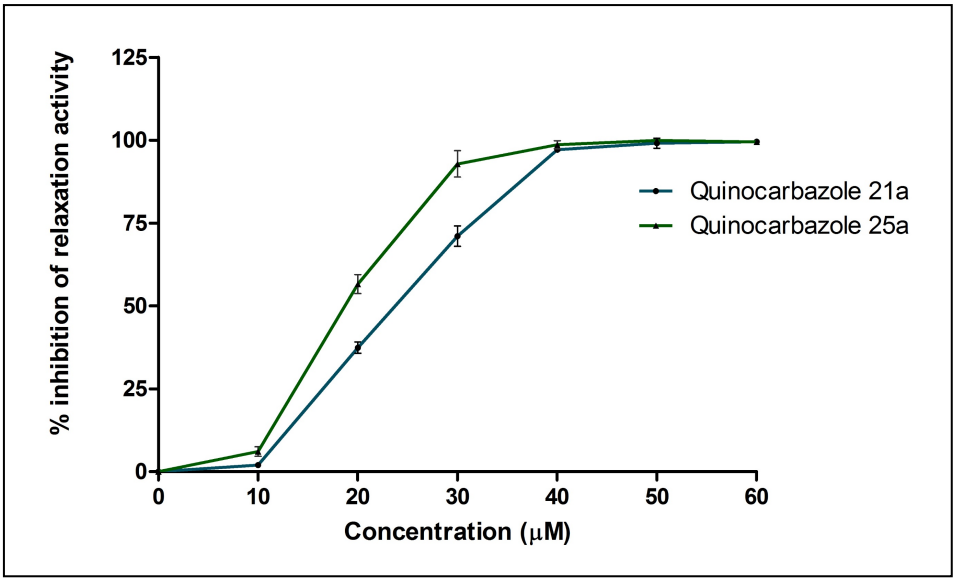

Fig. 8. Quantitative representation of enzyme inhibition as a function of concentrations of quinocarbazoles **21a** and **25a** under standard relaxation condition. Data represent mean value ± S.D. (n = 3).

Table 4. Inhibitory concentration of the compounds on human Topoisomerase II

Name of compound	**IC_{50}**μM± S.D.	**IC_{90}**μM± S.D.
Quinocarbazole **21a**	23.361 ± 0.104	41.514 ± 0.104
Quinocarbazole **25a**	19.086 ± 0.099	28.798 ± 0.099

Human TopII inhibitors can either stabilize the covalent DNA topoisomerase II complex (topoisomerase II poisons) or inhibit the catalytic activity of the enzyme (catalytic inhibitors). To identify the mode of hTopII inhibition by quinocarbazoles **21a** and **25a,** hTopII-mediated DNA cleavage assay was performed under equilibrium condition. The hTopII alone cleaved the pRYG DNA which resulted in the formation of nicked circular DNA (Form II) and linear DNA (Form III) (**Fig. 9**, lane 2). The positive control etoposide converted closed circular DNA (Form I) to linear DNA (Form III) by stabilization of the "cleavable complex" (**Fig. 9**, lanes 4 and 5) and resulted in a drastic increase in Form III. When the cleavage assay was performed with increasing concentrations of these quinocarbazoles, no remarkable linear products (**Fig. 9**, lanes 6–8 for **21a**, lanes 9–11 for **25a**) were observed. In addition, these quinocarbazoles could abrogate etoposide-mediated cleavage complex formation thereby rescuing Form I (**Fig. 9**, lane

12 for **21a** and lane 13 for **25a**) when they were preincubated (40 μM) with hTopII prior to etoposide (50 μM) addition. These results clearly established that **21a** and **25a** does not act as a topoisomerase II poison instead they inhibit the binding of enzyme to substrate DNA and thus inhibit etoposide mediated cleavable complex formation.

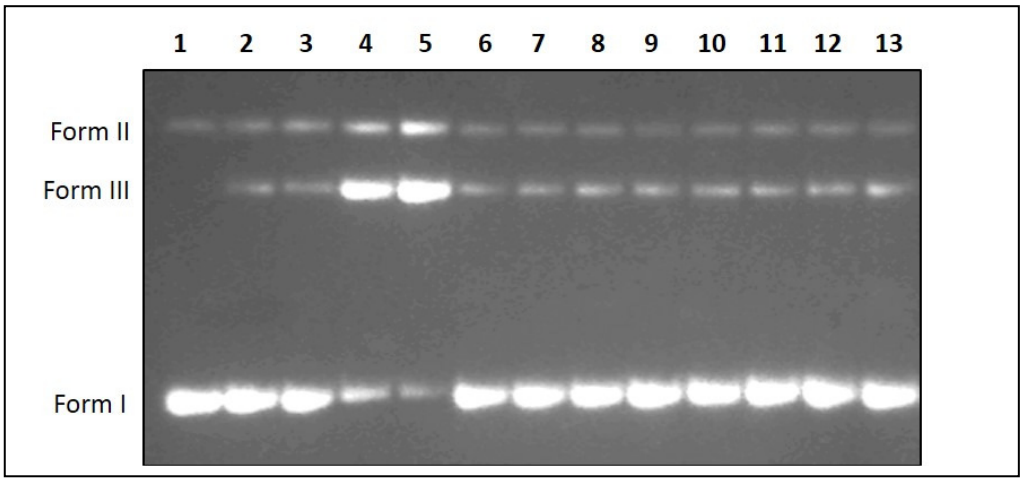

Fig. 9. Inhibition of etoposide-induced cleavage complex formation by quinocarbazole analogues was analyzed by cleavage reaction and agarose gel electrophoresis. Lane 1, negatively supercoiled pRYG DNA; lane 2, pRYG DNA with hTopII alone; lane 3 same as lane 2 but in presence of proteinase k treatment; Lanes 4, 5 same as lane 2 but in presence of increasing concentration (25 and 50μM) of etoposide; Lanes 6-8 and 9-11 same as lane 2 but in presence of increasing concentration (30, 40 and 50μM) of **21a** and **25a**, respectively; lane 12 and 13, hTopPII was incubated with 40 μM of **21a** and **21b**, respectively, followed by the addition of 50 μM of etoposide and pRYG DNA. Form I, closed circular DNA; Form II, nicked circular DNA; Form III, linear DNA. All results depicted were performed three times and representative data are from one set of these experiments.

The results from topoisomerase inhibition studies revealed that calothrixin B (**2**) weakly inhibit hTopI whereas its deoxygenated derivative quinocarbazole **21a** selectively targets human hTopII. The exception being *N*-oxide bearing calothrixin A (**1**) which inhibited both these enzymes although at different potency. Thus, it appears that the quinone functionality in calothrixin bestows topo I inhibition and the absence of such unit in quinocarbazoles favors hTopII inhibition. Compounds **21a** and **25a**, which displayed the most significant catalytic inhibition of topoisomerase II with their IC_{50} values falling below 23 μM, showed only moderate cytotoxicity. Meanwhile, the other tested 4-fluoroquinocarbazole **21b** had no effect

on hTopII activity nevertheless showed promising cellular cytotoxicity suggesting that this compound might target DNA or other proteins in cancer cells. Also, the disparity between the observed cytotoxicity and hTopI inhibition profile among calothrixins, namely calothrixin A (**1**), calothrixin B (**2**) and 4-fluorocalothrixin B **15h** indicate that topo I not to be a target for calothrixins.

Calothrixins are redox active and cleaves plasmid DNA

In order to gain insight into the effects on the DNA-damage profiles of the calothrixin/quiniocarbazole analogues, nuclease assay of supercoiled plasmid DNA incubated with these derivatives were qualitatively analyzed by agarose gel electrophoresis. The DNA nuclease assay for the synthesized analogues was planned in the presence of a reducing agent and ferric ion due to the redox active quinone functionality in calothrixins. The nuclease activity of calothrixin A (**1**), calothrixin B (**2**), calothrixin B analogues **15b-p** and quinocarbazoles (**21a-c**, **25a**, **25b** and **29**) in the presence as well as absence of reducing agent dithiothreitol (DTT) has been investigated on pBluescript SK(+) supercoiled plasmid DNA by agarose gel electrophoresis at 60 min incubation period at 37°C (**Fig. 10** A&C).

The nuclease activity of calothrixin analogues are seen only in the presence of a reducing agent (DTT) and metal ion ($FeCl_3$). Mono halo derivatives of calothrixin B (**15f**, **15g, 15i and 15k**) show higher propensity of cleavage of super coiled (SC) form to closed circular (CC) except for calothrxins (**2**) and **15l** (**Fig. 10A**). The 3-fluoro derivative **15h** of calothrixin B or its quinocarbazole **21b** shows complete degrading of SC form to CC and linear form which is comparable to the nuclease activity of calothrixin A (**1**).

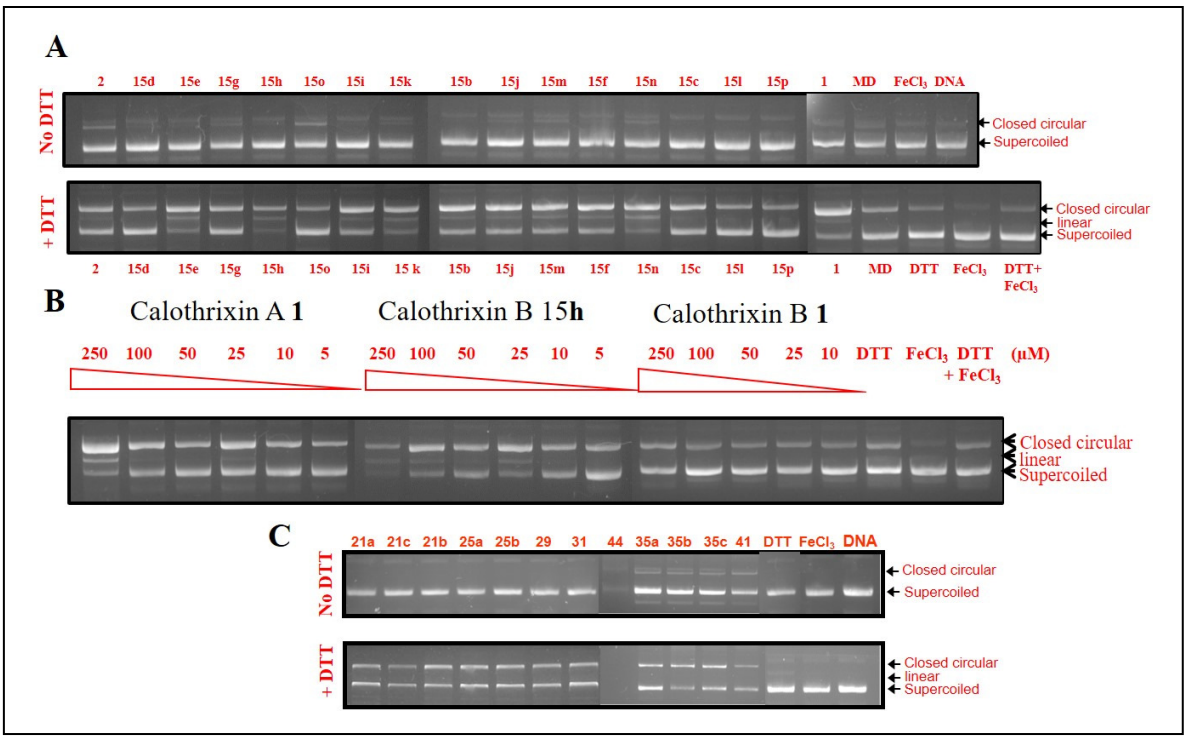

Fig. 10. Cleavage of plasmid DNA by calothrixins and quinocarbazoles in a cell free system. (A & C) Supercoiled plasmid DNA was incubated for 1 h with 250 µM of calothrixins or quinocarbazoles, 200 µM of ferric chloride in the presence or absence of DTT (200 µM). Plasmid DNA was separated by agarose gel and stained with ethidium bromide. Menadione (250 µM) was used as a positive control. (B) Dose dependent cleavage of plasmid DNA by calothrixins. Different concentrations of calothrixin A (**1**), **15h** and Calothrixin B (**2**) was incubated for 1 h with supercoiled plasmid DNA in the presence of DTT (200 µM) and ferric chloride (200 µM).

As can be seen in Fig. **10A** & **10C**, there is a general reduction in band intensities with 250 µM of compound **15h** or **21b**, indicating a partial digestion of plasmid DNA, an effect which is not seen with calothrixin A (**1**). Again the presence of fluorine atom at 3-position of calothrixin B or 4-position of quinocarbazole imparts distinct cleavage pattern (linearization and partial digestion of plasmid DNA) which should be highlighted in the context of higher cytotoxic potencies of these analogues. Significant cleavage of plasmid DNA is seen only at higher concentrations of calothrixin A (**1**) or B (**2**) (250 µM), whereas 4-fluoro calothrixin **15h** causes plasmid DNA cleavage even at low concentration of 25 µM (**Fig. 10B**). Although, calothrixin B analogues with dichloro substitution (**15o** and **15p**) or methylenedioxy unit (**15e**) at the E-ring

cleave and linearise the plasmid DNA, they were inactive in cellular cytotoxicity assay. Similar is the case with many quinocarbazole analogues reported in this paper where cleavage of plasmid DNA is seen but with no cytotoxic activity. This might be due to the intrinsic ability of DTT to cleave plasmid DNA in the presence of ferric ions (**Fig. 10 B,** last lane). One of the most striking observations about dimethyl amino propyl quinocarbazole **44** was the complete digestion of plasmid DNA even in the absence of DTT (**Fig. 10C**, lane 8).

E-ring fluoro analogues of calothrixins/quinocarbazoles shows enhanced DNA damage compared to other derivatives

Accumulation of DNA damage might lead to arrest of cells at either G1-S or G2/M checkpoints. In order to assess cellular DNA damage as a potential cause of cell cycle arrest by 4-fluoro analogues of calothrixin B **15h** or quinocarbazole **21b**, the ability of these analogues to induce DNA damage was investigated by performing alkaline single-cell gel electrophoresis (comet assay). This assay allows detection of DNA strand breaks, alkaline-labile DNA sites, and cross-links in individual cells. Electrophoresis of cell possessing damaged or fragmented

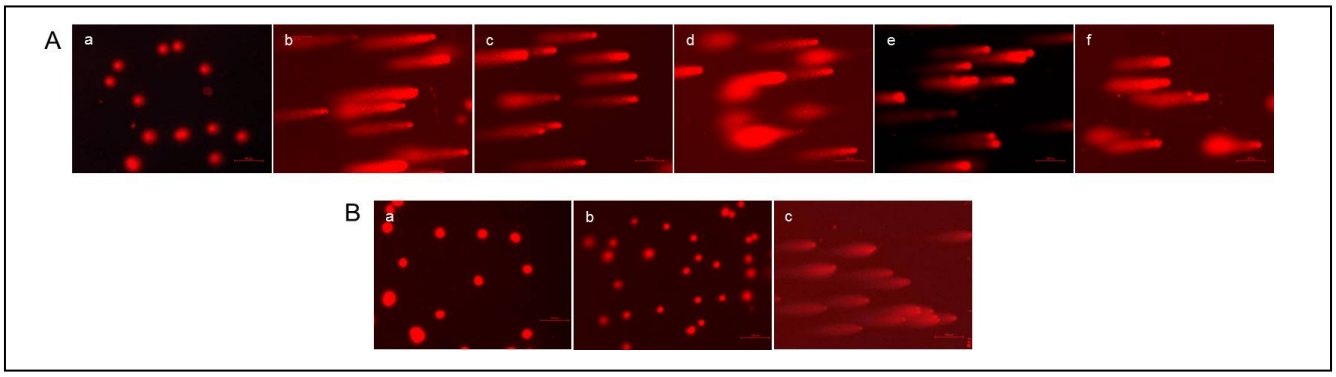

Fig. 11. Single-cell gel electrophoresis data (comet assay) in HCT116 cells (A) or NCI-H460 cells (B). Representative images of HCT116 cells (A) treated for 48 h with 0.5 μM Calothrixin A **1** (b) ; 5 μM Calothrixin B **2** (c) ; 5 μM **15h** (d) ; 5 μM **21a** (e) ; 5 μM **21b** (f) and untreated cells (a). Representative images of NCI-H460 cells (B) treated with 5 μM **21a** (b) ; 0.1 μM **21b** (c) and untreated cells (a)

DNA appears as a comet following staining with an intercalating agent and the length and fluorescence intensity of the comet tail represents the extent of the DNA damage. HCT116 and NCI-H460 cells were incubated with calothrixins/quinocarbazoles for 48 h, cells were harvested and the levels of DNA damage was quantified in single cells using the alkaline comet assay (**Fig. 11**).

Treatment of HCT116 with 0.5 μM Calothrixin A (**1**) resulted in extensive DNA damage, as reflected from the tail length of the comet after 48 h (**Fig. 11 Ab**). Similarly, the calothrixin B (**2**) (5 μM) induced significant levels of DNA damage (**Fig.11 Ac**) whereas its 4-fluro analogue **15h** at a low concentration of 3 μM for 48 h, (**Fig. 11 Ad**) caused a significant increase in DNA strand breaks (tail length) as compared with untreated cells (**Fig. 11 Aa**). In the case of quinocarbazoles under identical conditions, the fluoro analogue **21b** treated cells were considerably damaged (**Fig. 11 Af**) although its parent analogue **21a** showed reduced amount of DNA damage or fragmentation (**Fig. 11 Ae**). In contrast, the comet tail occurred (**Fig. 11 Bc**) when NCI-H460 cells were treated with as low as 0.1 μM of **21b** for 48 h and the tailing of comet is more pronounced in a dose dependent manner (data not shown) while the quinocarbazole **21a** failed to induce DNA damage even at 5 μM treatment for 48 h to NCI-H460 cells (**Fig. 11 Bb**).

Enhanced Apoptosis in E-ring fluoro analogues of calothrixin/quinocarbazole treated HCT116 and NCI-H460 Cells

Cell fate in HCT116, NCI-H460 and HeLa cells following treatment with calothrixins and quinocarbazoles at different time points were studied using fluorescence microscopy and by western blotting. The effect of calothrixins and quinocarbazoles on the cellular morphology of HCT116 and NCI-H460 cells was studied after of 48 h of treatment. Cells stained green

(acridine orange positive) represent viable cells, whereas reddish staining (propidium iodide positive) represents apoptotic cells. The results of acridine orange (AO)/propidium iodide (PI) staining showed that the control cells of HCT 116 or NCI-H460 presented intact green fluorescence (**Fig. 12**), showing the normal nuclear structures. Whereas calothrixin A (**1**) (2 µM) or 5 µM of calothrixin B (**2**), **15h** treated cells revealed chromatin condensation and

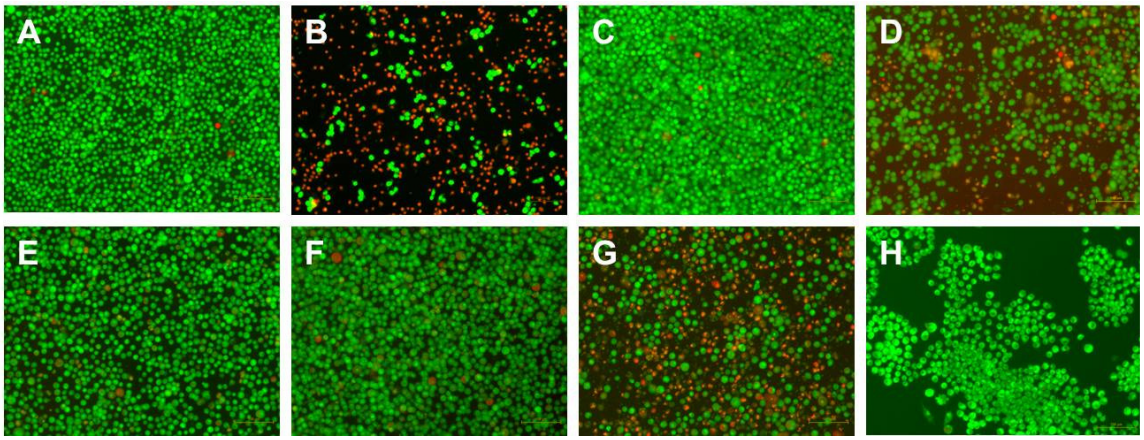

Fig.12. HCT116 cells were stained with acridine orange/propidium iodide after 48 h of treatment with calothrixins/quinocarbazoles. Cells were observed under fluorescence microscope (x100 magnification). Viable cells show green fluorescence. Necrotic and apoptotic cells show orange and yellow fluorescence. (A & E) Untreated HCT116 or NCI-H460 control cells, respectively. Cells were treated with 2 µM of calothrixin A **1** (B) 5 µM of calothrixin B **2** (C), 5 µM of 3-fluorocalothrixin B **15h** (D), 5 µM of quinocarbazole **21a** (F), 0.5 µM of 3-fluoroquinocarbazole **21b** (G), 5 µM of quinocarbazole **25b**.

nuclear fragmentation, as seen by the presence of nuclei stained with PI (red colour). The 3-fluoroquinocarbazole **21b** treated NCI-H460 cells at a low concentration of 0.5 µM showed significant apoptotic cell morphology.

As HeLa and NCI-H460 cells showed higher sensitivity to 3-fluorocalothrixin B **15h** and 4-fluoroquinocarbazole **21b**, respectively in the preliminary cytotoxicity assay, these cell lines were taken for mechanistic study. The proteolytic cleavage of poly (ADP-ribose) polymerase (PARP) by caspases is considered to be a hallmark of apoptosis.[37] Western blot analysis of cell

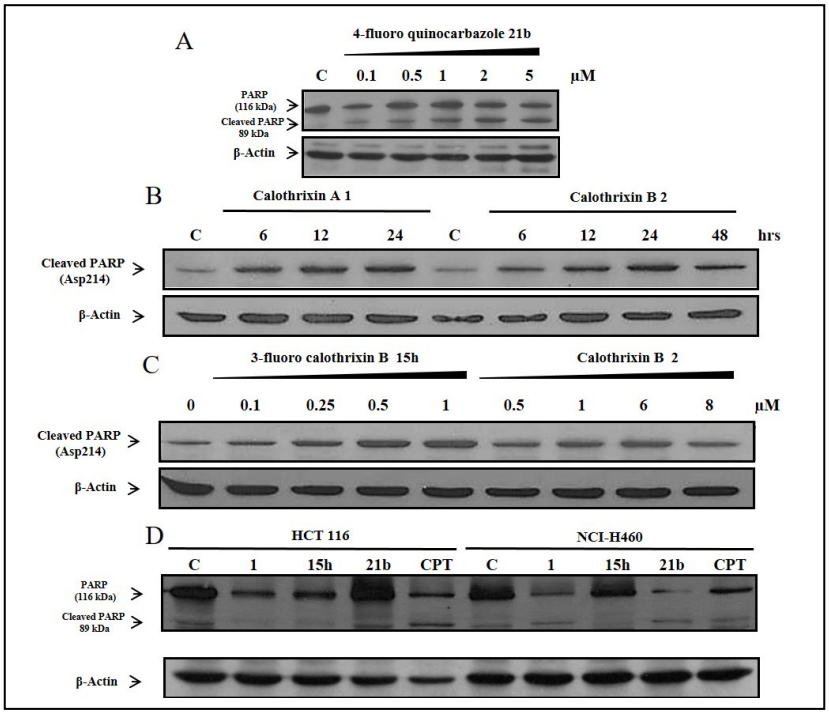

Fig. 13. Induction of apoptosis by calothrixins/quinocarbazoles. Detection of cleaved PARP protein levels by western blotting in the lysates from **A**. NCI-H460 cells treated with increasing concentrations (0.1, 0.5, 1, 2 and 5 µM) of 4-fluoroquinocarbazole **21b** for 48 h **B & C**. HeLa cells treated with calothrixins for different time points (1 µM of calothrixin A **1** for 6, 12, and 24 h ; 10 µM of calothrixin B **2** for 6, 12, 24 and 48 h) and varying concentrations (0.1, 0.25, 0.5 and 1 µM of 3-fluorocalothrixin B **15h** ; 0.5, 1, 6 and 8 µM of calothrixin B **2** for 48 h) **D**. HCT116 or NCI-H460 cells treated with calothrixins/quinocarbazoles (5 µM in case of calothrixin B **2**, compounds **15h** and **21b**; 3 µM of calothrixin A **1,** 0.5 µM of camptothecin) for 48 h. β-Actin staining was used as loading control.

lysates from NCI-H460 cells treated with increasing concentrations of 4-fluoroquinocarbazole **21b** for 48 h resulted in significant cleavage of PARP even at a lower dose of 1 µM (**Fig. 13A**). Immunoblot study with HeLa cells treated with 1 µM of calothrixin A (**1**) or 10 µM of calothrixin B (**2**) showed a time-dependent increase in the protein levels of cleaved PARP (**Fig. 13B**). After exposure to varying concentrations of calothrixin B (**2**) or its 3-fluoro analogue **15h**, a dose-dependent activation of PARP was seen. However, the 3-fluorocalothrixin B **15h** is more potent in causing cell death at lower doses (≥ 0.25 µM) in comparison to its parent compound calothrixin B (**2**) (**Fig. 13C**). Similar increase in the protein levels of cleaved PARP were seen in NCI-H460 cells treated with calothrixins/quinocarbazoles but in case of

HCT116 cells, there is a reduction in total PARP protein level after drug treatment without appearance of cleaved PARP protein bands (**Fig. 13D**). These data suggest that the inhibition of cell growth following drug treatment is mediated through apoptosis induction.

Quinocarbazoles interacts with DNA by intercalation

The mode of cytotoxicity of calothrixins/quinocarbazoles might be based on DNA damage, such as intercalation into DNA as seen in the case of ellipticine.[38] This has prompted us to initiate an investigation of interactions with DNA. Compounds studied in this paper can be divided into two groups, the quinone containing calothrixins and their deoxygenated quinocarbazoles. Due to their structural difference, calothrixins or quinocarbazoles can interact differently with the biological target. To better understand the structure and biological activity relationship, DNA interaction studies of representative calothrixins **1**, **2** and its analogue **15h**, quinocarbazoles **21a**, **21b**, **25a**, **35a, 35c** and **44** with calf-thymus DNA (CT-DNA) were carried out by UV-Vis spectroscopy (**Fig. 14**).

Addition of CT-DNA to quinocarbazoles **21a**, **21b** resulted in strong hypochromic effects (30% at 299 nm for **21a** and 46%, 41% at 258 nm, 302 nm respectively, for **21b**) with red shift (14 nm for **21b** at 258nm) suggesting an intercalative mode of binding[38] involving a stacking interaction between an aromatic chromophore of **21a**, **21b** and the base pairs of DNA. Unlike quinocarbazoles, titrations with CT-DNA induced no change or only minor changes (6.4% hypochromism at 264 nm) in UV-Vis spectra of calothrixin B (**2**) and 3-fluorocalothrixin B **15h**, respectively. One isosbestic point was observed for calothrixin A**1** (333 nm) and 3-fluorocalothrixin B **15h** (330 nm), whereas quinocarbazoles exhibited two isosbestic points

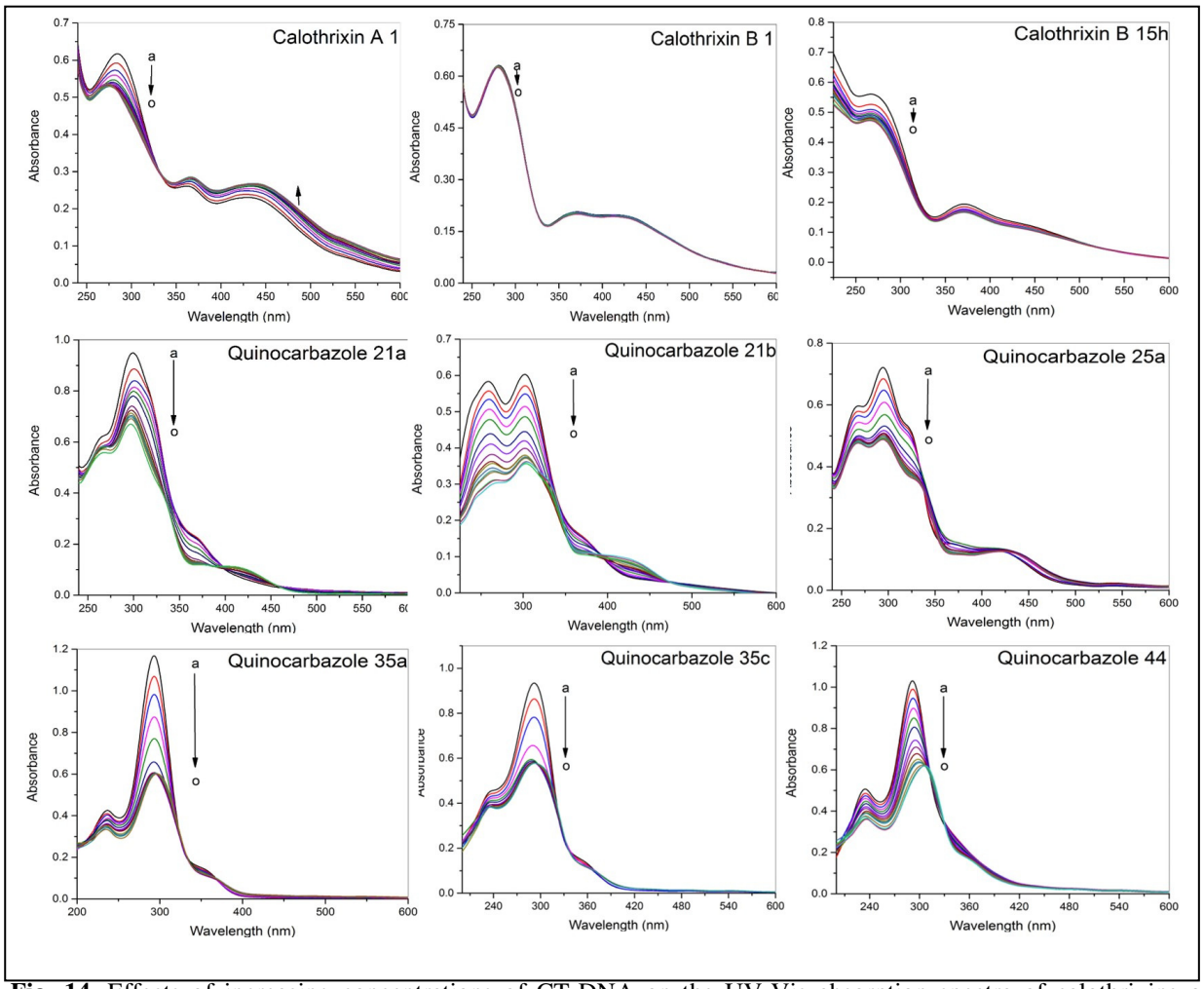

Fig. 14. Effects of increasing concentrations of CT-DNA on the UV-Vis absorption spectra of calothrixins or quinocarbazoles. Conditions: $C_{calothrixins\ or\ quinocarbazoles}$, 3×10^{-5}mol L^{-1}; C_{ctDNA} ($\times10^{-6}$mol L^{-1}); a→o: 0; 2; 5; 10; 15; 20; 25; 30; 35; 40; 45; 50; 60; 80; 100. The arrow shows the intensity changes in increasing CT-DNA concentration

(~337 nm and ~390 nm for **21a**, **21b** and **25a**) signifying additional binding modes between quinocarbazoles and CT-DNA as against a single isosbestic point seen with ellipticine-DNA complex.[39] However, it should be noted that a second, but minor, binding mode only contributes marginally to the overall absorption spectrum and might not have a significant influence on the isosbestic points. In contrast to quinocarbazole **21a**, the corresponding napthocarbazole **31** showed no change in UV-absorption spectra following addition of increasing concentrations of CT-DNA (**SI: Fig. 2**), thus highlighting the requirement of

quinoline nitrogen for DNA intercalation. In the case of amino quinocarbazoles, fluoro derivative **35c** showed strong hypochromism (38%) whereas the dimethyl amino propyl substituent bearing amino quinocarbazole **44** showed hypochromic (40%) and bathochromic shift (15 nm) following CT-DNA addition indicating stronger intercalative mode of interaction with DNA.[38] The 1-amino quinocarbazoles **35a** and **35c** too exhibited two isosbestic points at ~328 nm and ~367 nm indicative of multiple binding modes, although their contribution is very little. On the other hand, titration of calothrixin A (**1**) with CT-DNA showed little hypochromism (13%) with hypsochromic shift (10 nm) at 284 nm and hyperchromic shift (12% at 362 nm, 13% at 432 nm) indicating multimodal interaction, possibly both intercalation as well as electrostatic groove binding.

To quantitatively compare the binding property of different analogues of calothrixin or quinocarbazoles with CT-DNA, the intrinsic binding constants K_b, for drug-DNA complexes were determined using the linear fitting equation[40], Eq (1).

$$[DNA]/(\mathcal{E}_a - \mathcal{E}_f) = [DNA]/(\mathcal{E}_b - \mathcal{E}_f)] + [K_b(\mathcal{E}_b - \mathcal{E}_f)] \quad \ldots(1)$$

Where [DNA] is the concentration of CT-DNA, $\mathcal{E}_a$, $\mathcal{E}_f$ and $\mathcal{E}_b$ correspond to the extinction coefficients of drug at a given CT-DNA concentration, the free drug in solution and the fully bound drug with DNA, respectively. By plotting the $[DNA]/(\mathcal{E}_a - \mathcal{E}_f)$ versus [DNA], K_b can be obtained as the ratio of the slope to the intercept of the equation. Thus, the binding constants obtained from UV-Vis titrations with CT-DNA revealed the binding affinity of the calothrixin or quinocarbazole derivatives in the range of 10^5-10^6 M^{-1} indicative of strong drug-DNA interaction which is comparable to the intercalating drug, ethidium bromide (**Table 5**). Among the calothrixins, the magnitude of DNA binding was greater for both the calothrixin A (**1**) and 3-fluorocalothrixin B **15h** with K_b values of 4.77×10^6 M^{-1} and 5.74×10^6 M^{-1}, respectively.

While with quinocarbazoles, the substituted derivatives **21b** and **25a** showed greater binding strength to CT-DNA and the binding constants were 9.66×10^6 M^{-1} and 9.68×10^6 M^{-1}, respectively, whereas the quinocarbazole **21a** has comparatively lower K_b value of 1.01×10^5 M^{-1}. With the introduction of amino group to 4-fluoroquinocarbazole as in **35c** exhibit better binding strength ($K_b = 6.11 \times 10^6$ M^{-1}) than its parent amino quinocarbazole **35a** signifying additional bonding sites provided by the fluoro functionality to bind with DNA. However, derivatisation of amino functionality of **35a** to *N, N*-(dimethylamino)propyl group **44** resulted in higher DNA binding strength ($K_b = 3.70 \times 10^5$ M^{-1}) (**SI:Fig. 3**).

Sl.No.	Compound	Binding constants (K_b in L mol^{-1})
1	**1**	4.77 (± 0.04) x 10^6
2	**2**	No interaction
3	**15h**	5.74 (± 0.12) x 10^6
4	**21a**	1.01 (± 0.07) x 10^5
5	**21b**	1.36 (± 0.13) x 10^5 9.66 (± 0.11) x 10^6
6	**25a**	9.68 (± 0.20) x 10^6
7	**35a**	1.12 (± 0.34) x 10^5
8	**35c**	6.11 (± 0.24) x 10^6
9	**44**	3.70 (± 0.32) x 10^5
10	Ethidium bromide	6.8 (± 0.22) x 10^7

Table 5. Binding constants (K_b in L mol^{-1}) for the interaction of calothrixins or quinocarbazoles with CT-DNA at 298 K

Results from CT-DNA titration studies reveal strong intercalative binding to DNA by quinocarbazoles which is contributed primarily by the quinoline nitrogen atom and the introduction of *p*-quinone unit as is the case with calothrixin B **2/15h** support weak non-

intercalative binding to DNA. The exception being calothrixin A (**1**), which can interact with DNA by both intercalation and electrostatic groove binding possibly due to the *N*-oxide unit.

Effects of calothrixins or quinocarbazoles on change in DNA morphology during drug-DNA interaction was followed using circular dichroism (CD) spectroscopy (**Fig. 15**). The CD spectra of CT-DNA in absence of drug exhibits a positive CD band at 275 nm for the nucleobase stacking and a negative band at 246 nm for the B conformation. After the addition of calothrixins or quinocarbazoles to CT-DNA, there were changes in either or both positive and negative CD bands, suggesting perturbation in the DNA conformation. In the case of calothrixins B (**2**) and 3-fluorocalothrixin B **15h**, there is decrease in both the positive and negative CD bands which indicate that calothrixins interact with CT-DNA by a groove binding or electrostatic interaction. The decrease of negative CD band following DNA interaction is more pronounced with the 3-fluoro analogue of calothrixin B **15h** in comparison to calothrixin B (**2**). The planar aromatic quinocarbazoles **21a** and **21b** were optically inactive but following interaction with CT-DNA, it exhibits positive induced band which can be attributed to intercalation within DNA base pairs.[41] Optically asymmetric environment of DNA give rise to induced CD bands in the absorption region of quinocarbazole whose intensity increase in a concentration dependent manner. The induced CD of **21b** is less intense in comparison to **21a** suggesting weaker intercalation of the former compound. However, there is a decrease in positive and negative CD band indicating that the intercalation of quinocarbazoles into CT-DNA due to relaxation of DNA winding angle and the base pairs separated resulting in change in DNA conformation from the B-form to A-form. Results from CD studies with CT-DNA support the findings from UV-Vis spectral studies that the interaction mechanism of calothrixin

B (**2**) and its analogue **15h** with DNA is by means of groove binding or electrostatic interaction whereas quinocarbazoles **21a** and **21b** intercalate into the DNA base pairs.

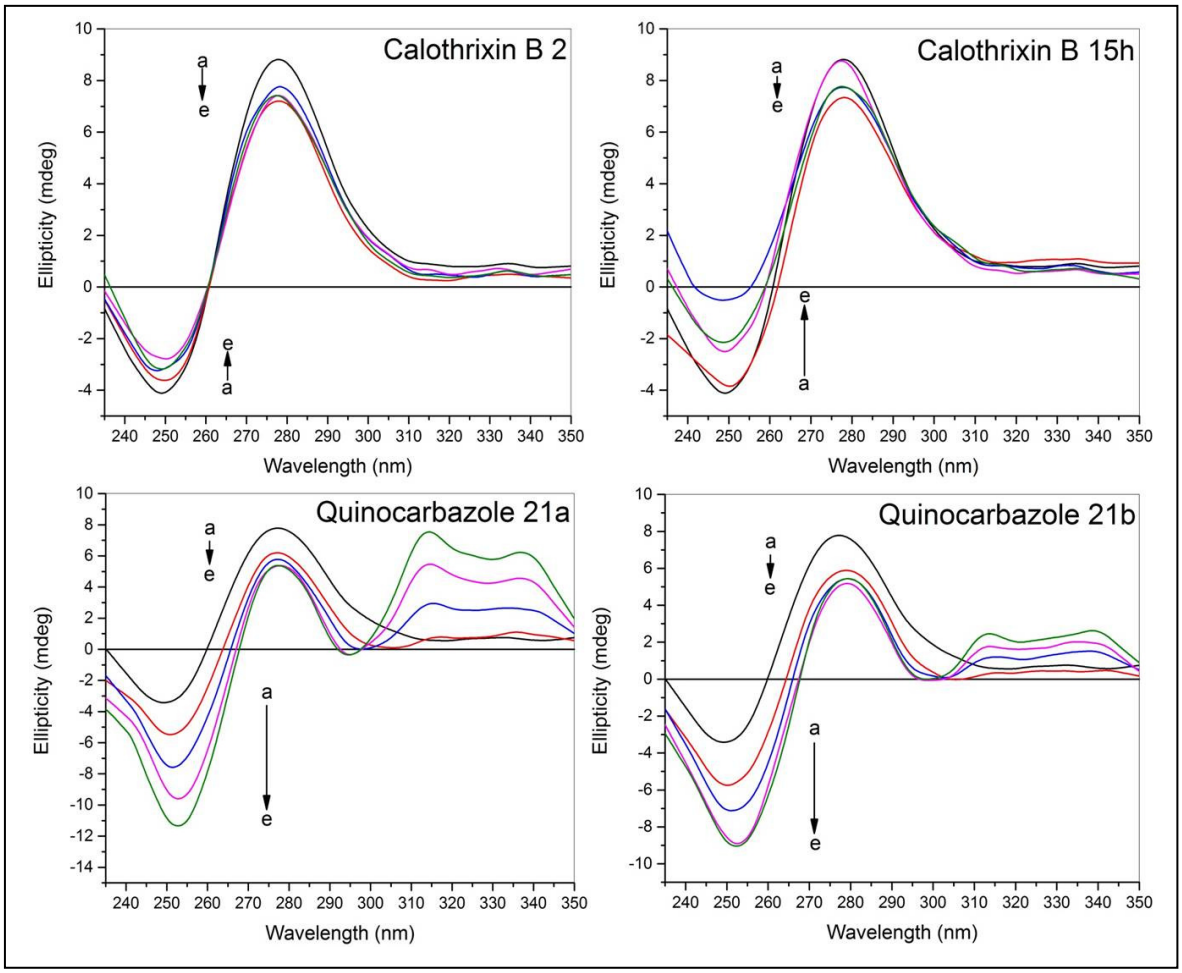

Fig. 15. Circular dichroism spectra of CT-DNA (1 $\times 10^{-4}$mol L^{-1}) in the presence of increasing amounts of calothrixin or quinocarbazoles. $C_{compounds}$ ($\times 10^{-6}$mol L^{-1}); a→e: 0; 6.6; 13.5; 20; 26.6. The arrow shows the intensity changes in increasing compound concentration.

The ability of quinocarbazoles to intercalate within DNA was determined by a topoisomerase I-catalysed unwinding assay, which is based on the ability of intercalating compounds to unwind the DNA duplex and thereby change the DNA twist.[42] The hTopI relaxed plasmid DNA substrate was purified as described in the materials and methods section and used as a substrate for the unwinding assay. In the presence of a strong intercalative agent, such as

ethidium bromide, supercoiling of the relaxed substrate DNA was induced at a concentration of 10 μM (**Fig. 16**, lane 3). On the contrary, no DNA unwinding was observed with the non-intercalative drug etoposide even at 200 μM concentration (**Fig. 16**, lane 4). The quinocarbazole **21b**, induced a concentration dependent net negative supercoiling (**Fig. 16**, lanes 5-8) similar to that of the intercalating drug ethidium bromide (**Fig. 16**, lane 3). A similar concentration dependent effect on the topological state of DNA was seen with the quinocarbazoles **21a** and **25a** (**SI: Fig. 4**). Thus, the above findings from DNA unwinding assays strongly indicate that the quinocarbazoles intercalates into DNA which was also supported by spectroscopic studies.

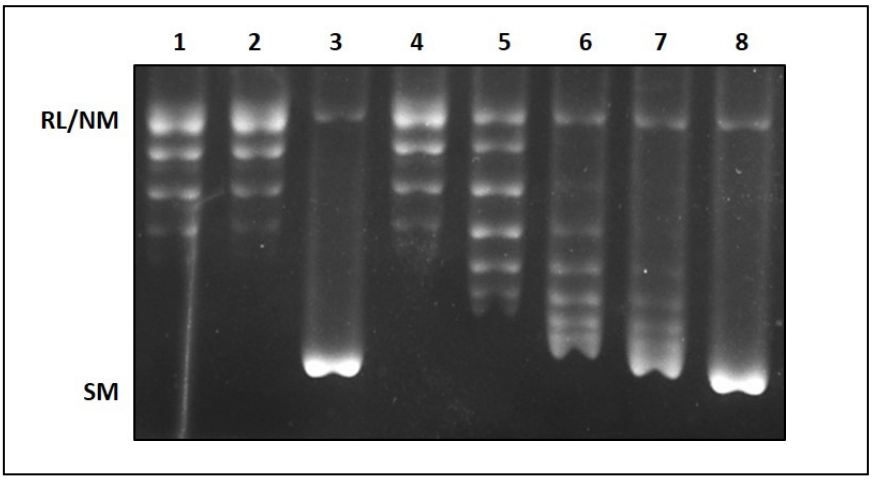

Fig. 16. Analysis of binding mode of quinocarbazole**21b** with DNA by agarose-gel electrophoresis. Lane1, relaxed pBluescript (SK+) plasmid DNA generated by treatment of plasmid DNA with excess hTopI, followed by phenol/chloroform extraction and ethanol precipitation; lane 2, relaxed plasmid DNA with hTopI; lane 3 and 4, same as lane 2 but in presence of 10 μM EtBr or 200 μM Etoposide, respectively; lane 5-8, same as lane 2, but in presence of increasing concentration (60, 70, 80, 90 and 100 μM) of quinocarbazole **21b**. NM, nicked monomer; RL, relaxed monomer; SM, supercoiled monomer.

Lowest conformational energy and DNA binding affinities of calothrixin/quinocarbazole analogues

Molecular docking has become the promising computational technique to understand the mode of interaction of ligand with the macromolecules. This technique has also become a blend

with the experimental techniques and helps in reducing time and labour efforts. Molecular docking interactions are elucidated in the terms of binding energy. Lower the binding energy signifies higher the binding affinity and *vice versa*.[43]

In our study, the DNA binding mode of calothrixin A, B and its analogues, quinocarbazoles were evaluated by docking studies with the 3D structure of 1DSC DNA. The binding conformation for each calothrixins/quinocarbazoles into the 1DSC DNA is determined and the one having lowest binding energy among the different conformations were generated. Among the AutoDock proposed confirmations for calothrixin analogues, **2** and **15h** were found to have lower binding energy values whereas the quinocarbazoles **21a**, **21b** too have low binding energy values. Among the calothrixins, **2** has highest binding affinity with 1DSC (binding energy value = -7.2 kcal/mol), where as binding energy values for 3-chlorocalothrixin B **15g** and 3-fluorocalothrixin B **15h** were -6.5 kcal/mol and -5.6 kcal/mol, respectively. In case of quinocarbazoles, the compounds **21a** and **21b** have binding energy values lower than -6.5 kcal/mol and -6.8 kcal/mol, respectively. From the docking results, highest binding affinity was observed in compound **2** with a least binding energy of -7.2 kcal/mol in comparison to other compounds. Although there is little correlation between predicted DNA binding energy values and the experimental cytotoxicity profile, all the calothrixin/quinocarbazoles analogues have negative binding energies (**SI: Fig. 5, Table 5**) indicating that these compounds can bind with DNA molecule.

Molecular docking studies of calothrixins with Topoisomerase I and II

Calothrixins (**1**, **2** and **15h**) and quinocarbazole derivatives (**21a**, **21b**, **25a**, and **25b**) were docked with topoisomerase I and II retrieved from protein data bank (PDB ID: 1T8I; PDB ID: 4LPB). Free energy of binding (ΔG) analysis for these derivatives docked to topo I indicated

that calothrixins (**1**, **2** and **15h**) docked with the lowest ΔG value (**SI: Fig. 6, Table 6**). Among calothrixins and quinocarbazoles, the binding affinity of 3-fluorocalothrixin B **15h** was found to be higher (-53.38 kcal/mol) and comparable to that of the known topo I inhibitor camptothecin (-50.04 kcal/mol). The binding affinity of rest of the compounds were found to be relatively lower (-39.28 to -46.82 kcal/mol) than camptothecin. Binding of calothrixins to topo I suggested that the quinone unit is essential in making hydrogen bond (H-bond length 2.81 Å) with Arg364 residue at the catalytic site as observed in the case of camptothecin. Interestingly, mutation of the Arg364 to His resulted in topo I resistant to camptothecin.[44] Thus, it might be possible that the weak inhibition of topo I by calothrixins A (**1**) and B (**2**) seen in an *in vitro* enzyme assay could be attributed to this key interaction. In case of quinocarbazoles, which lack the quinone unit failed to interact with the Arg364 might indicate its inability to inhibit topo I.

Docking studies with ATPase binding domain of type II topoisomerase showed that quinocarbazoles **21a**, **21b**, 3-fluorocalothrixin **15h** and calothrixin A (**1**) interacted favorably with target protein-topoisomerase (**SI: Fig. 7, Table 7**). Results of induced fit docking of these compounds showed binding affinity of quinocarbazoles and topo II inhibition seen in *in vitro* assays were comparable.

Drug-likeness of calothrixin and quinocarbazole analogues

Through a combination of *in silico* and experimental techniques,[45] the physico-chemical properties of some of the promising calothrixin or quinocarbazole analogues were evaluated. The partition coefficient (P) is defined as the concentration of a compound in octanol over the concentration of the same in water. The calothrixin A (**1**) was found to be more lipophilic at the physiologic pH of 7.4 than calothrixin B (**2**) possibly due to the *N*-oxide unit. Partition coefficient value of the calothrixin B (**2**) was considerably low in comparison to its fluoro

substituted analogue **15h** which has a $logD_{(pH7.4)}$ value of -1.96 (Table 6). However, a significant increase in lipophilicity (>1000 fold) was observed for fluoro-substituted quinocarbazole **21b** compared to the parent quinocarbazole **21a**. The physico-chemical parameters as shown in Table 6 were found to lie within acceptable range for "drug-like" compounds.

Compound	Lipinski's rule of five (highest permitted value) Calculated				Experimental	
	Molecular Weight[a] (500)	HBD[b] (5)	HBA[c] (10)	ClogP[d] (5)	logP[e]	logD[f] at pH7.4
1	314.3	1	5	2.352	1.32	1.02
2	298.3	1	5	2.418	-1.81	-2.11
15h	316.3	1	5	2.651	-1.66	-1.96
21a	268.3	1	1	4.485	-1.25	-1.55
21b	286.3	1	1	4.754	1.91	1.61

Table 6. Evaluation of drug-likeness of selected calothrixin and quinocarbazole analogues with respect to the Lipinski's Rule of Five and experimentally determined logP and logD in an octanol/water system.

[a] Molecular weights were calculated for nonionized calothrixin or quinocarbazole analogues. [b] Calculated number of hydrogen bond donor (HBD) groups. [c] Calculated number of hydrogen bond acceptor (HBA) groups. [d] Calculated octanol-water partition coefficient ClogP of the neutral species of the compounds. [e] Experimentally determined logP values in an octanol/water system. [f] Experimentally determined logD values in an octanol/buffer system at physiological pH of 7.4. All predictions were calculated using the Schrodinger QikProp application included in the Schrodinger's Maestrosoftware v9.1.

Toxicological evaluation of 3-fluorocalothrixin B 15h

In general, the widely reported cytotoxic quinones being oxidant and electrophilic manifest toxicological profile due to oxidative stress leading to the destruction of unsaturated lipids, DNA, proteins, and other essential cellular molecules. However, the nature of substituents greatly determines the toxicology of quinone in particular, the presence of an electronegative substituent (eg. halogen) confer stronger oxidant properties on the quinone and the corresponding hydroquinone is less readily oxidized, thus preventing its subsequent re-oxidation resulting in a safer pharmacological profile.[46] Accordingly, the potential toxicity of

15h which bears a fluorine substituent on the E-ring of quinoid calothrixin B was evaluated in an acute oral mice toxicity studies. In addition, the low growth inhibitory concentration of **15h** together with lethal concentration (LC_{50}) greater than 4 μM (**SI: Table 2-4**) indicate a wider therapeutic index, thus motivating investigation of *in vivo* toxicological profile of 3-fluorocalothrixin **15h** in SCID mice at 4 log higher dose (i.e. 50mg/kg) of LC_{50}. Pathological evaluation was done on compound **15h** treated SCID mice for the signs of acute toxicity. Thirty six 6-week-old female SCID mice were randomized into four groups (n = 6) to receive 0 (vehicle only), 10, 30 and 50 mg/kg of **15h** per orally every day for a period of seven days.

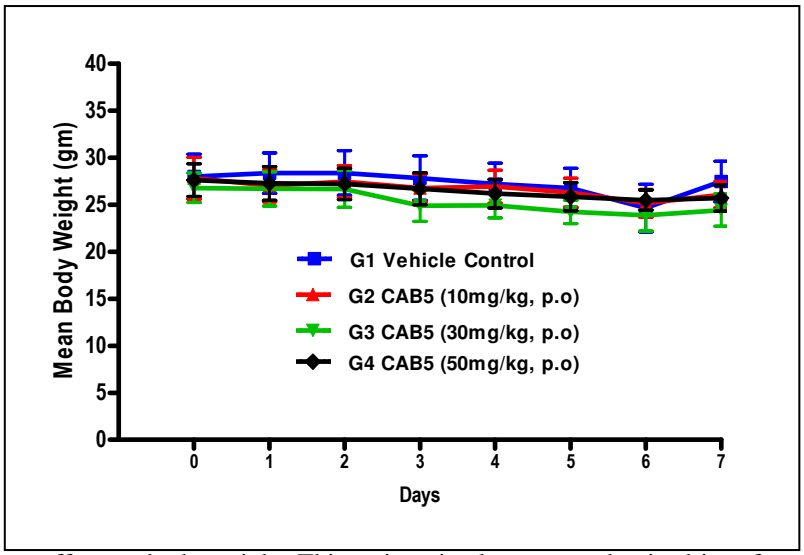

Fig. 17. No significant effect on body weight. Thirty six animals were randomized into four groups. The treated animals were administered compound **15h** at doses of 10, 30, and 50 mg/kg. The animals were dosed po daily for 7 days and were weighed daily for 1 week.

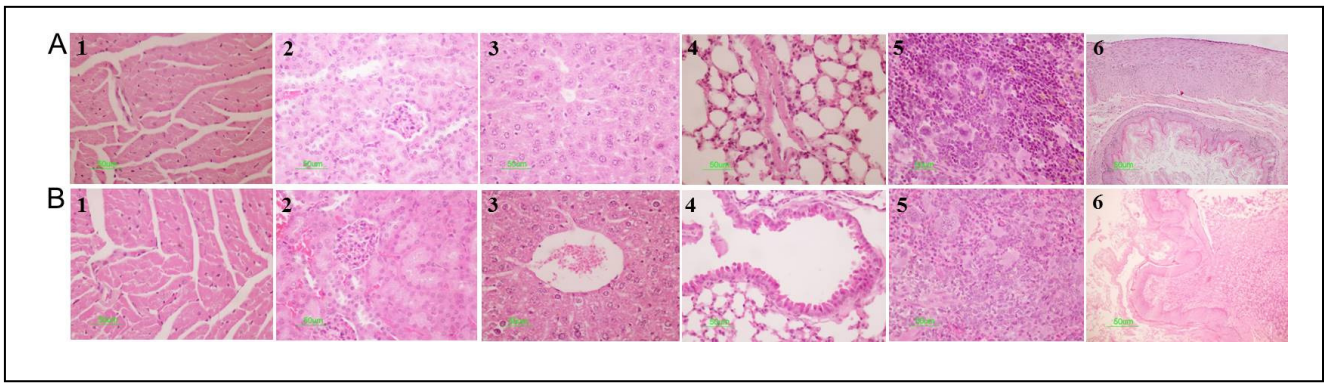

Fig. 18. Histopathological examination of major organs for signs of toxicity. Formalin-fixed heart (1) kidney (2) liver (3) lung (4) spleen (5) and stomach (6) from animals with oral administration of vehicle (**A**) or with 50 mg/kg **15h** (**B**), were embedded in paraffin. Tissue sections were stained with hematoxyline and eosin (H&E). Stained sections were evaluated histopathologically for signs of inflammatory cell infiltration or tissue degeneration. No signs of toxicity in major organs following treatment with 50mg/kg.

Throughout the study period, no deaths or significant clinical findings were noted in control as well as in **15h** treated animal groups. Despite wine red coloration of the drug substance in the dosing formulation the fecal matter from the entire drug treated animals were of normal shape and color. All animals in the treated group showed no changes in water/ food consumption or significant loss of body weight (**Fig. 17**) and were as healthy as the non-treated control animals. Compared to the control group, there were no treatment-related changes on any of the hematological (**SI: Table 8**) or clinical biochemistry parameters (data not shown). Gross necropsy performed at the end of the study period revealed no significant macroscopic changes between control and **15h** treated groups. No other significant differences in absolute or relative organ weights between the control and the treated groups were observed (**SI: Table 9**). The histopathological findings in the tissues sections from the heart, liver, lung, stomach, kidney and spleen from control and treated animals were not considered to be of toxicological significance. Thus it can be concluded from these studies that **15h** treated animals showed no adverse effects on the key organs (**Fig. 18**) and the animals tolerated without any apparent toxicity with 50 mg/kg of **15h**. Highest dose of 50mg/kg was chosen for the acute toxicity study because of the extreme *in vitro* potency of **15h**, hence a likely effective dose would be 5 mg/kg (1/10 MTD) and an intermediate dose of 10mg/kg.

Conclusions

Using $FeCl_3$-mediated domino reaction of enamines as a key strategy, synthesis of sixteen calothrixin B analogues containing different substituents on "E" ring was carried out. The synthesis of quinocarbazoles lacking quinone unit were also achieved. The cytotoxicities of calothrixins **1**, **2**, **15b-p** and quinocarbazole analogues (**21a-c**, **25a**, **25b**, **35a-c**, **44**) were evaluated against nine cancer cell lines. Among the analogues of calothrixin B **15b-p**, the 3-fluoro derivative **15h** was found to be more potent than the parent calothrixin B (**2**). The quinocarbazole analogues lacking quinone unit displayed cytotoxicity comparable to that of calothrixin B and its analogues. Notably, 4-fluoroquinocarbazole **21b** was as potent as that of 3-fluorocalothrixin B **15h** and far more potent than calothrixin B (**2**) in majority of the cell lines. Further, the observed cytotoxicity of 1 nM and 5 nM for 4-fluoroquinocarbazole **21b** in NCI-H460 cells and HEK293 cells, respectively indicate that these cell lines from different tissue of origin might share common molecular mechanism of action. On the other hand, the relative resistance of the lung adenocarcinoma cancer cell line A549 indicates that the observed potency of **21b** is not a general property to lung cancer cell lines. From the cytotoxicity data presented, it appears that the quinone unit in calothrixin does not contribute to the anti-cancer property.

Data from cell cycle analysis, *in vitro* DNA cleavage experiments together with alkaline COMET assay clearly indicate that calothrixin A (**1**) and the 3-fluorocalothrixin B **15h** have comparable effects in causing cellular DNA damage and arresting the cells in G1-S phase which is maintained even in the presence of nocodazole. Unlike in Jurkat or CEM leukemia cells, which after treatment with calothrixin A (**1**) resulted in accumulation of cells in S and G2/M cell cycle phases,[28] HCT116 and HeLa cells in our study showed arrest of cells in G1-S phase boundary following treatment with 5 μM (for HCT116 cells) or 1 μM (for Hela cells) of

calothrixin A (**1**) and 3-fluoro calothrixin B **15h**. From our study, calothrixin A (**1**) caused DNA cleavage in cells which resulted in cell cycle arrest in G1-S phase, such an effect was not seen in calothrixin B (**2**) treated cells. On the other hand, the 4-fluoroquinocarbazole **21b** showed little cleavage of plasmid DNA, caused arrest of cells in G2-M phase in HCT116 cells. Data from cytotoxicity studies and cell cycle analysis in cells differing in p53 gene activity indicates that calothrixins act much downstream of this tumour suppressor and the cytotoxicity or the G1-S phase arrest induced by calothrixins is not mediated by p53 functionality.

Given the ability to interact with DNA, calothrixin A (**1**) and the quinocarbazoles **21a**, **25a** were found to interfere with the catalytic activity of human topoisomerases II in a cell free assay. While calothrixin A (**1**) showed moderate hTopII inhibition whereas, the quinocarbazoles **21a** and **25a** with IC_{50} value of ~20 μM closely resembling with their observed GI_{50} values (5-15 μM) indicating that the cytotoxicities of these analogues might be mediated through topo II inhibition. However, it is surprising to note the inability of 4-fluoroquinocarbazole analogue **21b** to inhibit topo II activity even though it showed potent cytotoxicity profile and unique cell cycle effects whereas its parent analogue **21a** inhibits topo II but with moderate cytotoxicity. It is therefore assumed that the DNA damage by **21b** as evident from COMET assay might be accountable for the observed cytotoxicity and cell cycle effects in cancer cells.

The UV-Vis spectral properties of representative calothrixin and quinocarbazole analogues in presence of CT-DNA indicated that the presence of quinone unit in calothrixins eliminates intercalative mode of interaction with DNA, an effect which is seen with quinocarbazoles. The exception being calothrixin A (**1**), which not only intercalates but also has electrostatic interaction with CT-DNA. Owing to the shape and planar nature, it might be expected that the

quinocarbazoles intercalates by stacking interactions with DNA base pairs and as a result there might be unwinding and lengthening of DNA as evident from decrease in negative CD band. Further, the quinoline nitrogen atom is very essential for DNA intercalation as the napthocarbazole **31** failed to perturb changes in the UV-Vis spectra following addition of CT-DNA.

Considering all our results it seems that the quinone unit of calothrixins might be less important in comparison to the quinoline nitrogen atom with respect to their interaction with the biological target. This work on the synthesis of calothrixin B (**2**) analogues and its deoxygenated derivatives besides detailing the structural features of calothrixins on mechanistic aspects of cellular cytotoxicity, identified two of the novel fluoro analogues namely, 3-flurocalothrixin B **15h** and 4-fluoroquinocarbazole **21b** as having potent cytotoxicity and unique cell cycle effects. The 4-fluoroquinocarbazole **21b** is active on the lung carcinoma cell line NCI-H460 with a GI_{50} of 1 nM with no clonal growth at this concentration. The profound cytotoxic effect of compound **21b** on certain cell lines taken in the study might be attributed to the formation of covalent DNA adducts following metabolic activation as suggested for ellipticine.[36] The prominent *in vitro* anticancer profile with no adverse effects in animal experiments together with acceptable physico-chemical properties indicate that compound **15h** might be a promising candidate for further preclinical development. Topo II inhibition by compounds (calothrixin A (**1**), quinocarbazole **21a** and **25a**) might lead to the development of novel topo inhibitors for cancer therapy. Further, the 4-fluoroquinocarbazole **21b** with unique *in vitro* cytotoxicity has a potential that is worth pursuing.

Experimental section

All melting points were uncorrected. Dry THF was prepared by refluxing with sodium. Dry DCM/DCE was prepared by refluxing with P_2O_5. The progression of reaction was monitored by TLC using mixture of hexane/ethyl acetate as an eluent. Column chromatography was carried out on silica gel (230-400 mesh, Merck) by using increasing polarity. ^{1}H, ^{13}C and DEPT 135 spectra were recorded in $CDCl_3$ using TMS as an internal standard on a 300 MHz spectrometer at room temperature and Bruker 500 MHz at elevated temperature. Chemical shift values were quoted in parts per million (ppm) and coupling constants (*J*) were quoted in hertz (Hz). IR spectra were recorded on ABB MB3000 series FTIR spectrometers. High-resolution mass spectra (HRMS) were recorded using Micro Qtof mass spectrometer (ESI), Waters-Q-Tof premier-HAB 213 (ESI), JEOL GC Mate II (EI) and Varian FTMS (ESI). Purity of all final compounds were determined by analytical HPLC using the following conditions: Agilent Technologies with a Zorbax Rx-C18 column (250 mm x 4.6 mm, 5.0 µm) eluted at 1 mL/min with ammonium formate, acetonitrile and methanol as diluent. Column types and elution methods are described in the Supporting Information section. The purity of all the biologically evaluated compounds was determined to be ≥95% purity. Solvents used for HPLC analysis and sample preparation were HPLC grade. The required phosphonium ylide **8** was prepared from the published procedure.[33] Experimental procedure and analytical data of **13a-p**, **17a-c**, **31**, **32**, **33a-c**, **37**, **38**, **39** (see SI for details).

Calothrixin A 1

To a suspension of calothrixin B **2** (50 mg, 0.16 mmol) in dry DCM (80 mL), *m*-CPBA (250 mg, excess amount) was added. The reaction mixture was heated at reflux for 18 h (completion of the reaction detected by TLC, EtOAc/hexanes 2:1). Removal of solvent followed by washing

with 5 mL of methanol and 2 mL of DCM afforded calothrixin A **1** as a red solid. Yield: 40 mg (75%); mp: ≥280 °C (dec); IR (film): 3441, 1659 cm^{-1}; ^{1}H NMR (300 MHz, DMSO-d_6): δ 13.19 (s, 1 H, NH), 9.65 (d, J = 8.7 Hz, 1 H, ArH), 8.85 (s, 1 H, ArH), 8.60-8.56 (m, 1 H, ArH), 8.09 (d, J = 7.8 Hz, 1 H, ArH), 7.98-7.95 (m, 2 H, ArH), 7.58 (d, J = 7.8 Hz, 1 H, ArH), 7.43 (t, J = 7.4 Hz, 1 H, ArH), 7.35 (t, J = 7.4 Hz, 1 H, ArH); ^{13}C NMR (75 MHz, DMSO-d_6): δ 178.7, 178.2, 143.6 139.1, 138.6 132.4, 132.3, 132.2, 130.3, 128.6, 127.5, 127.3, 124.9, 123.9, 122.5, 122.3 119.6, 115.6, 114.5; DEPT 90: δ 131.9, 131.8, 131.7, 128.1, 127.0, 124.4, 122.0, 119.1, 114 ppm; HRMS (ESI-MS): m/z calcd for $C_{19}H_{11}N_2O_3$ $[M+H]^+$: 315.0770; found 315.0765. HPLC purity: 97.3%.

Calothrixin B (7*H*-indolo[3,2-*j*]phenanthridine-7,13(12*H*)-dione) 2

To a solution of enamine **14a** (500 mg, 1 mmol) in dry DMF (20 mL), anhydrous $FeCl_3$ (490 mg, 3 mmol) was added and refluxed for 3 h under N_2. It was then poured over crushed ice (50 g) containing Conc. HCl (1 mL). The crude product was filtered and dried. The resulting reddish brown solid was washed successively with 10 mL of chloroform and 4 mL of DCM. The solid obtained was crystallised from THF to afford calothrixin B **2** (198 mg, 65%) as a red solid. mp: ≥ 300 °C; IR (film): 3441, 1659 cm^{-1}; ^{1}H NMR (300 MHz, DMSO-d_6): δ 13.06 (s, 1 H; NH), 9.51 (s, 1 H, ArH), 9.49 (d, J = 8.4 Hz, 1 H, ArH), 8.08 (d, J = 8.1 Hz, 2 H, ArH), 7.88 (t, J = 7.5 Hz, 1 H, ArH), 7.81 (t, J = 7.5 Hz, 1 H, ArH), 7.54 (d, J = 8.4 Hz, 1 H, ArH), 7.39 (t, J = 7.5 Hz, 1 H, ArH), 7.31 (t, J = 7.5 Hz, 1 H, ArH); ^{13}C NMR (75 MHz, DMSO-d_6): δ 181.2, 180.7, 151.7, 147.9, 138.9, 138.4, 133.0, 132.0, 130.7, 130.3, 127.6 (2C), 125.2, 124.8, 123.8, 123.0, 122.8, 116.0, 114.4. DEPT 90: δ 147.4, 131.5, 130.1, 129.7, 127.1, 127.0, 124.2, 122.2, 113.8 ppm; HRMS (ESI-MS): m/z calcd for $C_{19}H_{11}N_2O_2$ $[M+H]^+$: 299.0821; found: 299.0830. HPLC purity: 96.6%.

General procedure for the preparation of enamines 14a-p

A mixture of 3-acetyl-2-nitroarylvinylenes **13a-p** (1 eq) and glycocyamine (50 mol%) in excess of DMF-DMA (8 eq) was heated at 100 ^{o}C for 3-4 h under N_2. After consumption of the starting material (monitored by TLC), the reaction mass was poured over crushed ice (50 mL) containing Conc. HCl (1 mL). The precipitated solid was filtered, washed with water and air dried to obtain crude compound which was purified by trituration with cold methanol (10 mL) to afford enamines as yellow/orange solid.

(*E*)-3-(Dimethylamino)-1-(2-(2-nitrostyryl)-1-(phenylsulfonyl)-1*H*-indol-3-yl)prop-2-en-1-one 14a

The reaction of methyl ketone **13a** (3 g, 6.72 mmol) with DMF-DMA (7.1 mL, 53.76 mmol) in the presence of glycocyamine (0.39 g, 3.36 mmol) at 100 ^{o}C for 3 h followed by workup using the above-mentioned procedure gave enamine **14a** (3.0 g, 89%) as a yellow solid. mp: 198-200 °C; ^{1}H NMR (300 MHz, $CDCl_3$): δ 8.23 (d, J = 8.1 Hz, 1 H, ArH), 7.99 (d, J = 8.1 Hz, 1 H, ArH), 7.81-7.79 (m, 3 H, ArH), 7.69-7.61 (m, 3 H, ArH), 7.49 (d, J = 7.8 Hz, 2 H, ArH), 7.42-7.36 (m, 5 H, ArH), 7.29-7.24 (m, 1 H, ArH), 5.29 (d, J = 12.6 Hz, 1 H, vinylic -CH), 3.03 (s, 3 H, -NCH_3), 2.75 (s, 3H, -NCH_3); ^{13}C NMR (75 MHz, $CDCl_3$): δ 186.9, 148.0, 137.7, 136.3, 135.4, 134.1, 133.5, 132.6, 132.4, 129.5, 129.3, 129.1, 128.9, 126.9, 125.8, 124.7, 124.6, 122.8, 121.7, 114.9, 45.1, 37.2 ppm; HRMS (EI): m/z calcd for $C_{27}H_{23}N_3O_5S$ [M^+]: 501.1358; found: 501.1356.

(*E*)-3-(Dimethylamino)-1-(2-(3-methoxy-2-nitrostyryl)-1-(phenylsulfonyl)-1*H*-indol-3-yl)prop-2-en-1-one 14 b

The reaction of methyl ketone **13b** (2 g, 4.20 mmol) with DMF-DMA (4.50 mL, 33.61 mmol) in the presence of glycocyamine (0.25 g, 2.10 mmol) at 100 ^{o}C for 4 h followed by workup

using the above-mentioned procedure gave enamine **14b** (1.89 g, 85%) as a yellow solid. mp: 192-196 °C; ^{1}H NMR (300 MHz, $CDCl_3$): δ 8.22 (d, J = 8.4 Hz, 1 H, ArH), 7.76-7.70 (m, 4 H, ArH), 7.52-7.46 (m, 3 H, ArH), 7.43-7.32 (m, 4 H, ArH), 7.28-7.23 (m, 1 H, ArH), 7.00 (d, J = 8.1 Hz, 1 H, ArH), 6.84 (d, J = 16.2 Hz, 1 H, vinylic CH), 5.25 (d, J = 12.6 Hz, 1 H, vinylic CH), 3.91 (s, 3 H, -OMe), 3.05 (s, 3 H, -NCH_3), 2.77 (s, 3 H, -NCH_3); ^{13}C NMR (75 MHz, $CDCl_3$): δ 186.7, 150.9, 140.4, 137.8, 136.4, 134.7, 134.1, 131.1, 130.5, 129.5, 129.3, 129.1, 126.8, 125.9, 124.6, 123.4, 121.4, 118.5, 114.9, 112.0, 56.5, 45.1, 37.2 ppm.

(*E*)-3-(Dimethylamino)-1-(2-(5-methoxy-2-nitrostyryl)-1-(phenylsulfonyl)-1*H*-indol-3-yl)prop-2-en-1-one 14c

The reaction of methyl ketone **13c** (2 g, 4.20 mmol) with DMF-DMA (4.50 mL, 33.61 mmol) in the presence of glycocyamine (0.25 g, 2.10 mmol) at 100 ^{o}C for 4 h followed by workup using the above-mentioned procedure gave enamine **14c** (2.0 g, 90%) as an orange solid. mp: 188-192 °C; ^{1}H NMR (300 MHz, $CDCl_3$): δ 8.22 (d, J = 8.4 Hz, 1 H, ArH), 8.11 (d, J = 9.0 Hz, 1 H, ArH), 7.82-7.80 (m, 2 H, ArH), 7.69 (s, 1 H, ArH), 7.60-7.49 (m, 3 H, ArH), 7.42-7.28 (m, 4 H, ArH), 7.25 (d, J = 8.4 Hz, 1 H, ArH), 7.20 (d, J = 15.0 Hz, 1 H, vinylic -CH), 6.93 (d, J = 8.4 Hz, 1 H, ArH), 5.31 (d, J = 12.6 Hz, 1 H, vinylic -CH), 3.06 (s, 3 H, -NCH_3), 2.80 (s, 3 H, -NCH_3); ^{13}C NMR (75 MHz, $CDCl_3$): δ 163.5, 140.9, 137.7, 136.3, 135.8, 135.5, 134.1, 133.7, 129.5, 129.3, 127.6, 126.9, 125.8, 124.6, 122.7, 121.3, 114.9, 114.1, 113.8, 56.1, 45.1, 37.2 ppm; HRMS (EI): m/z calcd for $C_{28}H_{25}N_3O_6S$ [M^+]: 531.1464; found: 531.1460.

(*E*)-1-(2-(4,5-Dimethoxy-2-nitrostyryl)-1-(phenylsulfonyl)-1*H*-indol-3-yl)-3-(dimethylamino)prop-2- en-1-one 14d

The reaction of methyl ketone **13d** (3 g, 5.93 mmol) with DMF-DMA (6.3 mL, 47.42 mmoml) in the presence of glycocyamine (0.35 g, 2.97 mmol) at 100 ^{o}C for 3 h followed by workup

using the above-mentioned procedure gave enamine **14d** (3.24 g) as a yellow solid. The crude product was used as such for next step without any further characterization.

(*E*)-3-(Dimethylamino)-1-(2-((*E*)-2-(6-nitrobenzo[d][1,3]dioxol-5-yl)vinyl)-1-(phenylsulfonyl)-1*H*-indol-3-yl)prop-2-en-1-one 14e

The reaction of methyl ketone **13e** (3 g, 6.12 mmol) with DMF-DMA (6.5 mL, 4.90 mmol) in the presence of glycocyamine (0.36 g, 3.06 mmol) at 100 ^{o}C for 3 h followed by workup using the above-mentioned procedure gave enamine **14e** (2.84 g, 85%) as a yellow solid. mp: 172-174 °C; ^{1}H NMR (300 MHz, $CDCl_3$): δ 8.22 (d, J = 8.4 Hz, 1 H, ArH), 7.79 (d, J = 7.8 Hz, 2 H, ArH), 7.68-7.67 (m, 1 H, ArH), 7.54-7.51 (m, 2 H, ArH), 7.48-7.47 (m, 1 H, ArH), 7.42-7.33 (m, 4 H, ArH), 7.28-7.14 (m, 2 H, ArH), 7.15 (s, 1 H, ArH), 6.16 (s, 2 H, ArH), 5.29 (d, J = 12.9 Hz, 1 H, vinylic CH), 3.04 (s, 3 H, -NCH_3), 2.77 (s, 3 H, -NCH_3) ppm; HRMS (EI): m/z calcd for $C_{28}H_{23}N_3O_7S$ [M^+]: 545.1257; found: 545.1260.

(*E*)-1-(2-(4-Bromo-2-nitrostyryl)-1-(phenylsulfonyl)-1*H*-indol-3-yl)-3-(dimethylamino)prop-2-en-1-one 14f

The reaction of methyl ketone **13f** (2 g) with DMF-DMA (4.0 mL) in the presence of glycocyamine (0.22 g) at 100 ^{o}C for 4 h followed by workup using the above-mentioned procedure gave enamine **14f** as a yellow solid. The crude product was used as such for next step without any further characterization. Yield: 2.12 g (96%).

(*E*)-1-(2-(4-Chloro-2-nitrostyryl)-1-(phenylsulfonyl)-1*H*-indol-3-yl)-3-(dimethylamino)prop-2-en-1-one 14g

The reaction of methyl ketone **13g** (3 g, 6.24 mmol) with DMF-DMA (6.6 mL, 50 mmol) in the presence of glycocyamine (0.36 g, 3.12 mmol) at 100 ^{o}C for 3 h followed by workup using the above-mentioned procedure gave enamine **14g** (3.08 g, 92%) as an orange solid. mp: 166-168

°C; ^{1}H NMR (300 MHz, $CDCl_3$): δ 8.22 (d, J = 8.4 Hz, 1 H, ArH), 7.99 (s, 1 H, ArH), 7.78-7.75 (m, 3 H, ArH), 7.66-7.61 (m, 3 H, ArH), 7.53-7.49 (m, 2 H, ArH), 7.41-7.34 (m, 4 H, ArH), 7.29-7.24 (m, 1 H, ArH), 5.29 (d, J = 12.6 Hz, 1 H, vinylic -CH), 3.03 (s, 3 H, -NCH_3), 2.75 (s, 3 H, -NCH_3); ^{13}C NMR (75 MHz, $CDCl_3$): δ 186.6, 154.5, 148.0, 137.7, 136.3, 134.9, 134.5, 134.1, 133.5, 131.1, 130.8, 130.1, 129.4, 129.3, 126.8, 125.9, 124.8, 124.6, 123.4, 121.3, 114.9, 98.3, 45.1, 37.2 ppm; HRMS (EI): m/z calcd for $C_{27}H_{22}ClN_3O_5S$ [M^+]: 545.1257; found: 545.1260.

(*E*)-3-(Dimethylamino)-1-(2-(4-Fluoro-2-nitrostyryl)-1-(phenylsulfonyl)-1*H*-indol-3-yl)prop-2-en-1-one 14h

The reaction of methyl ketone **13h** (3 g, 6.47 mmol) with DMF-DMA (6.9 mL, 51.72 mmol) in the presence of glycocyamine (0.38 g, 3.24 mmol) at 100 ^{o}C for 4 h followed by workup using the above-mentioned procedure gave enamine **14h** (3.05 g, 91%) as an orange solid. mp: 156-158 °C; ^{1}H NMR (300 MHz, $CDCl_3$): δ 8.22 (d, J = 8.1 Hz, 1 H, ArH), 7.82-7.72 (m, 4 H, ArH), 7.68-7.66 (m, 1 H, ArH), 7.58 (m, 2 H, ArH), 7.50 (d, J = 7.5 Hz, 1 H, ArH), 7.42-7.36 (m, 5 H, ArH), 7.33-7.29 (m, 1 H, ArH), 5.29 (d, J = 12.6 Hz, 1 H, vinylic -CH), 3.04 (s, 3 H, -NCH_3), 2.77 (s, 3 H, -NCH_3); ^{13}C NMR (75 MHz, $CDCl_3$): δ 186.7, 161.7 (d, J = 247.5 Hz), 148.1 (d, J = 8.25 Hz), 137.7, 136.3, 135.1, 134.1, 132.1 (d, J = 10 Hz), 131.1, 130.8 (d, J = 7.8 Hz), 129.4, 129.3, 128.5 (d, J = 3.8 Hz), 126.8, 125.8, 124.6, 123.0, 121.3, 121.0 (d, J = 21.2 Hz), 120.9, 114.9, 112.3 (d, J = 26.4 Hz), 45.1, 37.2 ppm; HRMS (EI): m/z calcd for $C_{27}H_{22}FN_3O_5S$ [M^+]: 519.1264; found: 519.1250.

(*E*)-1-(2-(5-Bromo-2-nitrostyryl)-1-(phenylsulfonyl)-1*H*-indol-3-yl)-3-(dimethylamino)prop-2-en-1-one 14i

The reaction of methyl ketone **13i** (2 g, 3.82 mmol) with DMF-DMA (4.0 mL, 30.53 mmol) in the presence of glycocyamine (0.22 g, 1.91 mmol) at 100 ^{o}C for 5 h followed by workup using the above-mentioned procedure gave enamine **14i** (2.03 g, 92%); as a orange solid. mp: 198-200 °C; ^{1}H NMR (300 MHz, $CDCl_3$): δ 8.22 (d, J = 8.1 Hz, 1 H, ArH), 7.92-7.79 (m, 4 H, ArH), 7.66-7.51 (m, 4 H, ArH), 7.44-7.30 (m, 6 H, ArH), 5.28 (d, J = 12.6 Hz, 1 H, vinylic -CH), 3.06 (s, 3 H, -NCH_3), 2.79 (s, 3H, -NCH_3); ^{13}C NMR (75 MHz, $CDCl_3$): δ 185.7, 153.8, 145.5, 136.6, 135.3, 133.9, 133.5, 133.2, 131.1, 130.7, 130.2, 128.3, 127.3, 125.9, 125.3, 125.0, 123.6, 122.8, 120.3, 113.9, 97.2, 44.1, 36.2 ppm; HRMS (EI): m/z calcd for $C_{27}H_{22}BrN_3O_5S$ [M^+]: 579.0464; found: 574.0460.

(*E*)-1-(2-(5-Chloro-2-nitrostyryl)-1-(phenylsulfonyl)-1*H*-indol-3-yl)-3-(dimethylamino)prop-2-en-1-one 14j

The reaction of methyl ketone **13j** (2 g) with DMF-DMA (4.0 mL) in the presence of glycocyamine (0.22 g) at 100 ^{o}C for 3 h followed by workup using the above-mentioned procedure gave enamine **14j** as a yellow solid. The crude product was used as such for next step without any further characterization. Yield: 2.12 g (96%).

(*E*)-1-(2-(2-Chloro-6-nitrostyryl)-1-(phenylsulfonyl)-1*H*-indol-3-yl)-3-(dimethylamino)prop-2-en-1-one 14k

The reaction of methyl ketone **13k** (2 g, 4.17 mmol) with DMF-DMA (4.4 mL, 33.33 mmoml) in the presence of glycocyamine (0.24 g, 2.08 mmol) at 100 ^{o}C for 4 h followed by workup using the above-mentioned procedure gave enamine **14k** (1.96 g, 88%) as a yellow solid. mp: 180-184 °C; ^{1}H NMR (300 MHz, $CDCl_3$): δ 8.14 (d, J = 8.4 Hz, 1 H, ArH), 7.73-7.70 (m, 2 H, ArH), 7.60-7.55 (m, 3 H, ArH), 7.46-7.41 (m, 3 H, ArH), 7.33-7.29 (m, 4 H, ArH), 7.16 (d, J = 7.5 Hz, 1 H, ArH), 6.95 (d, J = 16.2 Hz, 1 H, vinylic -CH), 5.30 (d, J = 12.3 Hz, 1 H, vinylic -

CH), 2.97 (s, 3 H, -NCH_3), 2.77 (s, 3H, -NCH_3); ^{13}C NMR (75 MHz, $CDCl_3$): δ 150.4, 137.6, 136.2, 135.3, 134.0, 133.5, 129.9, 129.5, 129.3, 128.7, 127.9, 126.9, 126.2, 125.9, 124.5, 122.4, 114.8, 45.2, 37.2 ppm; HRMS (EI): m/z calcd for $C_{27}H_{22}ClN_3O_5S$ [M^+]: 535.0969; found: 535.0960.

(*E*)-1-(2-(3-Chloro-2-nitrostyryl)-1-(phenylsulfonyl)-1*H*-indol-3-yl)-3-(dimethylamino)prop-2-en-1-one 14l

The reaction of methyl ketone **13l** (2 g, 4.17 mmol) with DMF-DMA (4.5 mL, 33.33 mmol) in the presence of glycocyamine (0.24 g, 2.09 mmol) at 100 ^{o}C for 4 h followed by workup using the above-mentioned procedure gave enamine **14l** (2.01 g, 91%) as an orange solid. mp: 202-204 °C; ^{1}H NMR (300 MHz, $CDCl_3$): δ 8.22 (d, J = 8.4 Hz, 1 H, ArH), 7.80-7.70 (m, 5 H, ArH), 7.55-7.45 (m, 3 H, ArH), 7.42-7.34 (m, 3 H, ArH), 7.29-7.24 (m, 2 H, ArH), 6.84 (d, J = 15.9 Hz, 1 H, vinylic -CH), 5.24 (d, J = 12.9 Hz, 1 H, vinylic -CH), 3.09 (s, 3 H, -NCH_3), 2.18 (s, 3 H, -NCH_3); ^{13}C NMR (75 MHz, $CDCl_3$): δ 148.2, 137.7, 136.3, 134.1, 131.2, 131.0, 129.7, 129.3, 129.2, 127.8, 126.6, 126.0, 125.4, 125.3, 124.6, 124.3, 121.3, 114.8, 45.1, 37.2 ppm.

(*E*)-1-(2-(5-Bromo-4-fluoro-2-nitrostyryl)-1-(phenylsulfonyl)-1*H*-indol-3-yl)-3-(dimethylamino)prop-2-en-1-one 14m

The reaction of methyl ketone **13m** (2 g, 3.69 mmol) with DMF-DMA (3.9 mL, 29.52 mmol) in the presence of glycocyamine (0.22 g, 1.85 mmol) at 100 ^{o}C for 4 h followed by workup using the above-mentioned procedure gave enamine **14m** (1.96 g, 89%) as an orange solid. mp: 206-210 °C; ^{1}H NMR (300 MHz, $CDCl_3$): δ 8.21 (d, J = 8.4 Hz, 1 H, ArH), 7.94-7.90 (m, 1 H, ArH), 7.84-7.77 (m, 3 H, ArH), 7.67-7.65 (m, 1 H, ArH), 7.56-7.50 (m, 2 H, ArH), 7.43-7.34 (m, 4 H, ArH), 7.29-7.24 (m, 2 H, ArH), 5.28 (d, J = 12.6 Hz, 1 H, vinylic -CH), 3.06 (s, 3 H, -NCH_3), 2.80 (s, 3 H, -NCH_3); ^{13}C NMR (75 MHz, $CDCl_3$): δ 158.7 (d, J = 254.8 Hz), 146.6 (d,

J = 7.5 Hz), 137.7, 136.3, 134.8, 134.2, 134.1, 130.4 (2 C), 129.3, 129.2, 126.9, 126.5, 126.0, 124.6, 123.9, 121.3, 120.1, 115.9 (d, *J* = 48.0 Hz), 114.9, 113.1 (d, *J* = 10.8 Hz), 45.1, 37.2 ppm; HRMS (EI): m/z calcd for $C_{27}H_{22}ClN_3O_5S$ [M^+]: 597.0369; found: 597.0382.

(*E*)-1-(2-(5-Chloro-4-fluoro-2-nitrostyryl)-1-(phenylsulfonyl)-1*H*-indol-3-yl)-3-(dimethylamino)prop-2-en-1-one 14n

The reaction of methyl ketone **13n** (2 g, 4.01 mmol) with DMF-DMA (4.3 mL, 32.13 mmol) in the presence of glycocyamine (0.23 g, 2.00 mmol) at 100 °C for 5 h followed by workup using the above-mentioned procedure gave enamine **14n** (1.96 g, 88%) as an orange solid. mp: 218-220 °C; ^{1}H NMR (300 MHz, $CDCl_3$): δ 8.21 (d, *J* = 7.8 Hz, 1 H, ArH), 7.87 (d, *J* = 8.4 Hz, 1 H, ArH), 7.79-7.67 (m, 3 H, ArH), 7.67-7.65 (m, 1 H, ArH), 7.58-7.50 (m, 3 H, ArH), 7.43-7.37 (m, 4 H, ArH), 7.34-7.29 (m, 2 H, ArH), 5.28 (d, *J* = 12.6 Hz, 1 H, vinylic -CH), 3.05 (s, 3 H, -NCH_3), 2.79 (s, 3 H, -NCH_3); ^{13}C NMR (75 MHz, $CDCl_3$): δ 186.6, 157.0 (d, *J* = 255.6 Hz), 145.9, 137.7, 136.3, 134.7, 134.2, 131.1, 130.3 (2 C), 129.3, 127.5 (d, *J* = 18.1 Hz), 126.9, 126.0, 124.6, 123.9, 121.3, 114.9, 113.5 (d, *J* = 26.4 Hz), 45.1, 37.2 ppm.

(*E*)-1-(2-(4,5-Dichloro-2-nitrostyryl)-1-(phenylsulfonyl)-1*H*-indol-3-yl)-3-(dimethylamino)prop-2-en-1-one 14o

The reaction of methyl ketone **13o** (3 g, 5.84 mmol) with DMF-DMA (6.2 mL, 46.72 mmol) in the presence of glycocyamine (0.37 g, 2.92 mmol) at 100 °C for 4 h followed by workup using the above-mentioned procedure gave enamine **14o** (2.94 g, 88%) as an orange solid. mp: 202-204 °C; ^{1}H NMR (300 MHz, $CDCl_3$): δ 8.22 (d, *J* = 8.7 Hz, 1 H, ArH), 8.15 (s, 1 H, ArH), 7.83 (s, 1 H, ArH), 7.77 (d, *J* = 7.8 Hz, 2 H, ArH), 7.67-7.63 (m, 1 H, ArH), 7.58-7.50 (m, 2 H, ArH), 7.43-7.35 (m, 4 H, ArH), 7.30-7.27 (m, 2 H, ArH), 5.27 (d, *J* = 12.3 Hz, 1 H, vinylic -CH), 3.06 (s, 3 H, -NCH_3), 2.79 (s, 3 H, -NCH_3); ^{13}C NMR (75 MHz, $CDCl_3$): δ 186.6, 154.6,

145.8, 138.4, 137.7, 136.4, 134.6, 134.2, 132.7, 132.5, 130.5, 130.1, 129.3, 126.8, 126.7, 126.5, 126.1, 124.7, 124.3, 121.3, 114.9, 97.9, 45.1, 37.2; HRMS (EI): m/z calcd for $C_{27}H_{21}Cl_2N_3O_5S$ [M^+]: 569.0579; found: 569.0568.

(*E*)-1-(2-(3,5-Dichloro-2-nitrostyryl)-1-(phenylsulfonyl)-1*H*-indol-3-yl)-3-(dimethylamino)prop-2-en-1-one 14p

The reaction of methyl ketone **13p** (2 g, 3.89 mmol) with DMF-DMA (3.7 mL, 31.13 mmol) in the presence of glycocyamine (0.23 g, 1.95 mmol) at 100 ^oC for 4 h followed by workup using the above-mentioned procedure gave enamine **14p** (1.90 g, 86%) as an orange solid. mp: 176-178 °C; ^1H NMR (300 MHz, $CDCl_3$): δ 8.13 (d, J = 7.8 Hz, 1 H, ArH), 7.69-7.57 (m, 5 H, ArH), 7.44-7.42 (m, 2 H, ArH), 7.37-7.59 (m, 5 H, ArH), 7.19 (s, 1 H, ArH), 6.75 (d, J = 15.9 Hz, 1 H, ArH), 5.16 (d, J = 12.3 Hz, 1 H, vinylic -CH), 2.99 (s, 3 H, -NCH_3), 2.73 (s, 3 H, -NCH_3); ^{13}C NMR (75 MHz, $CDCl_3$): δ 186.4, 154.8, 146.8, 137.8, 136.8, 136.5, 134.2, 133.5, 132.6, 129.3, 126.7, 126.5, 126.2, 125.6, 125.5, 124.7, 121.4, 115.0, 98.0, 45.1, 37.2 ppm; HRMS (EI): m/z calcd for $C_{27}H_{21}Cl_2N_3O_5S$ [M^+]: 569.0579; found: 569.0570.

General procedure for the preparation of calothrixin B analogues (15b-p)

To a solution of enamine **14b-p** (1 eq) in dry DMF (20 mL), $FeCl_3$ (3 eq) was added. The reaction mixture was refluxed for 3 h under N_2 atmosphere. It was then poured over crushed ice (50 g) containing Conc. HCl (1 mL). The crude product was filtered and dried. The resulting reddish brown/black solid was washed successively with 10 mL of chloroform and 4 mL of DCM. The solid obtained was crystallised from THF to afford calothrixin B and its analogues as red/red-orange solids.

4-Methoxy-7*H*-indolo[3,2-*j*]phenanthridine-7,13(12*H*)-dione 15b

The reaction of enamine **14b** (1 g, 1.88 mmol) with $FeCl_3$ (0.91 g, 5.65 mmol) in dry DMF (30 mL) at reflux for 3 h under N_2 followed by workup using the above-mentioned procedure gave **15b** (0.28 g, 45%); as a red solid. mp: ≥ 300 °C ; IR (film): 3438, 1672 cm^{-1}; ^1H NMR (500 MHz, DMSO-d_6, 100 ^oC) δ 9.61 (s, 1 H, ArH), 9.14 (d, *J* = 9.0 Hz, 1 H, ArH), 8.23 (d, *J* = 9.0 Hz, 1 H, ArH), 7.78 (t, *J* = 7.5 Hz, 1 H, ArH), 7.67 (d, *J* = 7.0 Hz, 1 H, ArH), 7.50-7.47 (m, 1 H, ArH),7.41 (t, *J*= 8.5 Hz, 2 H, ArH, 4.10 (s, 3 H, -OMe); DEPT 135 ($CDCl_3$+TFA-d (4:1)): δ 141.0, 134.9, 130.5, 127.0, 123.2, 120.0, 115.0, 113.7, 56.7 ppm; HRMS (EI): m/z calcd for $C_{20}H_{12}N_2O_3$ [M^+]: 328.0848 found: 328.0840. HPLC purity: 96.5%.

2-Methoxy-7*H*-indolo[3,2-*j*]phenanthridine-7,13(12*H*)-dione 15c

The reaction of enamine **14c** (1 g, 1.88 mmol) with $FeCl_3$ (0.91 g, 5.65 mmol) in dry DMF (30 mL) at reflux for 3 h under N_2 followed by workup using the above-mentioned procedure gave **15c** (0.40 g, 65%) as a red solid. mp: ≥ 300 °C; ^1H NMR (300 MHz, DMSO-d_6) δ 13.09 (s, 1 H, NH), 9.44 (s, 1 H, ArH), 9.02 (s, 1 H, ArH), 8.18 (d, *J* = 7.2 Hz, 1 H, ArH), 8.07 (d, J = 9.0 Hz, 1 H, ArH), 7.64-7.62 (m, 2 H, ArH), 7.48 (t, J = 7.5 Hz, 1 H, ArH), 7.40 (t, J = 7.5 Hz, 1 H, ArH); ^{13}C NMR (75 MHz, $CDCl_3$+TFA-d (4:1)): δ 177.8, 177.2, 164.6, 139.3, 138.5, 137.9, 137.5, 137.4, 131.9, 130.6, 129.2, 128.6, 127.1, 124.2, 123.7, 123.1, 118.1, 113.9, 106.0, 56.6; DEPT 135: δ 138.1, 131.6, 130.2, 126.7, 123.3, 122.7, 113.6, 105.6, 56.2 ppm; HRMS (EI): m/z calcd for $C_{20}H_{12}N_2O_3$ [M^+]: 328.0848 found: 328.0790. HPLC purity: 95.2%.

2, 3-Dimethoxy-7*H*-indolo[3,2-*j*]phenanthridine-7,13(12*H*)-dione 15d

The reaction of crude enamine **14d** (500 mg, 0.89) with $FeCl_3$ (433 mg, 2.67 mmol) in dry DMF (20 mL) at reflux for 3 h under N_2 atmosphere followed by workup using the above-mentioned procedure furnished **15d** (182 mg, 57%) as a red orange solid. mp: > 300 °C; IR(film): 3441, 1651, 1242 cm^{-1}; ^1H NMR (500 MHz, DMSO-d_6, 100 °C): δ 12.72 (s, 1 H, NH), 9.42 (s, 1 H,

ArH), 9.03 (s, 1 H, ArH), 8.23 (d, *J* = 7.5 Hz, 1 H, ArH), 7.60 (d, *J* = 8 Hz, 1 H, ArH), 7.53 (s, 1 H, ArH), 7.48 (t, *J* = 8.5 Hz, 1 H, ArH), 7.39 (t, *J* = 7.3 Hz, 1 H, ArH), 4.07 (s, 3 H, -OCH_3), 4.05 (s, 3 H, -OCH_3); ^{13}C NMR (75 MHz, $CDCl_3$+TFA-d (4:1)) : δ 178.0, 177.6, 160.1, 156.3, 141.3, 139.3, 138.1, 137.6, 136.1, 130.5, 126.9, 126.4, 124.2, 124.0, 123.7, 118.4, 113.9, 105.5, 100.0, 57.6, 57.1; DEPT 135: δ 137.8, 130.3, 126.6, 123.5, 113.5, 105.1, 99.8, 57.2, 56.7 ppm; HRMS (ESI-MS): m/z calcd for $C_{21}H_{15}N_2O_4$ $[M+H]^+$: 359.1032; found: 359.1037. HPLC purity: 98.1%.

7*H*-[1,3]Dioxolo[4,5-*b*]indolo[3,2-*j*]phenanthridine-7,13(12*H*)-dione 15e

The reaction of enamine **14e** (500 mg, 0.92 mmol) with $FeCl_3$ (448 mg, 2.76 mmol) in dry DMF (20 mL) at reflux for 3 h under N_2 atmosphere followed by workup using the above-mentioned procedure furnished **15e** (189 mg, 60%) as a red solid. mp: > 300 °C; IR (film): 3441, 1651, 1242, 1065, 1034 cm^{-1}; ^{1}H NMR (500 MHz, DMSO-d_6, 100 ^{o}C) δ 12.75 (bs, 1 H, NH), 9.37 (s, 1 H, ArH), 8.91 (s, 1 H, ArH), 8.20 (d, *J* = 8.0 Hz, 1 H, ArH), 7.64 (d, *J* = 8 Hz, 1 H, ArH), 7.46 (m, 2 H, ArH), 7.38 (t, *J* = 7.5 Hz, 1 H, ArH), 6.30 (s, 2 H, -CH_2); ^{13}C NMR (75 MHz, $CDCl_3$+TFA-d (4:1)) : δ 177.8, 177.3, 158.2, 155.3, 142.7, 139.3, 138.5, 137.5, 137.2, 130.6, 126.9, 125.7, 124.2, 123.8, 118.4, 113.8, 105.6, 103.7, 98.5; DEPT 135: δ 138.5, 130.6, 126.9, 123.8, 113.8, 105.6, 103.6, 98.5 ppm; HRMS (ESI-MS): m/z calcd for $C_{20}H_{11}N_2O_4$ $[M+H]^+$: 343.0713; found: 343.0718. HPLC purity: 97.0%.

3-Bromo-7*H*-indolo[3,2-*j*]phenanthridine-7,13(12*H*)-dione 15f

The reaction of enamine **14f** (1 g, 1.73 mmol) with $FeCl_3$ (0.84 g, 5.18 mmol) in dry DMF (30 mL) at reflux for 3 h under N_2 followed by workup using the above-mentioned procedure gave **15f** (0.43 g, 64% over two steps) as a red solid. mp: ≥ 300 °C ; IR (film): 3438, 1665 cm^{-1}; ^{1}H NMR (300 MHz, DMSO-d_6): δ 13.17 (s, 1 H, NH), 9.59 (s, 1 H, ArH), 9.46 (d, *J* = 9.3 Hz, 1

H, ArH), 8.37 (s, 1 H, ArH), 8.15 (d, J = 7.5 Hz, 1 H, ArH), 8.02 (d, J = 9.0 Hz, 1 H, ArH), 7.61 (d, J = 8.1 Hz, 1 H, ArH), 7.46 (t, J = 7.2 Hz, 1 H, ArH), 7.38 (t, J = 7.2 Hz, 1 H, ArH); ^{13}C NMR (75 MHz, $CDCl_3$+TFA-d (4:1)): δ 177.1, 176.5, 144.1, 141.2, 140.9, 139.8, 138.3, 137.3, 135.4, 131.1, 130.2, 128.5, 127.3, 124.9, 124.5, 124.4, 124.0, 118.5, 114.0; DEPT 135: δ 143.7, 137.9, 130.6, 129.7, 126.9, 124.1, 123.5, 113.5 ppm; HRMS (EI): m/z calcd for $C_{19}H_9BrN_2O_2$ $[M]^+$: 375.9847; found: 375.9840. HPLC purity: 97.4%.

3-Chloro-7*H*-indolo[3,2-*j*]phenanthridine-7,13(12*H*)-dione 15g

The reaction of enamine **14g** (500 mg, 0.94 mmol) with $FeCl_3$ (457 mg, 2.82 mmol) in dry DMF (20 mL) at reflux for 3 h under N_2 followed by workup using the above-mentioned procedure gave **15g** (210 mg, 67%) as a red orange solid. mp: > 300 °C; IR (film): 3441, 1651 cm^{-1}; ^{1}H NMR (500 MHz, DMSO-d_6, 100 °C): δ 12.84 (s, 1 H, NH), 9.64 (bs, 1 H, ArH), 9.55 (d, J = 9.0 Hz, 1 H, ArH), 8.20-8.19 (m, 2 H, ArH), 7.87-7.85 (m, 1 H, ArH), 7.64 (d, J = 8.5 Hz, 1 H, ArH), 7.48-7.45 (m, 1 H, ArH), 7.38 (t, J = 7.0 Hz, 1 H, ArH); ^{13}C NMR (125 MHz, DMSO-d_6, 100 °C): δ 180.7, 180.4, 152.2, 149.4, 139.3, 138.3, 137.0, 133.5, 130.9, 129.6, 128.9, 127.7, 125.7, 124.7, 124.0, 122.9, 121.8, 116.6, 114.4; DEPT 135: δ 143.0, 138.9, 131.0, 128.1, 127.3, 123.9, 123.2, 114.0 ppm; HRMS (ESI-MS): m/z calcd for $C_{19}H_{10}N_2O_2Cl$ $[M+H]^+$: 333.0431, found 335.0443. HPLC purity: 97.7%.

3-Fluoro-7*H*-indolo[3,2-*j*]phenanthridine-7,13(12*H*)-dione 15h

The reaction of enamine **14h** (500 mg, 0.96 mmol) with $FeCl_3$ (467 mg, 2.88 mmol.) in dry DMF (20 mL) at reflux for 3 h under N_2 followed by workup using the above-mentioned procedure gave **15h** (195 mg, 64%) as a red solid. mp: > 300 °C IR (film): 3294, 1643 cm^{-1}; ^{1}H NMR (300 MHz, DMSO-d_6): δ 13.2 (s, 1 H, NH), 9.61-9.56 (m, 2 H, ArH), 8.11 (d, J = 7.8 Hz, 1 H, ArH), 7.88-7.85 (m, 1 H, ArH), 7.83-7.77 (m, 1 H, ArH), 7.57 (d, J = 7.8 Hz, 1 H,

ArH), 7.43 (t, J = 7.2 Hz, 1 H, ArH), 7.34 (t, J = 7.2 Hz, 1 H, ArH); ^{13}C NMR (75 MHz, DMSO-d_6): δ 180.3, 179.9, 163.2 (d, J = 251.4 Hz), 152.5 (d, J = 12.7 Hz), 148.8, 138.3, 137.7, 132.7, 130.1 (d, J = 9.9 Hz), 127.1, 124.3, 124.2, 123.2, 122.2, 120.2 (d, J = 24.5 Hz), 119.6, 115.5, 113.8, 113.2 (d, J = 20.1 Hz); DEPT 90: δ 148.8, 130.2 (d, J = 9.3 Hz), 127.2, 124.3, 122.2, 120.3 (d, J = 24.2 Hz), 113.9, 113.2 (d, J = 19.7 Hz) ppm; HRMS (EI): m/z calcd for $C_{19}H_9F_2N_2O_2$ [M^+]: 316.0648; found: 316.0610. HPLC purity: 97.7%.

2-Bromo-7*H*-indolo[3,2-*j*]phenanthridine-7,13(12*H*)-dione 15i

The reaction of enamine **14i** (1 g, 1.73 mmol) with $FeCl_3$ (0.84 g, 5.18 mmol) in dry DMF (30 mL) at reflux for 3 h under N_2 followed by workup using the above-mentioned procedure gave **15i** (0.42 g, 65%) as a red solid. mp: ≥ 300 °C ; IR (film): 3431, 1669 cm^{-1}; ^{1}H NMR (300 MHz, DMSO-d_6): δ 13.15 (s, 1 H; NH), 9.74 (s, 1 H, ArH), 9.60 (s, 1 H, ArH), 8.14 (d, J = 7.5 Hz, 1 H, ArH), 8.10-8.07 (m, 2 H, ArH), 7.60 (d, J = 7.8 Hz, 1 H, ArH), 7.46 (t, J = 7.2 Hz, 1 H, ArH), 7.37 (t, J = 7.5 Hz, 1 H, ArH); ^{13}C NMR (75 MHz, $CDCl_3$+TFA-d (4:1)): δ 176.8, 176.0, 143.1, 141.3, 139.6, 139.4, 138.8, 137.0, 131.3, 130.8, 130.3, 129.2, 127.1, 126.6, 124.2, 123.9, 123.1, 118.34, 113.8; DEPT 135: δ 142.7, 141.0, 131.0, 130.5, 126.8, 123.6, 122.7, 113.5 ppm; HRMS (EI): m/z calcd for $C_{19}H_9BrN_2O_2$ [M]$^+$: 375.9847; found: 375.9840. HPLC purity: 97.4%

2-Chloro-7*H*-indolo[3,2-*j*]phenanthridine-7,13(12*H*)-dione 15j

The reaction of enamine **14j** (1 g, 1.87 mmol) with $FeCl_3$ (0.91 g, 5.61 mmol) in dry DMF (30 mL) at reflux for 3 h under N_2 followed by workup using the above-mentioned procedure gave **15j** (0.41 mg, 62% over two steps) as a red solid. mp: > 300 °C; IR (film): 3441, 1657 cm^{-1}; ^{1}H NMR (500 MHz, DMSO-d_6, 100 °C): δ 12.86 (s, 1 H, NH), 9.65-9.61 (m, 2 H, ArH), 8.22 (d, J = 8.0 Hz, 1 H, ArH), 8.19 (d, J = 8.5 Hz, 1 H, ArH), 7.94 (d, J = 8.0 Hz, 1 H, ArH), 7.67 (d, J

= 8.0 Hz, 1 H, ArH), 7.49 (t, *J* = 7.5 Hz, 1 H, ArH), 7.41 (t, *J* = 7.5 Hz, 1 H, ArH); ^{13}C NMR (75 MHz, $CDCl_3$+TFA-d (4:1)): δ 176.9, 176.3, 143.0, 142.3, 139.6, 139.5, 139.2, 138.9, 137.2, 130.9, 129.4, 128.1, 127.3, 126.6, 124.3, 123.9, 123.2, 118.3, 114.0; DEPT 135: *δ* 143.0, 138.9, 131.0, 128.1, 127.3, 123.9, 123.2, 114.0 ppm; HRMS (EI): m/z calcd for $C_{19}H_9ClN_2O_2$ $[M]^+$: 332.0353; found: 332.0350. HPLC purity: 98.6%

1-Chloro-7*H*-indolo[3,2-*j*]phenanthridine-7,13(12*H*)-dione 15k

The reaction of enamine **14k** (1 g, 1.87 mmol) with $FeCl_3$ (0.91 g, 5.61 mmol) in dry DMF (30 mL) at reflux for 3 h under N_2 followed by workup using the above-mentioned procedure gave **15k** (0.39 g, 65%) as a red solid. mp: ≥ 300 °C; IR (film): 3426, 1667 cm^{-1}; ^{1}H NMR (300 MHz, DMSO-d_6): *δ* 13.38 (s, 1 H, NH), 9.58 (s, 1 H, ArH), 8.17 (t, *J* = 8.1 Hz, 2 H, ArH), 7.98-7.91 (m, 2 H, ArH), 7.62 (d, *J* = 8.1 Hz, 1 H, ArH), 7.49 (t, *J* = 7.8 Hz, 1 H, ArH), 7.41 (t, *J* = 8.1 Hz, 1 H, ArH). ^{13}C NMR (75 MHz, DMSO-d_6) : *δ* 179.0, 178.0, 152.0, 147.9, 138.5, 138.3, 138.0, 132.0, 131.8, 130.7, 129.0, 127.1, 126.8, 124.4, 123.3, 122.1, 120.8, 115.8, 113.9; DEPT 135: *δ* 147.9, 132.0, 131.8, 129.0, 127.0, 124.3, 122.1, 113.9 ppm; HRMS (EI): m/z calcd for $C_{19}H_9ClN_2O_2$ $[M]^+$: 332.0353; found: 332.0350. HPLC purity: 96.8%.

4-Chloro-7*H*-indolo[3,2-*j*]phenanthridine-7,13(12*H*)-dione 15l

The reaction of enamine **14l** (1 g, 1.87 mmol) with $FeCl_3$ (0.91 g, 5.61 mmol) in dry DMF (30 mL) at reflux for 3 h under N_2 followed by workup using the above-mentioned procedure gave **15l** (0.32 g, 52%) as a red solid. mp: ≥ 300 °C ; IR (film): 3448, 1652 cm^{-1}; ^{1}H NMR (500 MHz, DMSO-d_6, 100 °C): *δ* 9.75 (s, 1 H, ArH), 9.57 (d, *J* = 8.5 Hz, 1 H, ArH), 8.23 (d, *J* = 8.0 Hz, 1 H, ArH), 8.12 (d, *J* = 7.0 Hz, 1 H, ArH), 7.84 (d, *J* = 8.0 Hz, 1 H, ArH), 7.68 (d, *J* = 8.5 Hz, 1 H, ArH), 7.49 (t, *J* = 7.5 Hz, 1 H, ArH), 7.41 (t, *J* = 7.5 Hz, 1 H, ArH); ^{13}C NMR (75 MHz, $CDCl_3$+TFA-d (4:1)): δ 176.9, 176.3, 143.0, 142.3, 139.6, 139.5, 139.2, 138.9, 137.2,

130.9, 129.4, 128.1, 127.3, 126.6, 124.3, 123.9, 123.2, 118.3, 114.0; DEPT 135: δ 139.8, 133.1, 129.7, 126.3, 124.1, 122.8, 119.0, 109.5 ppm; HRMS (EI): m/z calcd for $C_{19}H_9ClN_2O_2$ $[M]^+$: 332.0353; found: 332.0350. HPLC purity: 95.0%.

2-Bromo-3-fluoro-7*H*-indolo[3,2-*j*]phenanthridine-7,13(12*H*)-dione 15m

The reaction of enamine **14m** (1 g, 1.67 mmol) with $FeCl_3$ (0.82 g, 5.02 mmol) in dry DMF (30 mL) at reflux for 3 h under N_2 followed by workup using the above-mentioned procedure gave **15m** (0.42 g, 63%) as a red solid. mp: ≥ 300 °C ; IR (film): 3452, 1662 cm^{-1}; ^1H NMR (300 MHz, DMSO-d_6): δ 13.15 (s, 1 H, NH), 9.88 (d, J = 7.8 Hz, 1 H, ArH), 9.60 (s, 1 H, ArH), 8.14-8.07 (m, 2 H, ArH), 7.60 (d, J = 8.1 Hz, 1 H, ArH), 7.46 (t, J = 7.5 Hz, 1 H, ArH), 7.37 (t, J = 7.2 Hz, 1 H, ArH). ^{13}C NMR (75 MHz, $CDCl_3$+TFA-d (4:1)): δ 176.8, 176.5, 163.4, 144.5, 142.1 (d, J = 12 Hz), 139.9, 139.3, 137.3, 135.3, 131.2, 128.8, 127.5, 124.5, 123.9 (d, J = 11.3 Hz), 121.3, 121.0, 118.5, 114.1, 107.7 (d, J = 27.9 Hz); DEPT 135: δ 143.8, 134.6, 130.6, 126.9, 123.4, 113.5, 107.4 (d, J = 26.4 Hz) ppm; HRMS (EI): m/z calcd for $C_{19}H_8BrFN_2O_2$ $[M^+]$: 393.9753; found: 393.9750. HPLC purity: 97.1%.

2-Chloro-3-fluoro-7*H*-indolo[3,2-*j*]phenanthridine-7,13(12*H*)-dione 15n

The reaction of enamine **14n** (1 g, 1.67 mmol) with $FeCl_3$ (0.88 g, 5.42 mmol) in dry DMF (30 mL) at reflux for 3 h under N_2 followed by workup using the above-mentioned procedure gave **15n** (0.39 g (62%); as a red solid. mp: ≥ 300 °C ; IR (film): 3441, 1651 cm^{-1}; ^1H NMR (300 MHz, DMSO-d_6): δ 13.19 (s, 1 H, NH), 9.74 (d, J = 8.4 Hz, 1 H, ArH), 9.62 (s, 1 H, ArH), 8.18-8.15 (m, 2 H, ArH), 7.61 (d, J = 6.9 Hz, 1 H, ArH), 7.50-7.45 (m, 1 H, ArH), 7.39 (t, J = 8.1 Hz, 1 H, ArH). DEPT 135: δ 131.0, 130.6, 126.9, 123.6, 113.6, 108.1, 107.8 ppm; HRMS (EI): m/z calcd for $C_{19}H_8ClFN_2O_2$ $[M^+]$: 350.0258; found: 350.0250. HPLC purity: 97.9%.

2, 3-Dichloro-7*H*-indolo[3,2-*j*]phenanthridine-7,13(12*H*)-dione 15o

The reaction of enamine **14o** (500 mg, 0.88 mmol) with $FeCl_3$ (428 mg, 2.64 mmol) in dry DMF (20 mL) at reflux for 3 h under N_2 atmosphere followed by workup using the above-mentioned procedure furnished **15o** (198 mg, 65%) as a red solid. mp: > 300 °C; IR (film): 3294, 1643; ^{1}H NMR (500 MHz, DMSO-d_6, 40 ^{o}C) δ 13.10 (s, 1 H, NH), 9.71 (s, 1 H, ArH), 9.59 (s, 1 H, ArH), 8.40 (s, 1 H, ArH) 8.12 (d, *J* = 7 Hz, 1 H, ArH), 7.60 (d, J = 8 Hz, 1 H, ArH), 7.46 (t, J = 7.0 Hz, 1 H, ArH), 7.37 (t, J = 7.3 Hz, 1 H, ArH); ^{13}C NMR (75 MHz, $CDCl_3$+TFA-d (4:1)) : δ 176.4, 175.8, 144.7, 144.2, 141.0, 139.4, 138.9, 136.8, 130.9, 129.5, 128.7, 127.1, 124.5, 124.2, 123.9, 122.8, 118.2, 113.8; DEPT 90: δ 130.6, 129.2, 126.8, 123.6, 122.5, 113.5 ppm; HRMS (EI): m/z calcd for $C_{19}H_8Cl_2N_2O_2$ [M^+]: 365.9963 found: 365.9950. HPLC purity: 97.3%.

2,4-Dichloro-7*H*-indolo[3,2-*j*]phenanthridine-7,13(12*H*)-dione 15p

The reaction of enamine **14p** (1 g, 1.76 mmol) with $FeCl_3$ (0.86 g, 5.27 mmol) in dry DMF (30 mL) at reflux for 3 h under N_2 followed by workup using the above-mentioned procedure gave **15p** (0.42 g, 65%) as a red solid. mp: ≥ 300 °C ; IR (film): 3438, 1656 cm^{-1}; ^{1}H NMR (300 MHz, DMSO-d_6): δ 13.25 (s, 1 H, NH), 9.72 (s, 1 H, ArH), 9.63 (s, 1 H, ArH), 8.34 (s, 1 H, ArH), 8.19 (d, *J* = 7.5 Hz, 1 H, ArH), 7.65 (d, J = 7.8 Hz, 1 H, ArH), 7.50 (t, J = 7.5 Hz, 1 H, ArH), 7.45-7.40 (m, 1 H, ArH); ^{13}C NMR (75 MHz, $CDCl_3$+TFA-d (4:1)): δ 176.0, 175.5, 144.7, 141.5, 139.8, 139.7, 137.8, 137.3, 136.2, 131.0, 130.2, 127.7, 127.4, 127.2, 124.3, 123.9, 118.2, 114.0; DEPT 90: δ 144.3, 137.5, 130.7, 127.0, 126.9, 123.5, 113.7 ppm; HRMS (EI): m/z calcd for $C_{19}H_8Cl_2N_2O_2$ [M^+]: 365.9963 found: 365.9900. HPLC purity: 97.1%.

Ethyl 2-(2-nitrophenyl)-9-(phenylsulfonyl)-9*H*-carbazole-3-carboxylate 18a

A solution of divinyl compound **17a** (3 g) in dry xylenes (100 mL), 10% Pd/C (0.5 g) was added. The reaction mixture was refluxed for 24 h. It was then filtered through celite pad and

washed with hot xylenes (3 x 20 mL). Then, the combined filtrate was concentrated under *vacuo* and then triturated with MeOH (20 mL) to afford carbazole **18a** (2.46 g, 85%) as a pale yellow solid. mp: 200-202 ^{o}C. ^{1}H NMR (300 MHz, $CDCl_3$): δ 8.58 (s, 1 H, ArH), 8.30 (d, J = 8.0 Hz, 1 H, ArH), 7.83 (s, 1 H, ArH), 7.59 (d, J = 7.2 Hz, 2 H, ArH), 7.54-7.46 (m, 5 H, ArH), 7.44-7.32 (m, 5 H, ArH), 4.14 (q, J = 7.0 Hz, 2 H, -OCH_2), 1.17 (t, J = 7.4 Hz, 3 H, -CH_3) ppm.

Ethyl 2-(4-fluoro-2-nitrophenyl)-9-(phenylsulfonyl)-9*H*-carbazole-3-carboxylate 18b

The thermal electrocyclization of divinyl compound **17b** (3 g) using 10% Pd/C (0.5 g) in dry xylenes (100 mL) following the same procedure as that of **18a** afforded the compound **18b** (2.53g, 82%) as a pale yellow solid. mp: 228-230 ^{o}C; ^{1}H NMR (300 MHz, DMSO-d_6): δ 8.78 (s, 1 H), 8.34-8.28 (m, 2 H), 8.17-8.14 (m, 2 H), 7.88 (d, J = 7.5 Hz, 2 H), 7.76 (t, J = 8.1 Hz, 1 H) 7.69-7.61 (m, 3 H), 7.53-7.48 (m, 3 H), 4.07 (q, J = 6.9 Hz, 2 H, -OCH_2), 1.03 (t, J = 8.1 Hz, 3 H, -CH_3) ppm; ^{13}C NMR (75 MHz, $CDCl_3$): δ 165.9, 161.4 (d, J = 248 Hz), 149.1, 139.6, 138.6, 137.9, 136.5, 135.6, 133.9 (d, J = 8.3 Hz), 133.1 (d, J = 3.8 Hz), 130.3, 129.4, 126.7, 126.1, 125.4 (d, J = 9.8 Hz), 123.6, 122.0, 120.9 (d, J = 21 Hz), 116.6, 115.2, 112.0 (d, J = 27.2 Hz), 61.3, 14.1 ppm. DEPT 135: δ 135.2, 133.4 (d, J = 8.3 Hz), 133.4, 129.8, 128.9, 126.3, 125.0, 123.2, 120.4 (d, J = 21 Hz), 116.1, 114.7, 111.6 (d, J = 27.2 Hz), 60.6, 13.3 ppm; Anal. Calcd for $C_{27}H_{19}FN_2O_6S$, C: 62.54; H: 3.69; N: 5.40 Found, C: 62.32; H: 3.89; N: 5.64.

Ethyl 2-(4-chloro-2-nitrophenyl)-9-(phenylsulfonyl)-9*H*-carbazole-3-carboxylate 18c

The thermal electrocyclization of divinyl compound **17c** (3 g) using 10% Pd/C (0.5 g) in dry xylenes (100 mL) following the same procedure as that of **18a** afforded the compound **18c** (2.39 g, 80%) as a pale yellow solid. mp: 230-232 °C; ^{1}H NMR (300 MHz, DMSO-d_6): δ 8.57 (s, 1 H), 8.27 (d, J = 8.4 Hz, 1 H, ArH), 8.14 (s, 1 H, ArH), 8.09 (s, 1 H, ArH), 7.93 (d, J = 7.8

Hz, 1 H, ArH), 7.70 (d, *J* = 7.5 Hz, 2 H, ArH), 7.60 (d, *J* = 8.1 Hz, 1 H, ArH), 7.50 (t, *J* = 7.5 Hz, 1 H, ArH), 7.44-7.33 (m, 2H, ArH), 7.31-7.25 (m, 3 H), 4.08 (q, *J* = 6.3 Hz, 2 H, $-OCH_2$), 1.09 (t, *J* = 8.1 Hz, 3 H, $-CH_3$) ppm; ^{13}C NMR (75 MHz, $CDCl_3$): δ 165.9, 148.7, 140.2, 139.1, 137.8, 137.1, 136.1, 134.4, 134.2, 132.8, 132.6, 129.3, 128.5, 126.5, 126.4, 125.6, 124.9, 124.7, 124.3, 123.2, 120.6, 116.5, 115.4, 61.3, 14.0 ppm. Anal. Calcd for $C_{27}H_{19}ClN_2O_6S$, C: 60.62; H: 3.58; N: 5.24 Found, C: 60.79; H: 3.80; N: 5.42.

(2-(2-Nitrophenyl)-9-(phenylsulfonyl)-9*H*-carbazol-3-yl)methanol 19a

To a solution of carbazole **18a** (0.5 g, 1 mmol) in dry DCM (20 mL) kept at 0 ^{o}C for 10 min, DIBAL-H (20 % in toluene) (1.8 mL, 2.5 mmol) was slowly added under nitrogen atmosphere and stirred at the same temperature for 30 min. After the reaction was completed (monitored by TLC), it was quenched using 3N HCl (2 mL) and water (20 mL). The organic layer was extracted with DCM (2 x 20 mL) and washed with brine solution (10 mL) and dried (Na_2SO_4). Removal of solvent in vacuo afforded crude alcohol **19a** (0.42 g, 90%) as a thick yellow paste. The crude alcohol was used as such for the next step without further purification.

(2-(4-Fluoro-2-nitrophenyl)-9-(phenylsulfonyl)-9*H*-carbazol-3-yl)methanol 19b

The reduction of carbazole ester **18b** (0.5 g, 1 mmol) using DIBAL-H (1.8 mL, 2.5 mmol) in dry DCM (20 mL) following the same procedure as that of **19a** afforded crude alcohol **19b** (0.42 g, 91%) as a yellow paste. The crude alcohol was used as such for the next step without further purification.

(2-(4-Chloro-2-nitrophenyl)-9-(phenylsulfonyl)-9*H*-carbazol-3-yl)methanol 19c

The reduction of carbazole ester **18c** (0.5 g, 1 mmol) using DIBAL-H (1.7 mL, 2.5 mmol) in dry DCM (20 mL) following the same procedure as that of **19a** afforded crude alcohol **19c**

(0.39 g, 85%) as a yellow paste. The crude alcohol was used as such for the next step without further purification

2-(2-Nitrophenyl)-9-(phenylsulfonyl)-9*H*-carbazole-3-carbaldehyde 20a

A solution of crude benzyl alcohol **19a** (0.42 g, 0.9 mmol) in dry DCM (15 mL), PCC (0.26 g, 12 mmol) and celite (1 g) were added and the reaction mixture was stirred at room temperature for 2 h. Then, the reaction mixture upon filtration through celite followed by removal of solvent and subsequent column chromatographic purification (silica gel, 80 % DCM in hexane) gave aldehyde **20a** (0.37 g, 79% over two steps) as a pale yellow solid. mp: 236-238 °C; ^{1}H NMR (300 MHz, DMSO-d_6): δ 9.88 (s, 1 H, CHO), 8.84 (s, 1 H), 8.37-8.30 (m, 2 H), 8.25 (d, *J* =7.8Hz, 1 H), 8.16 (s, 1 H), 7.91-7.89 (m, 3 H), 7.80 (t, *J* = 7.5 Hz, 1 H), 7.71-7.65 (m, 3 H), 7.57-7.50 (m, 3 H) ppm; ^{13}C NMR (75 MHz, $CDCl_3$): δ 190.8, 148.6, 139.9, 138.9, 138.2, 136.0, 135.3, 133.5, 133.4, 132.5, 130.0, 129.9, 129.7, 129.0, 126.3, 125.8, 125.1, 124.9, 124.3, 124.1, 121.5, 115.6, 114.7. DEPT 135: *δ* 190.8, 135.3, 133.5, 132.5, 129.9, 129.7, 129.0, 126.3, 125.1, 124.3, 124.1, 121.5, 115.6, 114.7 ppm; Anal. Calcd for $C_{25}H_{16}N_2O_5S$, C: 65.78; H: 3.53; N: 6.14 Found, C: 65.94; H: 3.73; N: 6.02.

2-(4-Fluoro-2-nitrophenyl)-9-(phenylsulfonyl)-9*H*-carbazole-3-carbaldehyde 20b

The oxidation of crude alcohol **19b** (0.42 g, 0.9 mmol) using PCC (0.25 g, 11 mmol) in dry DCM (15 mL), following the same procedure as that of **20a** afforded the compound **20b (**0.36 g, 78% over two steps) as a pale yellow solid. mp: 244-246 ^{o}C; ^{1}H NMR (300 MHz, DMSO-d_6): *δ* 9.89 (s, 1 H, CHO), 8.34 (s, 1 H), 8.33 (t, *J* = 7.8 Hz, 2 H), 8.22-8.19 (m, 2 H), 7.91 (d, *J* = 7.8 Hz, 2 H), 7.80 (t, *J* = 7.2 Hz, 1 H), 7.75-7.66 (m, 3 H), 7.56-7.54 (m, 3 H); ^{13}C NMR (75 MHz, $CDCl_3$): *δ* 191.0, 161.4 (d, *J* = 248 Hz), 149.1(d, *J* = 7.5 Hz), 139.8, 138.2, 137.8, 136.0, 135.3, 134.3 (d, *J* = 8.3 Hz), 130.1, 129.9, 129.0, 126.3, 125.9, 125.1, 124.8, 124.5, 121.5, 120.6 (d, *J* = 22 Hz), 115.9, 114.7, 112.0 (d, *J* = 27.1 Hz); DEPT 135: *δ* 191.0, 135.2, 134.3 (d,

J = 8.3 Hz), 129.9, 129.1, 126.3, 125.1, 124.5, 121.5, 120.6 (d, *J* = 22 Hz), 115.9, 114.7, 112.0 (d, *J* = 27.1 Hz) ppm; Anal. Calcd for $C_{25}H_{15}FN_2O_5S$, C: 63.29; H: 3.19; N: 5.90 Found, C: 63.46; H: 3.07; N: 6.16.

2-(4-Chloro-2-nitrophenyl)-9-(phenylsulfonyl)-9*H*-carbazole-3-carbaldehyde 20c

The oxidation of crude alcohol **19c** (0.39 g, 0.8 mmol) using PCC (0.21 g, 1 mmol) in dry DCM (15 mL), following the same procedure as that of **20a** afforded the compound **20c (**0.33 g, 73% over two steps) as a pale yellow solid. mp: 248-250 °C; ^{1}H NMR (300 MHz, $CDCl_3$): δ 9.83 (s, 1 H, CHO), 8.44 (s, 1 H, ArH), 8.29 (d, *J* = 8.1 Hz, 1 H), 8.15 (s, 1 H, ArH), 8.14 (s, 1 H, ArH), 8.10 (s, 1 H, ArH), 7.95 (d, *J* = 7.2 Hz, 1 H, ArH), 7.73-7.70 (m, 2 H), 7.66-7.64 (m, 1 H), 7.55-7.53 (m, 1 H), 7.50-7.42(m, 2H, ArH), 7.39-7.32 (m, 3 H); ^{13}C NMR (75 MHz, $CDCl_3$): δ 190.1, 149.3, 140.9, 139.2, 138.0, 137.1, 135.3, 134.6, 133.6, 133.0, 132.8, 132.7, 129.9, 129.5, 128.9, 126.9, 126.5, 125.4, 124.9, 124.8, 123.4, 120.8, 116.2, 115.3; DEPT 135: δ 189.1, 133.5, 132.5, 131.9, 128.4, 127.8, 125.4, 123.7, 122.3, 119.7, 115.2, 114.2 ppm; Anal. Calcd for $C_{25}H_{15}ClN_2O_5S$, C: 61.16; H: 3.08; N: 5.71 Found, C: 61.39; H: 3.24; N: 5.82.

General procedure for preparation of quinocarbazoles 21a-c

To a solution of carbazole (1 mmol) in dry THF (50 mL), Ra-Ni (3-4 g) was carefully added and the reaction mixture was stirred at room temperature for 3 h. Then, the nickel residue was carefully filtered and washed with hot THF (3 x 30 mL). The combined filtrate was evaporated. To this, DMSO (20 mL) and 50% NaOH (3 mL) were added. The reaction mixture was stirred at room temperature for 6 h and then poured over ice (50 g). The solution was slightly warmed to avoid the emulsification, and the solid formed was filtered and dried ($CaCl_2$). The crude product was triturated with $CHCl_3$ to afford quinocarbazoles **21a-c**.

8*H*-Quino[4,3-*b*]carbazole 21a

Reductive cyclization of carbazole-3-carbaldehyde **20a** (0.45g, 1 mmol) using Ra-Ni (3-4 g) in THF (50 mL) adopting the above mentioned procedure afforded quinocarbazole **21a (**0.20 g, 76% over two steps) as a pale yellow solid. mp: 276-278°C; ^{1}H NMR (300 MHz, DMSO-d_6): δ 11.80 (s, 1 H, -NH), 9.43 (s, 1 H, ArH), 9.02 (s, 1 H, ArH), 8.85 (d, J = 6.9 Hz, 1 H), 8.72 (s, 1 H, ArH), 8.36 (d, J = 7.5 Hz, 1 H), 8.09 (d, J = 7.2 Hz, 1 H, ArH), 7.79-7.71 (m, 2 H, ArH), 7.64 (d, J = 7.8 Hz, 1 H, ArH), 7.56 (t, J = 7.5 Hz, 1 H, ArH), 7.32 (t, J = 7.2 Hz, 1 H, ArH); ^{13}C NMR (75 MHz, $CDCl_3$): 154.2, 143.6, 142.3, 141.9, 130.2, 129.4, 128.1, 127.5, 126.5, 124.6, 124.1, 122.9, 122.0, 121.1, 120.9, 120.2, 119.5, 111.2, 101.2; DEPT 135: δ 154.2, 129.4, 128.2, 127.5, 126.5, 122.9, 121.1, 120.9, 119.5, 111.2, 101.2 ppm; HRMS (EI): m/z calcd for $C_{19}H_{12}N_2$ [M^+]: 268.1000 found: 268.1000. HPLC purity: 95.1%.

4-Fluoro-8*H*-quino[4,3-*b*]carbazole 21b

Reductive cyclization of carbazole-3-carbaldehyde **20b** (0.45g, 1 mmol) using Ra-Ni (3-4 g) in THF (50 mL) adopting the above mentioned procedure afforded quinocarbazole **21b (**0.20 g, 73% over two steps) as a pale yellow solid. mp: 280-282 °C; ^{1}H NMR (300 MHz, DMSO-d_6): δ 11.90 (s, 1 H, -NH), 9.52 (s, 1 H, ArH), 9.09 (s, 1 H, ArH), 9.01-8.96 (m, 1 H, ArH), 8.76 (s, 1 H, ArH), 8.42 (d, J = 7.8 Hz, 1 H), 7.90-7.87 (m, 1 H, ArH), 7.71-7.59 (m, 3 H, ArH), 7.38 (t, J = 7.5 Hz, 1 H, ArH); ^{13}C NMR (75 MHz, $CDCl_3$): 162.2 (d, J = 245 Hz), 156.2, 145.4 (d, J = 9 Hz), 143.2, 142.5, 130.5, 128.8, 128.1, 126.0 (d, J = 9.8 Hz), 125.1, 122.5, 121.8, 121.7, 120.4, 120.2, 115.6 (d, J = 23.6 Hz), 114.3 (d, J = 20.4 Hz), 111.9, 101.8 ppm. DEPT 135: δ 155.6, 127.5, 125.4 (d, J = 9 Hz), 121.2, 121.1, 119.6, 115.0 (d, J = 22.6 Hz), 113.6 (d, J = 20.4 Hz), 111.3, 101.2 ppm; HRMS (EI): m/z calcd for $C_{19}H_{11}FN_2$[M^+]: 286.0906 found: 286.0906. HPLC purity: 95.1%.

4-Chloro-8*H*-quino[4,3-*b*]carbazole 21c

Reductive cyclization of carbazole-3-carbaldehyde **20c** (0.45g, 0.9 mmol) using Ra-Ni (3-4 g) in THF (50 mL) adopting the above mentioned procedure afforded quinocarbazole **21c** (0.20 g, 71% over two steps) as a pale yellow solid. mp: 272-274 °C; ^{1}H NMR (300 MHz, DMSO-d_6): δ 11.86 (s, 1 H, -NH), 9.45 (s, 1 H, ArH), 9.04 (s, 1 H, ArH), 8.88 (d, J = 9.0 Hz, 1 H), 8.71 (s, 1 H, ArH), 8.36 (d, J = 7.8 Hz, 1 H), 8.10 (s, 1 H, ArH), 7.75 (d, J = 8.7 Hz, 1 H), 7.63 (d, J = 7.8 Hz, 1 H, ArH), 7.57 (t, J = 7.5 Hz, 1 H, ArH), 7.32 (t, J = 7.8 Hz, 1 H, ArH); ^{13}C NMR (75 MHz, $CDCl_3$): 155.7, 144.3, 142.5, 141.9, 132.4, 129.6, 128.1, 127.7, 126.5, 125.0, 124.8, 123.0, 121.9, 121.3 (2C), 120.1, 119.6, 111.3, 101.4 ppm; DEPT 135: δ 155.7, 128.1, 127.7, 126.5, 125.0, 121.2, 119.6, 111.3, 101.4 ppm; HRMS (EI): m/z calcd for $C_{19}H_{11}ClN_2[M^+]$: 302.0611 found: 302.0610. HPLC purity: 97.8%.

(4-Methyl-2-(2-nitrophenyl)-9-(phenylsulfonyl)-9*H*-carbazol-3-yl)methanol 23a

The reduction of the known carbazole ester[32] **22a** (0.5 g, 1 mmol) using DIBAL-H (1.8 mL, 2.5 mmol) in dry DCM (20 mL) following the same procedure as that of **19a** afforded crude alcohol **23a** (0.4 g, 88%) as yellow paste. The crude alcohol was used as such for the next step without further purification.

(2-(4-Fluoro-2-nitrophenyl)-4-methyl-9-(phenylsulfonyl)-9*H*-carbazol-3-yl)methanol 23b

Reduction of carbazole ester **22b** (0.5 g, 1 mmol) using DIBAL-H (1.8 mL, 2.5 mmol) in dry DCM (20 mL) following the same procedure as that of **19a** afforded crude alcohol **23b** (0.39 g, 86%) as a yellow paste. The crude compound was used as such for the next step without further purification.

4-Methyl-2-(2-nitrophenyl)-9-(phenylsulfonyl)-9*H*-carbazole-3-carbaldehyde 24a

Oxidation of crude alcohol **23a** (0.40 g, 0.9 mmol) using PCC (0.24 g, 1.1 mmol) and celite (1 g) in dry DCM (15 mL), following the same procedure as that of **20a** afforded the compound **24a** (0.33 g, 74% over two steps) as a pale yellow solid. mp: 228-230 °C; ^{1}H NMR (300 MHz, DMSO-d_6): δ 10.23 (s, 1 H, CHO), 8.43 (d, *J* =8.4 Hz, 1 H), 8.36 (d, *J* =7.8 Hz, 1 H), 8.27 (d, *J* =7.5 Hz, 1 H), 8.08 (s, 1 H), 7.90-7.87 (m, 3 H), 7.82 (d, *J* =7.5 Hz, 1 H), 7.73-7.70 (m, 2 H), 7.61-7.53 (m, 4 H), 3.11(s, 3 H, -CH_3) ppm; ^{13}C NMR (75 MHz, $CDCl_3$): δ 193.2, 149.4, 140.6, 140.0, 139.0, 138.3, 137.0, 136.2, 135.6, 134.3, 133.1, 130.8, 130.4, 129.9, 129.1, 127.1, 126.4, 125.9, 125.8, 125.2, 124.8, 115.5, 114.2, 17.0; DEPT 135: *δ* 192.3, 135.3, 133.4, 132.2, 129.9, 129.5, 128.2, 126.2, 125.0, 124.3, 123.9, 114.6, 113.2, 16.1 ppm; Anal. Calcd for $C_{26}H_{18}N_2O_5S$, C: 66.37; H: 3.86; N: 5.95 Found, C: 66.26; H: 3.69; N: 5.84.

2-(4-Fluoro-2-nitrophenyl)-4-methyl-9-(phenylsulfonyl)-9*H*-carbazole-3-carbaldehyde 24b

Oxidation of crude alcohol **23b** (0.39 g, 0.8 mmol) using PCC (0.23 g, 1.1 mmol) and celite (1 g) in dry DCM (15 mL) following the same procedure as that of **20a** afforded the compound **24b** (0.32 g, 70% over two steps) as a pale yellow solid. mp: 240-242 ^{o}C; ^{1}H NMR (300 MHz, DMSO-d_6): δ 10.23 (s, 1 H, CHO), 8.40-8.32 (m, 2 H), 8.19 (d, *J* =8.4 Hz, 1 H), 8.05 (s, 1 H), 7.87 (d, *J* =7.8 Hz, 2 H), 7.79-7.34 (m, 1 H), 7.73-7.63 (m, 2 H), 7.60-7.58 (m, 1 H), 7.56-7.49 (m, 3 H), 3.08 (s, 3 H, -CH_3) ppm; Anal. Calcd for $C_{26}H_{17}FN_2O_5S$, C: 63.93; H: 3.51; N: 5.73 Found, C: 64.11; H: 3.24; N: 5.56.

13-Methyl-8*H*-quino[4,3-*b*]carbazole 25a

Reductive cyclization of carbazole-3-carbaldehyde **24a** (0.5 g, 1.1 mmol) using Ra-Ni (3-4 g) in THF (50 mL) following the same procedure as that of **21a** afforded quinocarbazole **25a** (0.22 g, 75% over two steps) as a pale yellow solid. mp: 286-288 °C; ^{1}H NMR (300 MHz, DMSO-d_6): *δ* 11.87 (s, 1 H, -NH), 9.80 (s, 1 H, ArH), 8.85 (d, *J* = 7.2 Hz, 1 H), 8.62 (s, 1 H, ArH), 8.46 (d, *J*

= 7.5 Hz, 1 H), 8.10 (d, *J* = 7.5 Hz, 1 H, ArH), 7.77-7.76 (m, 2 H, ArH), 7.65 (d, *J* = 7.8 Hz, 1 H, ArH), 7.57 (t, *J* = 7.2 Hz, 1 H, ArH), 7.33 (t, *J* = 7.2 Hz, 1 H, ArH, 2.51 (s, 3 H); ^{13}C NMR (75 MHz, $CDCl_3$): 150.4, 142.7, 142.0, 141.9, 132.5, 130.6, 129.0, 128.2, 126.8, 126.5, 124.0, 123.4, 123.0, 122.9, 122.7, 119.5, 118.3, 111.0, 99.3, 14.9; DEPT 135: δ 150.4, 129.1, 128.2, 126.8, 126.5, 123.5, 123.0, 119.5, 111.0, 99.3, 14.9 ppm; HRMS (EI): m/z calcd for $C_{20}H_{14}N_2[M^+]$: 282.1157 found: 282.1154. HPLC purity: 95.0%.

4-Fluoro-13-methyl-8*H*-quino[4,3-*b*]carbazole 25b

Reductive cyclization of carbazole-3-carbaldehyde **24b** (0.5 g, 1 mmol) using Ra-Ni (3-4 g) in THF (50 mL) following the same procedure as that of **21a** afforded quinocarbazole **25b** (0.22 g, 72% over two steps) as a pale yellow solid. mp: 274-276 °C; ^{1}H NMR (300 MHz, DMSO-d_6): δ 12.21 (s, 1 H, -NH), 9.97 (s, 1 H, ArH), 9.02 (dd, J_1= 9.0 Hz & J_2 = 5.7 Hz, 1 H), 8.65 (s, 1 H, ArH), 8.47 (d, *J* = 8.1 Hz, 1 H, ArH), 7.90 (d, *J* = 8.7 Hz, 1 H, ArH), 7.77-7.70 (m, 2 H, ArH), 7.61 (t, *J* = 7.5 Hz, 1 H, ArH), 7.38 (t, *J* = 7.5 Hz, 1 H, ArH), 2.51 (s, 3 H); DEPT 135: δ 150.1, 127.5, 126.3 (d, *J* = 9.8 Hz), 123.7, 120.3, 116.3 (d, *J* = 23.4 Hz), 111.5, 109.8, 99.8, 15.2 ppm; HRMS (EI): m/z calcd for $C_{20}H_{13}FN_2[M^+]$: 300.1063 found: 300.1062. HPLC purity: 97.7%.

3-(2-Nitrophenyl)-9-(phenylsulfonyl)-9*H*-carbazol-2-yl)methanol 27

To a solution of carbazole **26** (0.5 g, 1 mmol) in dry DCM (20 mL) kept at 0 ^{o}C for 10 min, DIBAL-H (20 % in toluene) (1.8 mL, 2.5 mmol) was slowly added under nitrogen atmosphere and stirred at the same temperature for 30 min. After the reaction was completed (monitored by TLC), it was quenched using 3N HCl (2 mL) and water (20 mL). The organic layer was extracted with DCM (2 x 20 mL) and washed with brine solution (10 mL) and dried (Na_2SO_4).

Removal of solvent in vacuo afforded crude alcohol **27** (0.39 g, 86%) as a thick yellow paste. The crude compound was used as such for the next step without further purification.

3-(2-Nitrophenyl)-9-(phenylsulfonyl)-9*H*-carbazole-2-carbaldehyde 28

Oxidation of crude alcohol **27** (0.39 g, 0.9 mmol) using PCC (0.22 g, 1 mmol) in dry DCM (15 mL), following the same procedure as that of **19c** afforded the compound **28** (0.34, 76% over steps) as a pale yellow solid. mp: 224-226; ^{1}H NMR (300 MHz, $CDCl_3$): δ 9.90 (s, 1 H, -CHO), 8.86 (s, 1 H), 8.31 (d, *J* =8.1 Hz, 1 H), 8.08 (d, *J* =7.8 Hz, 1 H), 7.86-7.83 (m, 3 H), 7.70 (s, 1 H), 7.63 (t, *J* =7.5 Hz, 1 H), 7.58-7.51 (m, 2 H), 7.46 (m, 1 H), 7.36-7.32 (m, 4 H); ^{13}C NMR (75 MHz, $CDCl_3$): δ 190.6, 148.9, 140.0, 137.8, 137.6, 135.9, 134.3 (2C), 132.8, 130.3, 129.5, 129.4, 129.2, 126.6, 124.9, 124.5, 121.3, 121.2, 117.4, 115.2; DEPT 135: *δ* 190.6, 134.3, 132.9, 132.7, 129.5, 129.2, 126.6, 124.5, 121.3, 117.4, 115.2 ppm; Anal. Calcd for $C_{25}H_{16}N_2O_5S$, C: 65.78; H: 3.53; N: 6.14 Found, C: 65.86; H: 3.74; N: 6.00.

12*H*-Quino[3,4-*b*]carbazole 29

Reductive cyclization of carbazole-2-carbaldehyde **28** (0.45 g, 1 mmol) using Ra-Ni (3-4 g) in THF (50 mL) following the same procedure as that of **21a** afforded quinocarbazole **29** (0.19 g, 74% over two steps) as a pale yellow solid. mp: ≥ 300 °C; ^{1}H NMR (300 MHz, DMSO-d_6): *δ* 12.25 (s, 1 H, -NH), 10.1 (s, 1 H, ArH), 9.98 (s, 1 H, ArH), 9.22 (d, *J* = 7.8 Hz, 1 H), 8.68 (s, 1 H, ArH), 8.62 (d, *J* = 7.8 Hz, 1 H), 8.32 (d, *J* = 7.5 Hz, 1 H), 8.02 (t, *J* = 7.5 Hz, 1 H), 7.95 (t, *J* = 7.4 Hz, 1 H, ArH), 7.71-7.70 (m, 2 H, ArH), 7.43-7.41 (m, 1 H, ArH); ^{13}C NMR (75 MHz, DMSO-d_6): *δ* 151.0, 143.4, 139.7, 132.5, 131.6, 129.9, 129.3, 129.1, 125.6 (2C), 123.4, 122.7, 122.4, 122.0, 121.2, 120.0, 114.3, 112.2, 111.7; DEPT 135: *δ* 151.0, 129.9, 129.3, 129.2, 123.4, 122.7, 122.3, 120.0, 114.3, 112.3, 111.7 ppm; HRMS (ESI-MS): m/z calcd for $C_{19}H_{12}N_2$ $[M+H]^+$: 269.1079; found: 269.1073. HPLC purity: 97.0%

2-(2-Nitrophenyl)-9-(phenylsulfonyl)-9*H*-carbazole-3-carbonitrile 34a

Thermal electrocyclization of divinyl compound **33a** (1 g, 2.2 mmol) using 10% Pd/C (0.1 g) in dry xylenes (80 mL) following the same procedure as that of **18a** afforded the compound **34a** (0.81 g, 81%) as a pale yellow solid. mp: 226-229 °C; ^{1}H NMR (300 MHz, $CDCl_3$): δ 8.38-8.36 (m, 2 H), 8.30 (s, 1 H), 8.20 (d, J = 8.1 Hz, 1 H), 7.96 (d, J = 7.8 Hz, 1 H), 7.81-7.77 (m, 3 H), 7.70 (t, J = 7.8 Hz, 1 H), 7.63-7.51 (m, 3 H), 7.48-7.39 (m, 3 H); ^{13}C-NMR (75 MHz, DMSO-d_6,): δ 148.1, 140.2, 139.3, 138.1, 135.9, 135.4, 134.0, 132.6, 132.4, 130.7, 129.9, 129.4, 126.3, 125.7, 125.2, 124.9, 124.0, 121.7, 117.5, 115.0, 114.6, 107.0 ppm; Anal. Calcd for $C_{25}H_{15}N_3O_4S$, C, 66.22; H, 3.33; N, 9.27 Found, C: 66.09; H: 3.18; N: 9.48.

2-(4-Fluoro-2-nitrophenyl)-9-(phenylsulfonyl)-9*H*-carbazole-3-carbonitrile 34b

Thermal electrocyclization of divinyl compound **33b** (0.8 g, 1.7 mmol) using 10% Pd/C (0.1 g) in dry xylenes (80 mL) following the same procedure as that of **18a** afforded the compound **34b** (0.66 g, 83%) as a pale yellow solid. mp: 262-264 °C; ^{1}H NMR (300 MHz, $CDCl_3$): δ 8.38-8.31 (m, 3 H), 7.98-7.93 (m, 2 H), 7.81-7.74 (m, 2 H), 7.65-7.47 (m, 4 H), 7.44-7.39 (m, 3 H); ^{13}C-NMR (75 MHz, DMSO-d_6): δ 161.8 (d, J = 249.8 Hz), 148.9 (d, J = 9.8 Hz), 139.3, 139.2, 138.1, 135.9, 135.4, 134.7 (d, J = 8.3 Hz), 129.9, 129.7, 128.9 (d, J = 3 Hz), 126.2, 125.9, 125.2, 123.9, 121.7, 121.1 (d, J = 21 Hz), 117.5, 115.3, 114.6, 112.7 (d, J = 27.8 Hz), 107.2 ppm; Anal. Calcd for $C_{25}H_{14}FN_3O_4S$, C, 63.69; H, 2.99; N, 8.91 Found, C, 63.52; H, 2.84; N, 9.06.

2-(4-Chloro-2-nitrophenyl)-9-(phenylsulfonyl)-9*H*-carbazole-3-carbonitrile 34c

Thermal electrocyclization of divinyl compound **33c** (0.8 g, 1.6 mmol) using 10% Pd/C (0.1 g) in dry xylenes (80 mL) following the same procedure as that of **18a** afforded the compound **34c** (0.68 g, 85%) as a pale yellow solid. mp: 276-278 °C; ^{1}H NMR (300 MHz, $CDCl_3$): δ 8.37 (d,

J = 8.4 Hz, 1 H), 8.32 (d, *J* = 7.5 Hz, 2 H), 8.20 (d, *J* = 1.5 Hz, 1 H), 7.97 (d, *J* = 7.8 Hz, 1 H), 7.80-7.76 (m, 3 H), 7.62 (t, *J* = 7.95 Hz, 1 H), 7.54-7.50 (m, 2 H), 7.47-7.39 (m, 3 H); ^{13}C-NMR (75 MHz, DMSO-d_6): δ 148.8, 139.2, 138.9, 138.1, 135.9, 135.4, 134.8, 134.2, 133.6, 131.2, 129.9, 129.5, 126.4, 125.9, 125.2, 124.8, 123.9, 121.7, 117.4, 115.2, 114.6, 107.0 ppm.

General procedure for preparation of aminoquinocarbazoles 35a-c

To a solution of carbazole-3-carbonitrile **34a-c** (1 mmol) in dry THF (30 mL), Ra-Ni (3-4 g) was carefully added and the reaction mixture was refluxed for 30 min. After consumption of the starting material (monitored by TLC), the nickel residue was carefully filtered and washed with hot THF (3 x 20 mL). The combined filtrate was evaporated. To this, DMSO (20 mL) and 50% NaOH (3 mL) were added. The reaction mixture was stirred at room temperature for 3 h and then poured over ice (50 g). The solution was slightly warmed to avoid the emulsification, and the solid formed was filtered and dried ($CaCl_2$). The crude product was triturated with CH_2Cl_2 to afford aminoquinocarbazoles **35a-c**.

1-Amino-8*H*-quino[4,3-*b*]carbazole 35a

Reductive cyclization of carbazole-3-carbonitrile **34a** (0.5 g, 1.1 mmol) using Ra-Ni (3-4 g) in THF (50 mL) adopting the above mentioned procedure afforded aminoquinocarbazole **35a** (0.24 g, 78% over two steps) as a pale yellow solid. mp: >310 ˚C; ^{1}H NMR (300 MHz, DMSO-d_6): δ 13.49, (bs, 1 H, NH exchangeable with D_2O), 12.18 (bs, 1 H, NH exchangeable with D_2O), 9.64 (s, 1 H), 8.70-8.68 (m, 2 H), 8.23 (d, *J* = 7.5 Hz, 1 H), 7.69-7.57 (m, 5 H), 7.38 (t, *J* = 7.35 Hz, 1 H); ^{13}C-NMR (75 MHz, DMSO-d_6): δ 154.7, 143.9, 141.9, 132.1, 131.0, 129.8, 128.0, 125.0, 124.5, 123.4, 121.7, 120.8, 120.3, 119.7, 119.5, 117.7, 111.8, 108.8, 103.3; DEPT-135: δ 129.9, 128.1, 125.0, 123.5, 120.8, 120.5, 119.5, 117.8, 111.8, 103.4 ppm: HRMS (EI): m/z calcd for $C_{19}H_{13}N_3[M^+]$: 283.1109 found: 283.1109. HPLC purity: 97.1%

1-Amino-4-fluoro-8*H*-quino[4,3-*b*]carbazole 35b

Reductive cyclization of carbazole-3-carbonitrile **34b** (0.5 g, 1.06 mmol) using Ra-Ni (3-4 g) in THF (50 mL) adopting the above mentioned procedure afforded aminoquinocarbazole **35b** (0.24 g, 76% over two steps) as a pale yellow solid. mp: >310 °C; ^{1}H NMR (300 MHz, DMSO-d_6): δ 12.15 (s, 1 H, NH exchangeable with D_2O), 9.64 (s, 1 H), 9.15 (bs, 2 H, NH exchangeable with D_2O), 8.72 (dd, J_1 = 8.85 Hz, J_2 = 6.3 Hz, 1 H), 8.59 (s, 1 H), 8.20 (d, J = 7.8 Hz, 1 H), 7.69-7.64 (m, 1 H), 7.58 (t, J = 7.5 Hz, 1 H), 7.50-7.47 (m, 1 H), 7.42-7.34 (m, 2 H); ^{13}C-NMR (75 MHz, DMSO-d_6): δ 162.2 (d, J = 249 Hz), 155.2, 143.9, 141.9, 130.7, 128.0, 126.1 (d, J = 9.8 Hz), 124.3, 121.7, 120.8, 120.4, 119.5, 116.6, 112.6 (d, J = 22.5 Hz), 111.8, 108.6, 104.2 (d, J = 25.8 Hz), 103.2; DEPT-135: δ 128.0, 126.1, 120.8, 120.4, 119.5, 112.6 (d, J = 22.5 Hz), 111.8, 104.2 (d, J = 25.8 Hz), 103.2 ppm; HRMS (EI): m/z calcd for $C_{19}H_{12}FN_3[M^+]$: 301.1015 found: 301.1040. HPLC purity: 97.1%.

1-Amino-4-chloro-8*H*-quino[4,3-*b*]carbazole 35c

Reductive cyclization of carbazole-3-carbonitrile **34c** (0.5g, 1.02 mmol) using Ra-Ni (3-4 g) in THF (50 mL) adopting the above mentioned procedure afforded aminoquinocarbazole **35c** (0.24 g, 74% over two steps) as a pale yellow solid. mp: >310 °C; ^{1}H NMR (500 MHz, DMSO-d_6): δ 11.73 (s, 1 H, NH exchangeable with D_2O), 9.28 (s, 1 H), 8.56-8.54 (m, 2 H), 8.20 (d, J = 7.5 Hz, 1 H), 7.60 (d, J = 8.5 Hz, 1 H), 7.54-7.52 (m, 4 H, NH exchangeable with D_2O), 7.31 (d, J = 7.5 Hz, 2 H); ^{13}C-NMR (75 MHz, DMSO-d_6): δ 157.0, 144.2, 142.1, 141.8, 132.5, 131.0, 127.3, 124.4, 123.9, 123.1, 122.2, 121.6, 120.5, 119.7, 119.5, 117.1, 111.4, 102.2; DEPT-135: δ 127.3, 123.3, 121.6, 120.5, 119.5, 117.1, 111.4, 102.2 ppm; HRMS (EI): m/z calcd for $C_{19}H_{12}ClN_3[M^+]$: 317.0720 found: 317.0715. HPLC purity: 98.2%.

3-(2-Nitrophenyl)-9-(phenylsulfonyl)-9*H*-carbazole-2-carbonitrile 40

Thermal electrocyclization of divinyl compound **39** (1 g, 2.2mmol) using 10% Pd/C (0.1 g) in dry xylenes (80 mL) following the same procedure as that of **18a** afforded the compound **40** (0.83 g, 83%) as a pale yellow solid. mp: 239-241 ˚C; ^{1}H NMR (300 MHz, $CDCl_3$): δ 8.76 (s, 1 H), 8.36 (d, J = 8.7 Hz, 1 H), 8.20 (d, J = 8.1 Hz, 1 H), 7.91 (d, J = 7.8 Hz, 3 H), 7.87 (s, 1 H), 7.78-7.74 (m, 1 H), 7.70-7.63 (m, 2 H), 7.60-7.52 (m, 2 H), 7.50-7.40 (m, 3 H); ^{13}C-NMR (75 MHz, $CDCl_3$): δ 148.4, 139.6, 137.4, 137.3, 136.9, 134.5, 133.3, 133.2, 132.7, 130.0, 129.5, 126.6, 125.1, 124.7, 124.6, 121.1, 120.6, 119.5, 117.9, 115.2, 110.4 ppm.

1-Amino-12*H*-quino[3,4-*b*]carbazole 41

Reductive cyclization of carbazole-2-carbonitrile **40** (0.5g, 1.1 mmol) using Ra-Ni (3-4 g) in THF (50 mL) following the same procedure as that of **35a** afforded aminoquinocarbazole **41** (0.23 g, 75% over two steps) as a greenish yellow solid. mp: >310 ˚C; ^{1}H NMR (300 MHz, DMSO-d_6): δ 13.74 (bs, 1 H, NH exchangeable with D_2O), 12.13 (s, 1 H, NH exchangeable with D_2O), 9.68 (s, 1 H), 8.85 (d, J = 7.8 Hz, 1 H), 8.81 (s, 1 H), 8.53 (d, J = 7.8 Hz, 1 H), 7.77-7.74 (m, 1 H), 7.71-7.63 (m, 3 H), 7.61-7.56 (m, 1 H), 7.36 (t, J = 6.15 Hz, 1 H); ^{13}C-NMR (75 MHz, DMSO-d_6): δ 156.0, 143.1, 140.1, 129.2, 128.8, 128.5, 126.1, 124.3, 123.4, 123.0, 122.6, 122.3, 121.9, 120.4, 116.9, 114.9, 112.1, 106.1; DEPT-135: δ 129.0, 128.8, 125.1, 123.0, 122.3, 119.8, 115.2, 111.7, 107.3 ppm; HRMS (EI): m/z calcd for $C_{19}H_{13}N_3[M^+]$: 283.1109 found: 283.1109. HPLC purity: 96.0%.

8*H*-Quino[4,3-*b*]carbazol-1(2*H*)-one 42

To a solution of carbazole **18a** (0.5 g, 1 mmol) in dry THF (50 mL), Ra-Ni (3-4 g) was carefully added and the reaction mixture was refluxed for 4 h. After consumption of the starting material (monitored by TLC), the nickel residue was carefully filtered and washed with hot

THF (3 x 20 mL). The combined filtrate was evaporated. To this, DMSO (20 mL) and 50% NaOH (3 mL) were added. The reaction mixture was stirred at room temperature for 3 h and then poured over ice (50 g). The solution was slightly warmed to avoid the emulsification, and the solid formed was filtered and dried ($CaCl_2$). The crude product was recrystalized from DMSO afforded amide compound **42** (0 .22 g, 78%) as a colourless solid. m.p: >310 ˚C; ^{1}H NMR (300 MHz, DMSO-d_6): δ 11.73 (bs, 1 H, NH exchangeable with D_2O), 11.48 (s, 1 H, NH exchangeable with D_2O), 9.13 (s, 1 H), 8.46-8.42 (m, 2H), 8.33 (d, J = 7.5 Hz, 1 H), 7.59 (d, J = 7.5 Hz, 1 H), 7.52-7.44 (m, 2H), 7.37 (d, J = 7.5 Hz, 1 H), 7.30-7.24 (m, 2H) ppm.

1 –Chloro-8*H*-quino[4,3-*b*]carbazole 43

To a suspension of amide **42** (0.2 g, 0.7 mmol) in distilled $POC1_3$ (30 mL) was refluxed under N_2 atmosphere for 24 h. Then, the excess $POC1_3$ was removed in *vacuo*. To the cooled residue was added saturated solution of $NaHCO_3$ (50 mL) and then the reaction mixture was allowed to settle for 1 h. The chloroquinoline was filtered and dried ($CaC1_2$). The crude product was triturated with ethyl acetate to afford chloroquinocarbazole **43** (0 .17 g, 79%) as a colourless solid. mp: >310 ˚C; ^{1}H NMR (300 MHz, DMSO-d_6): δ 9.24 (s, 1 H, -NH), 8.86-8.83 (m, 1 H), 8.79 (s, 1 H), 8.48 (d, J = 7.8 Hz, 1 H), 8.02-7.99 (m, 1 H), 7.81-7.74 (m, 2 H), 7.66 (d, J = 8.1 Hz, 1 H), 7.58 (t, J = 7.5 Hz, 1 H), 7.33 (t, J = 7.5 Hz, 1 H); ^{13}C NMR (75 MHz, DMSO-d_6): δ 151.3, 142.6, 142.1 (2C), 132.2, 128.9, 128.5, 127.9, 127.2, 125.1, 124.2, 123.0, 121.9, 121.5, 119.8, 119.2, 117.5, 111.4, 102.3 ppm.

1-[3'-(*N*,*N*-Dimethylamino)propyl]-8*H*quino[4,3-*b*]carbazole 44

A mixture of chloroquinoline **43** (0.15 g, 0.5 mmol) and 3-(*N*,*N*-dimethylamino)-l-propylamine (20 mL) was refluxed under N_2 atmosphere for 20 h. The excess amine was then removed in vacuo. The sticky residue was washed with aq. Na_2CO_3 solution and extracted with $CHC1_3$ (3 x

50 mL) and dried (Na_2SO_4). The removal of solvent in *vacuo* afforded crude product, which upon trituration with diethylether furnished aminoquinocarbazole **44** (0.14 g, 75%) as a brownish yellow solid. mp: 92-94 ˚C; ^{1}H NMR (300 MHz, CD_3OD): δ 8.94 (s, 1 H), 8.45 (s, 1 H), 8.22 (d, J = 7.8 Hz, 1 H), 7.69 (d, J = 8.1 Hz, 1 H), 7.54-7.41 (m, 4 H), 7.31-7.25 (m, 2 H), 3.76 (t, J = 7.05 Hz, 2H), 2.57 (t, J = 7.35 Hz, 2H), 2.33 (s, 6H), 2.06 (p, J = 6.82 Hz, 2H); ^{13}C NMR (75 MHz ,CD_3OD): 156.6, 145.5, 143.5 (2C), 129.2, 128.2, 126.6, 125.6, 124.2, 123.1 (2C), 122.7, 121.5, 120.5, 115.9, 114.3, 112.0, 102.9, 58.8, 45.5, 41.2, 27.9; DEPT-135 δ 129.2, 128.2, 126.6, 123.1 (2 C), 121.5, 120.5, 115.9, 112.0, 102.9, 58.8, 45.5, 41.2, 27.9 ppm. HRMS (EI): m/z calcd for $C_{24}H_{24}N_4[M^+]$: 368.2001 found: 368.2000. HPLC purity: 95.4%.

12*H*-Naphtho[1,2-*b*]carbazole 46

To a solution of known N-phenylsulfonyl napthocarbazole[34] **45** (0.3 g, 0.7 mmol) in DMSO (20 mL), 50% NaOH (3 mL) was added and the reaction mixture was stirred at room temperature for 6 h and poured over crushed ice (50 g). The solution was slightly warmed to avoid the emulsification, and the solid formed was filtered and dried ($CaCl_2$). The crude product was triturated with methanol to afford napthocarbazole **46** (0.16 g, 84%) as a pale yellow solid. mp: 268-270 °C; ^{1}H NMR (300 MHz, DMSO-d_6): δ 11.45 (s, 1 H, -NH), 8.87 (d, J = 7.8 Hz, 1 H), 8.77-8.73 (m, 2 H), 8.28 (d, J = 7.5 Hz, 1 H), 7.98-7.95 (m, 2 H), 7.72-7.56 (m, 4 H,), 7.49 (t, J = 7.8 Hz, 1 H), 7.24 (t, J = 7.5 Hz, 1 H), ^{13}C NMR (75 MHz, CDCl3): δ 141.8, 139.9, 131.5, 129.8, 128.6, 128.3, 127.8, 126.9, 126.4, 126.2, 125.2, 124.0, 123.2, 122.9, 122.0, 120.8, 119.4, 118.8, 110.9, 102.3 ppm. DEPT 135: δ 128.3, 127.8, 126.9, 126.4, 126.2, 123.2, 122.9, 120.9, 119.4, 118.8, 110.9, 102.3 ppm; HRMS (EI): m/z calcd for $C_{20}H_{13}N[M^+]$: 267.1048 found: 267.1057. HPLC purity: 95.9%.

Cell lines and Cytotoxicity Assays

Human cancer cell lines, colon cancer (HCT116 p53 WT), lung cancer (NCI-H460, A549), glioblastoma (U251), breast cancer (MCF7 and MDA-MB 231), leukemic (Jurkat), cervical cancer (HeLa and SiHa) and human embryonic kidney (HEK) cells used in the study were purchased from ATCC (Manassas, VA). The p53 double knock out of HCT116 (p53-/-) was generously provided by Dr. Bert Vogelstein (John Hopkins, Baltimore, MD). The human tumor cell lines were grown in DMEM medium containing 10% Fetal Bovine serum, 2mM L-Glutamine and Pen-strep antibiotic solution media at 37 ^{o}C with 5% CO_2. The leukemic cell line Jurkat was grown as suspension in complete RPMI-1640 medium. For cytotoxicity assay, cells are seeded into 96 well cell culture plates with seeding densities ranging from 1500 -3000 cells /well for adherent cells and 20,000 cells/well for Jurkat. Stock concentrations of calothrixin analogues were prepared at 1 mM in DMSO (Sigma) and diluted to working concentrations of 4 μM in culture media. Growth inhibition assays were performed in the presence of different drug concentrations ranging from 4 μM to 0.2 nM for 48 hrs. The cytotoxic effects of calothrixins on these tumor cell lines were measured using procedure developed at NCI[47] by Sulphorhodamine-B assay[48] or CCK-8 (Dojindo, Kumamoto, Japan) for adherent and suspension cell lines, respectively. The half-Maximal growth inhibition (GI_{50}) values which are the reduction in cell number by 50 % in comparison with that of vehicle control were obtained and standard deviation from at least two independent experiments were computed using Microsoft excel.

Clonogenic cell survival assay

HCT116 and NCI-H460 cells were seeded at concentrations of 100 cells/well of a six well plate (in triplicate), after overnight adherence the cells were treated with different concentrations of calothrixins/quinocarbazoles in culture medium for 48 h and then washed with Dulbecco's Phosphate buffered saline followed by addition of fresh drug-free medium. Cells were incubated for an additional 14 days, then the colonies in each well were stained and photographed.

Flow cytometry studies

Cell cycle analysis was carried out to study the effect of calothrixins on cell cycle progression. HCT116 and HeLa cells were treated with calothrixins alone (5 μM for HCT116 cells and 1 μM for HeLa cells) for 20 h or pre-treatment of cells with calothrixins for 3 h followed by 0.4μM nocodazole for additional 17 h. After drug treatments, the cells were collected by trypsinisation, washed twice with phosphate-buffered saline (PBS) and fixed with 70% ethanol. Before staining, cells were washed with PBS to remove ethanol. Fixed cells were stained with propidium iodide (20μg/ml) in PBS containing Triton X-100 (0.1% v/v) and RNase A (0.2mg/ml) for 1 h at room temperature. Cell cycle status was analysed using a Beckman-Coulter flow cytometer.

Purification of recombinant human topoisomerase I

The wild-type human topoisomerase I (91 kDa) was purified from Sf-9 insect cells infected with the recombinant baculovirus (a kind gift from Prof. J.J. Champoux). Approximately, 1 x 10^9 Sf-9 cells were infected with the recombinant virus, and cells were harvested after 48-h infection. The cells were lysed and enzyme was purified as described.[49]

Plasmid relaxation assay

DNA topoisomerases were assayed by decreased mobility of the relaxed isomers of supercoiled pBS (SK+) [pBluescript (SK+)] DNA in 1.2% agarose gel. For recombinant human topoisomerase I (HTopI), the enzyme was purified as mentioned in preceding section and relaxation assay was carried out in the relaxation buffer (25 mM Tris-HCl, pH 7.5, 5% glycerol, 0.5 mM DTT, 10 mM $MgCl_2$, 50 mM KCl, 25 mM EDTA and 150 µg/mL BSA).[50,51] For studies involving human topoisomerase II, the enzyme was purchased from TopoGEN Inc. (Human Topo IIa, TopoGEN Inc.) and the assay was performed as per manufacturer's protocol. For all the experiments, the temperature of the DNA and buffer mixture was raised to 37 °C before enzyme addition. The reactions were rapidly quenched using stop solution and kept in ice. The gels were stained with ethidium bromide (EtBr) (0.5 µg/mL) and the amount of supercoiled monomer DNA band fluorescence was quantified by integration using Gel Doc 2000 under UV illumination (Bio-Rad Quantity One Software).

Plasmid cleavage reaction

Cleavage reaction was performed as described previously.[52] In brief, a 20 µl reaction mixture (200 ng negatively supercoiled pRYG DNA, 10 mM Tris-HCl (pH 7.5), 100 mM KCl, 0.1 mM EDTA, 5 mM $MgCl_2$, 0.5 mM DTT, 30 µg BSA and 10 pmol of htopII) was incubated at 37 ^{o}C for 30 min and terminated by the addition of 0.5% SDS and 10 mM EDTA. The mixture was further incubated with 100 µg/ml proteinase K at 37 $^{\circ}$C for 30 min and analyzed by 1% agarose gel electrophoresis. To resolve the linear product (Form III) from the supercoiled molecule (Form I), ethidium bromide at a final concentration of 0.5 µg/ml was included in the gel.

DNA cleavage studies

The *in vitro* nuclease activity of calothrixins was evaluated using pBSK plasmid DNA in presence of Dithiothreitol (DTT) and ferric chloride by agarose gel electrophoresis. The oxidative cleavage of plasmid DNA (250 ng) was studied at pH 8.0 in 20mM Hepes buffered solution containing varying concentrations of calothrixins, 200 µM DTT and 200 µM $FeCl_3$.The reactions were carried out at 37°C for 1 hour and electrophoresed at 100V in Tris-acetate-EDTA (TAE) buffer using 1.5% Agarose gel containing 0.5 µg/mL ethidium bromide and photographed under UV light.

Alkaline COMET assay

A total of 10^4 cells were suspended in 150 µl pre-warmed low melting point (LMP) agarose (0.5% PBS) and were rapidly spread on doubly-frosted microscope slides (Rohem, India) pre-coated with normal melting (NMP) agarose (1%) and covered with a coverslip. After gelling for 10 min at 0 $^{\circ}$C, the coverslip was gently removed and a third layer of 100 µl NMP agarose (0.5% PBS) was added. Slides were then put in a tank filled with lysis solution (2.5 M NaCl, 0.1 M EDTA, 10 mM Tris–HCl pH 10, 10% DMSO and 1% Triton X-100 both freshly added) for 1 h at room temperature. Slides were then removed from lysis solution and incubated in fresh electrophoresis buffer (0.3 M NaOH and 1 mM EDTA, pH >13) for 40 min at room temperature to allow unwinding of DNA. Electrophoresis was then carried out at room temperature in fresh electrophoresis buffer for 24 min (0.7 V/cm; 300 mA). After electrophoresis, slides were gently washed twice for 5 min in fresh neutralisation buffer (0.4 M Tris–HCl pH 7.5). After drying overnight at 4 $^{\circ}$C, slides were stained with 50 µl of ethidium bromide solution (20 µg/ml), covered with a coverslip and photographed under a UV-fluorescent microscope (magnification, x100; Nikon, Japan).

Western blot analysis

HeLa cells after treatment with different concentration of calothrixins for 48 h were collected by trypsinization, washed once with ice cold PBS, pelleted at 400 xg (rcf) for 10 minutes at 4 °C. The cell pellets were lysed in modified RIPA buffer (10 mM Tris-Cl (pH 8.0), 140 mM NaCl, 1 mM EDTA, 1% Triton X-100, 0.1% SDS) containing protease (Cat. No.539134, Calbiochem, Merck-Millipore, CA) and phosphatase (Cat. No.524627, Calbiochem, Merck-Millipore, CA) inhibitor cocktail. Whole cell lysates were separated by SDS-PAGE and transferred to nitrocellulose membrane (Bio-Rad Laboratories, CA). The membrane after blocking with 5% nonfat dry milk (Fluka, Sigma-Aldrich) in 0.1% Tween-20 in TBS for 1 h was incubated overnight at 4 °C with primary antibodies to either PARP (Cat. No. 9532, Cell signaling technology) or cleaved PARP (Asp214) (Cat. No. 9541, Cell signaling technology) or β-Actin, Clone AC-15 (Cat. No. A1978, Sigma). After incubation with the appropriate horseradish peroxidase (HRP)-conjugated secondary antibody, a chemiluminence substrate kit (Supersignal west pico, Thermo Scientific Pierce) was used for detection.

Fluorescence microscopy assay using acridine orange and propidium iodide staining

To detect the apoptotic properties of the treated HCT116 and NCI-H460 cells, a propidium iodide (PI) and acridine orange (AO) double staining assay was performed using a fluorescent microscope (Nikon TiE attached with NIS-AR Software) according to the standard procedure. HCT116 and NCI-H460 cells (10-50 x 10^3 cells/well) were grown on a 12 well plate and cultured with different concentrations of calothrixins/quinocarbazoles for 48 h. After drug treatment, cells were washed with PBS, and then stained with acridine orange (20 µg/mL in PBS) and propidium iodide (40 µg/mL in PBS) for 10 min at room temperature in dark.

Following staining, the cells were washed twice with PBS and observed under a UV-fluorescent microscope (magnification, x100; Nikon, Japan).

DNA binding Studies

The preparation of CT-DNA stock solution was done as per the protocol of Ghosh et al.[53] The concentration of the CT-DNA solution was determined[54] from the UV absorbance at 260 nm using molar extinction coefficient ε_{260} = 6600 M^{-1} cm^{-1}. The absorbance at 260 and 280 nm was recorded in order to purity of DNA solution. The A_{260}/A_{280} ratio was found to be 1.85 depicting that the DNA was sufficiently free from protein. Various concentrations of DNA were used to obtain a varied molar ratio of the DNA-compound adduct.

Absorbance values were recorded on a double beam UV-2250 UV–VIS spectrophotometer (Shizmadju, Japan). Absorption titration experiments were conducted by keeping the concentration of calothrixin/quinocarbazoles constant (3×10^{-5} mol L^{-1}) while varying the CT-DNA concentration from 0 to 1×10^{-4} mol L^{-1}. Absorbance values were recorded after each successive addition of DNA solution.

CD studies

The CD measurements were made on a JASCO J715 spectropolarimeter (Tokyo, Japan) using a 1 cm cell at 0.2 nm intervals, with 3 scans averaged for each CD spectrum in the range of 230–350 nm. All CD measurements were performed in 1.3% DMSO solution by keeping the concentration of DNA constant (1×10^{-4} mol L^{-1}) while varying the drug concentration from 0 to 26.6×10^{-5} mol L^{-1}, at room temperature and observed CD spectra were baseline subtracted for blank. No alteration in the CD spectral shape or intensity of the CT-DNA was observed at 1.3% volume of DMSO in the final mixture. Hence, the observed changes in CD spectra were attributed solely to calothrixins/quinocarbazoles-CT DNA interaction.

DNA unwinding assay

Unwinding assay was performed using 50 fmol relaxed pBluscript (SK+) DNA in presence of quinocarbazoles in a concentration-dependent regime.[55] Relaxed DNA was prepared by incubating supercoiled plasmid DNA with excess of htopI, followed by proteinase K digestion at 37°C, phenol/chloroform extraction, and ethanol precipitation. The unwinding reaction was carried out at 37°C for 15 min, terminated by the addition of prewarmed stop solution (5% SDS, 15% Ficoll and 0.25% Bromophenol Blue) and electrophoresed on to 1% agarose gel.

***In silico* studies**

DNA-drug molecular docking studies

The DNA target of our interest 1DSC (an octamer complexed with actinomycin D) was selected from the protein databank (PDB), co-crystallized ligands were identified and removed from the structure of 1DSC and the nucleotide base pairs (5'-D(*GP*AP*AP*GP*CP*TP*TP*C)-3') was used for the analysis. The receptor DNA (1DSC) and the selected calothrixins such as **2**, **15b-p** were taken for *in silico* docking studies. The structure of the calothrixins was drawn using chemsketch.[56] The energy minimization for each compound was performed by using UCSF Chimera[57] for flexible conformations of the compounds during the docking. The flexible docking study was carried out using Autodock v4.0. Essential hydrogen atoms, Kollman united atom type charges and solvation parameters were added with the aid of Autodock tools.[58] This server integrates Lamarckian genetic algorithms. Each docking experiment was derived from ten different conformations. The relative stabilities were evaluated using free energy simulations and their binding affinities. The interaction analysis were calculated and visualised through the PyMol.[59]

Topoisomerase molecular docking studies

Docking Methods

Preparation of the Ligands and Protein:

The synthesized ligands were sketched using sketched module embedded in Schrodinger suite. Synthesized ligands namely, calothrixins (**1**, **2** and **15h**) and quinocarbazole derivatives (**21a**, **21b**, **25a** and **25b**) were taken for minimization using Ligprep module of Schrodinger 09 (Ligpep 2.3, Schrödinger Suite 2009)[60] where probable tautomeric and ionization states at pH = 7 ± 1 followed by minimization with OPLS 2005 force field (Ligpep 2.3, Schrödinger Suite 2009).[60] The protein preparation of different targets viz Topoisomerase I and II with PDB ID's: 1T8I and 4LPB[61] respectively was performed using Protein preparation wizard of Schrodinger 09 where missing hydrogen, bond order was assigned followed by energy minimization. The small molecules and all the water molecules were removed from coordinate file. The resultant PDB co-ordinates were taken for docking studies.

Molecular Docking:

Docking has been carried out using Schrodinger's Glide module. The receptor grid was prepared keeping co-crystallised ligand of Topoisomerases I and II (PDB ID: 1T8I and 4LPB respectively) at the centre of grid with 20Å edges bearing catalytic site. Initially docking study of the co-crystal was performed on prepared receptor grid for cross-validating the binding mode with respect to X-ray crystal structure binding mode. Further, molecular docking of calothrixins and quinocarbazole analogues were used as ligands against 1T8I and 4LPB using Glide XP 5.8 programme.[62, 63] The top analogues based on docking score as well as binding interaction with catalytic residues were allowed for induced fit docking. The docked conformation corresponding to the lowest free energy (or highest score) provided by Glide program was selected as the most probable binding pose of top calothrixins and quinocarbazole derivatives.

Visualisation of Docking Results

Once the docking was performed, best poses for hydrogen bonding, hydrophobic and π-π interactions were analysed using Chimera Visualisation tool,[64] PyMol version 1.3 (The PyMOL Molecular Graphics System;) and Glide (Schrödinger, LLC, New York, NY, USA) and LIGPLOT (Wallace AC et al) programs.

Pathological Evaluation of *in vivo* toxicity

Experiments were carried out using 6 weeks old female SCID (Severe Combined Immunodeficient) mice taken from in-house breeding facility of Orchid Pharma Limited (OPL), Chennai (India). Groups of six mice were housed in individually ventilated cages (IVC) at constant temperature (22±3 ^{o}C) and humidity (50±20%) at OPL, Oncology animal facility. Care of animals complied with the regulations of committee constituted for the purpose of Control and Supervision of Experiments on Animals (CPCSEA), Government of India. The study design was reviewed and approved by the Institutional Animal Ethics Committee of the OPL (Protocol No. 06/IAEC- 02/CAN/2014) and was performed according to the institutional guidelines. The animals were randomized into four group (n=6) to receive 0 (vehicle only), 10, 30 and 50 mg/kg of 3-fluorocalothrixin **15h** orally every day for a period of seven days. The body weights were taken daily prior to dosing and parameters such animal weight gain/loss and daily clinical toxic symptoms were observed and recorded. At the end of the study period, all the animals were euthanised by CO_2 and tissues from the heart, liver, lung, stomach, kidney and spleen were weighed (data not shown). Tissues were fixed in 10% formalin and embedded in paraffin. For histopathological examination, thin sections 3-5 µm in thickness were prepared, stained with hematoxylin and eosin (H&E) and were evaluated microscopically.

Supporting Information: Copies of ^{1}H, ^{13}C NMR (except for **15b** and **15n**), DEPT 135 and HRMS spectra (for selected compounds) for calothrixins **1, 2, 15b-p** and quinocarbazoles. CSV file containing molecular formula strings and the associated biological data. These materials are available free of charge *via* the Internet at http://pubs.acs.org.

Corresponding Author

*E-mail: mohanakrishnan@unom.ac.in; Phone: +91-44-22202813; Fax: 91-44-22300488

ORCID

A .K. Mohanakrishnan: 0000-0002-3758-4578

ACKNOWLEDGMENTS

We thank the Council of Scientific and Industrial Research (CSIR) New Delhi [02(0214)/14/EMR-II dt. 17/11/2014] for financial support. B.M.R. thanks Council of Scientific and Industrial Research (CSIR), New Delhi for fellowship. The authors thank the Department of Science and Technology Funds for the Improvement of Science and Technology (DST-FIST) for NMR facility. The authors also thank SAIF, IIT Madras for HRMS data. We acknowledge Dr. Ramesh, DMPK department, Jubilant Biosys Ltd, Banglaore for his help in the determination of experimental logP and logD values.

ABBREVIATIONS USED

MOM, Methoxymethyl ether; LTA, Lead tetraacetic acid; SAR, Structure activity relationship; PTC, Phase transfer catalyst; NBS, N-Bromosuccinimide; AIBN, Azabisisobutyronitrile; DCM, Dichloromethane; DCE, Dichloroethane; DMF, N, N-Dimethylformamide; DMA, N, N-Dimethylacetamide; DMFDMA, N, N-Dimethylformamide dimethyl acetal; *m*-CPBA, meta-chloroperoxybenzoic acid; DIBAL-H, Diisobutylaluminum hydride; THF, Tetrahydrofuran;

PCC, Pyridinium chlorochromate; DMSO, Dimethylsulphoxide; FT-IR, Fourier-transform infrared spectroscopy; HRMS, High resolution mass spectrometry; FACS, Flow assisted cell sorter; hTopI, Human topoisomerase I; hTopII, Human topoisomerase II; DTT, Dithiothreitol; AO, Acridine orange; PI, Propidium Iodide; ADP-ribose, Adenosine diphosphate ribose; PARP, Poly ADP-ribose polymerase; CT-DNA, Calf-thymus DNA; UV-Vis, Ultraviolet-Visible spectroscopy; CD, Circular Dichroism; ATPase, Adenosine triphosphatase; clogP, Calculated octanol-water partition coefficient; logP, Experimentally determined logP values in an octanol/water system; logD, Experimentally determined logD values in an octanol/buffer system at physiological pH of 7.4; HBD, Calculated number of hydrogen bond donor; HBA, Calculated number of hydrogen bond acceptor; SCID mice, Severe combined immune deficiency mice; MTD, Maximum tolerated dose; MCH, mean corpuscular hemoglobin; MCHC, mean corpuscular hemoglobin concentration; MCV, mean corpuscular volume; H&E stain, Haemotoxylin and Eosin stain.

REFERENCES

(1) Asche, C. Antitumour Quinones. *Mini Rev. Med. Chem.* **2005**, *5*, 449-467.

(2) O'Brien, P. J. Molecular Mechanisms of Quinone Cytotoxicity. *Chem. Biol. Interact.* **1991**, *80*, 1-41.

(3) Gewirtz, D. A. A Critical Evaluation of the Mechanisms of Action Proposed for the Antitumor Effects of the Anthracycline Antibiotics Adriamycin and Daunorubicin. *Biochem. Pharmacol.* **1999**, *57*, 727-741.

(4) Itoigawa, M.; Kashiwada, Y.; Ito, C.; Furukawa, H.; Tachibana, Y.; Bastow, K. F.; Lee, K. H. Antitumor agents. 203. Carbazole Alkaloid Murrayaquinone A and Related Synthetic Carbazolequinones as Cytotoxic Agents. *J. Nat. Prod.* **2000**, *63*, 893-897.

(5) Verweij, J.; Pinedo, H. M. Mitomycin C: Mechanism of Action, Usefulness and Limitations. *Anti-Cancer Drugs* **1990**, *1*, 5-13.

(6) Rickards, R. W.; Rothschild, J. M.; Willis, A. C.; De, C. N. M.; Kirk, J.; Kirk, K.; Saliba, K. J.; Smith, G. D. Calothrixins A and B, Novel Pentacyclic Metabolites from *Calothrix cyanobacteria* with Potent Activity Against Malaria Parasites and Human Cancer Cells. *Tetrahedron* **1999**, *55*, 13513-13520.

(7) Doan, N. T.; Stewart, P. R.; Smith, G. D. Inhibition of Bacterial RNA polymerase by the Cyanobacterial Metabolites 12-*epi*-Hapalindole E Isonitrile and Calothrixin A. *FEMS Microbiol. Lett.* **2001**, *196*, 135-139.

(8) Khan, Q. A.; Lu, J.; Hecht, S. M. Calothrixins, a New Class of Human DNA Topoisomerase I Poisons. *J. Nat. Prod.* **2009**, *72*, 438-442.

(9) Chen, X.; Smith, G. D.; Waring, P. Human Cancer Cell (Jurkat) Killing by the Cyanobacterial Metabolite Calothrixin A. *J. Appl. Phycol.* **2003**, *15*, 269-277.

(10) Mohanakrishnan, A. K.; Srinivasan, P. C. A Versatile Construction of the 8*H*-Quino[4,3-*b*]carbazole Ring System as a Potential DNA Binder. *J. Org. Chem.* **1995**, *60*, 1939-1946.

(11) Kelly, T. R.; Zhao, Y.; Cavero, M.; Torneiro, M. Synthesis of the Potent Antimalarials Calothrixin A and B. *Org. Lett.* **2000**, *2*, 3735-3737.

(12) Bernardo, P. H.; Chai, C. L. Friedel-Crafts Acylation and Metalation Strategies in the Synthesis of Calothrixins A and B. *J. Org. Chem.* **2003**, *68*, 8906-8909.

(13) Tohyama, S.; Choshi, T.; Matsumoto, K.; Yamabuki, A.; Ikegata, K.; Nobuhiro, J.; Hibino, S. A New Total Synthesis of an Indolo[3,2-*j*]phenanthridine Alkaloid Calothrixin B. *Tetrahedron Lett.* **2005**, *46*, 5263-5264.

(14) Yamabuki, A.; Fujinawa, H.; Choshi, T.; Tohyama, S.; Matsumoto, K.; Ohmura, K.; Nobuhiro, J.; Hibino, S. A Biomimetic Synthesis of the Indolo[3, 2- *j*]phenanthridine Alkaloid, Calothrixin B. *Tetrahedron Lett.* **2006**, *47*, 5859-5861.

(15) Sissouma, D.; Maingot, L.; Collet, S.; Guingant, A. Concise and Efficient Synthesis of Calothrixin B. *J. Org. Chem.* **2006**, *71*, 8384-8389.

(16) Bennasar, M. L.; Roca, T.; Ferrando, F. A New Radical-based Route to Calothrixin B. *Org. Lett.* **2006**, *8*, 561-564.

(17) McErlean, C. S. P.; Sperry, J.; Blake, A. J.; Moody, C. J. Synthesis of the Calothrixins, Pentacyclic Indolo[3,2-*j*]phenanthridine Alkaloids, Using a Biomimetic Approach. *Tetrahedron* **2007**, *63*, 10963-10970.

(18) Abe, T.; Ikeda, T.; Choshi, T.; Hibino, S.; Hatae, N.; Toyata, E.; Yanada, R.; Ishikura, M. Total Synthesis of Calothrixins A and B by Palladium Catalyzed Tandem Cyclization/cross Coupling Reaction of Indolylborate. *Eur. J. Org. Chem.* **2012**, 5018-5027.

(19) Kaliyaperumal, S.A.; Banerjee, S.; Syam Kumar, U. K. Palladium Mediated Intramolecular Multiple C-X/C-H Cross Coupling and C–H activation: Synthesis of Carbazole Alkaloids Calothrixin B and Murrayaquinone A. *Org. Biomol. Chem.* **2014**, *12*, 6105-6113.

(20) Bhosale, S. M.; Gawade, R. L.; Puranik, V. G.; Kusurkar, R. S. An Efficient Total Synthesis of Calothrixin B. *Tetrahedron Lett.* **2012**, *53*, 2894-2896.

(21) Ramkumar, N.; Nagarajan, R. Total Synthesis of Calothrixin A and B via C-H Activation. *J. Org. Chem.* **2013**, *78*, 2802-2807.

(22) Saravanan, V.; Muthu Ramalingam, B.; Mohanakrishnan, A. K. Total Synthesis of Calothrixin B and Its Analogues. *Eur. J. Org. Chem.* **2014**, 1266-1279.

(23) Xu, S.; Nguyen, T.; Pomilio, I.; Vitale, M. C.; Velu, S. E. Total Synthesis of Calothrixins A and B via Oxidative Radical Reaction of Cyclohexenone with Aminophenanthridinedione. *Tetrahedron* **2014**, *70*, 5928-5933.

(24) Mal, D. R.; Roy, J.; Biradha, K. Regiodivergent and Short Total Synthesis of Calothrixins. *Org. Biomol. Chem.* **2014**, *12*, 8196-8203.

(25) Dethe, D. H.; Murhade, G. M. Diversity-oriented Synthesis of Calothrixins and Ellipticines. *Eur. J. Org. Chem.* **2014**, 6953-6962.

(26) Bernardo, P. H.; Chai, C. L.; Heath, G. A.; Mahon, P. J.; Smith, G. D.; Waring, P.; Wilkes, B. A. Synthesis, Electrochemistry and Bioactivity of the Cyanobacterial Calothrixins and Related Quinones. *J. Med. Chem.* **2004**, *47*, 4958-4963.

(27) Bernardo, P. H.; Chai, C. L.; Le Guen, M.; Smith, G. D.; Waring, P. Structure-activity Delineation of Quinones Related to the Biologically Active Calothrixin B. *Bioorg. Med. Chem. Lett.* **2007**, *17*, 82-85.

(28) Xu, S.; Nijampatnam, B.; Dutta, S.; Velu, S, E. Cyanobacterial Metabolite Calothrixins: Recent Advances in Synthesis and Biological Evaluation. *Mar. Drugs* **2016**, *14*, 1-21.

(29) O′Sullivan, C.; Miller, C. M.; Deane, F. M.; McCarthy, F. O. Emerging Targets in the Bioactivity of Ellipticines and Derivatives: Chapter 6. Editor: Atta-ur-Rahman*, Studies in Natural Product Chemistry,* Eds. Elsevier*,* 2013, Vol. *39*, pp 189-232.

(30) Bolton, J. L.; Trush, M. a; Penning, T. M.; Dryhurst, G.; Monks, T. J. Role of Quinones in Toxicology. *Chem. Res. Toxicol.* **2000**, *13*, 135-160.

(31) Paoletti, C.; Le Pecq, J. B.; Dat-Xuong, N.; Juret, P.; Garnier, H.; Amiel, J. L.; Rouesse, J. Antitumor Activity, Pharmacology, and Toxicity of Ellipticines, Ellipticinium, and 9-

hydroxy Derivatives: Preliminary Clinical Trials of 2-Methyl-9-Hydroxy Ellipticinium (NSC 264-137). *Recent Results Cancer Res.* **1980**, *74*, 107-123.

(32) Ramalingam, B. M.; Saravanan, V.; Mohanakrishnan, A. K. Synthesis of Calothrixins and its Analogues Using $FeCl_3$-mediated Domino Reaction Protocol. *Org. Lett.* **2013**, *15*, 3726-3729.

(33) Rajeshwaran, G. G.; Mohanakrishnan, A. K. Synthetic Studies on Indolocarbazoles: Total Synthesis of Staurosporine Aglycon. *Org. Lett.* **2011**, *13*, 1418-1421.

(34) Raju, P.; Rajeshwaran, G. G.; Mohanakrishnan, A. K. Synthetic Studies on Indolocarbazoles: A Facile Synthesis of Staurosporine Analogues. *Eur. J. Org. Chem.* **2015**, 7131-7145.

(35) Mohanakrishnan, A. K.; Dhayalan, V.; Clement, A.; Balamurugan, R.; Sureshbabu, R.; Senthil Kumar, N. A One Pot Synthesis of Annulated Carbazole Analogues. *Tetrahedron Lett.* **2008**, *49*, 5850-5854.

(36) Stiborová, M.; Bieler, C. A.; Wiessler, M.; Frei, E. The Anticancer Agent Ellipticine on Activation by Cytochrome P450 Forms Covalent DNA Adducts. *Biochem. Pharmacol.* **2001**, *62*, 1675-1684.

(37) Kaufmann, S. H.; Desnoyers, S.; Ottaviano, Y. Davidson, N. E.; Poirier G. G. Specific Proteolytic Cleavage of Poly(ADP-ribose)polymerase: An Early Marker of Chemotherapy-Induced Apoptosis. *Cancer Res*. **1993**, *53*, 3976-3985.

(38) Monnot, M.; Mauffret, O.; Simon, V.; Lescot, E.; Psaume, B.; Saucier, J. M.; Belehradek, J.; Fermandjian, S. A CD Study of Interactions of Ellipticine Derivatives with DNA: Relations with the In vitro Cytotoxicity. *FEBS Lett.* **1990**, *273*, 71-74.

(39) Kohn, K. W.; Waring, M. J.; Glaubiger, D.; Friedman, C. A. Intercalative Binding of Ellipticine to DNA. *Cancer Res*. **1975**, *35*, 71-76.

(40) Kumar, C. V.; Asuncion, E. H. DNA Binding Studies and Site Selective Fluorescence Sensitization of an Anthryl Probe. *J. Am. Chem. Soc.* **1993**, *115*, 8547-8553.

(41) Allenmark, S. Induced Circular Dichroism by Chiral Molecular Interaction, *Chirality*, **2003**, *15*, 409-422.

(42) Waring, M. J. DNA Modification and Cancer. *Annu. Rev. Biochem.* **1981**, *50*, 159-192.

(43) Haq, I.; Ladbury, J. Drug-DNA Recognition: Energetics and Implications for Design. *J. Mol. Recognit.* **2000**, 188-197.

(44) Urasaki, Y.; Laco, G, S.; Pourquier, P.; Yuji Takebayashi, Y.; Kohlhagen, G.; Gioffre, C.; X Zhang, H.; Devasis Chatterjee, D.; Pantazis, P.; Pommier, Y. Characterization of a Novel Topoisomerase I Mutation from a Camptothecin-Resistant Human Prostate Cancer Cell line. *Cancer Res*. **2001**, *61*, 1964-1969.

(45) Chiang, P-C.; Hu. Y. Simultaneous Determination of logP, logD and pKa of Drugs by Using a Reverse Phase HPLC Coupled with a 96-well Plate Auto Injector. *Comb. Chem. High Throughput Screen.* **2009**, *12*, 250-257.

(46) Monks, T. J.; Jones, D. C. The Metabolism and Toxicity of Quinones, Quinonimines, Quinone Methides, and Quinone-Thioethers. *Curr. Drug Metab.* **2002**, *3*, 425-438.

(47) Skehan, P.; Storeng, R.; Scudiero, D.; Monks, A.; McMahon, J.; Vistica, D.; Warren, J. T.; Bokesch, H.; Kenney, S.; Boyd, M. R. New Colorimetric Cytotoxicity Assay for Anticancer-drug Screening. *J. Natl. Cancer Inst.* **1990**, *82*, 1107-1112.

(48) Vichai V.; Kirtikara K. Sulforhodamine B Colorimetric Assay for Cytotoxicity Screening. *Nat. Protoc.* **2006**, *1*, 1112-1116.

(49) Stewart, L.; Ireton, G. C.; Parker, L. H.; Madden K. R.; Champoux J. J. Biochemical and Biophysical Analyses of Recombinant Forms of Human Topoisomerase I. *J. Biol. Chem.* **1996,** *271*, 7593-7601.

(50) Ganguly, A.; Das, B. B.; Sen, N.; Roy, A.; Dasgupta S. B.; Majumder H. K. LeishMan' Topoisomerase I: An Ideal Chimera for Unraveling the Role of the Small Subunit of Unusual Bi-subunit Topoisomerase I from *Leishmania donovani*. *Nucl. Acid. Res.* **2006**, *34*, 6286-6297.

(51) Kumar, A.; Chowdhury, S. R.; Sarkar, T.; Chakrabarti, T.; Majumder, H. K.; Jha, T.; Mukhopadhyay, S. A New Bisbenzylisoquinoline Alkaloid Isolated from *Thalictrum foliolosum*, as a Potent Inhibitor of DNA Topoisomerase IB of *Leishmania donovani*. *Fitoterapia.* **2016**, *109,* 25-30.

(52) Sengupta, T.; Mukherjee, M.; Das, R.; Das, A.; Majumder, H. K. Characterization of the DNA-binding Domain and Identification of the Active Site Residue in the "Gyr A" Half of Leishmania Donovani Topoisomerase II. *Nucleic Acids Res.* **2005**, *33*, 2364-2373.

(53) (a) Amrita, A.; Priya, R.; Hridya, H.; Sivaramakrishna, A.; Babu, S.; Siva, R. Studies on Interaction of Norbixin with DNA: Multispectroscopic and In silico Analysis. *Spectrochimica Acta.* **2015**, *144*, 163-169. (b) Ghosh, P.; Devi, G. P.; Priya, R.; Amrita, A.; Sivaramakrishna, A.; Babu, S.; Siva, R. Spectroscopic and In silico Evaluation of Interaction of DNA with Six Anthraquinone Derivatives. *Appl. Biochem. Biotech.* **2013**, *170*, 1127-1137.

(54) Bhakta, D.; Siva, R. Morindone, an Anthraquinone, Intercalates DNA Sans Toxicity: A Spectroscopic and Molecular Modeling Perspective. *Appl. Biochem. Biotech.* **2012**, *167*, 885-896.

(55) Pommier, Y.; Covey, J. M.; Kerrigan, D.; Markovits, J.; Pham, R. DNA Unwinding and Inhibition of Mouse Leukemia L1210 DNA Topoisomerase I by Intercalators. *Nucleic Acids Res.* **1987**, *15,* 6713-6731.

(56) Li, Z.; Wan, H.; Shi, Y.; Ouyang, P. Personal Experience with Four Kinds of Chemical Structure Drawing Software: Review on ChemDraw, ChemWindow, ISIS/Draw, and ChemSketch. *J. Chem. Inf. Comput. Sci.* **2004**, *44*, 1886-1890.

(57) Pettersen, E. F.; Goddard, T. D.; Huang, C. C.; Couch, G.S.; Greenblatt, D. M.; Meng, E. C.; Ferri, T. E. UCSF Chimera Visualization System for Exploratory Research and Analysis. *J. Comput. Chem.* **2004**, *25*, 1605-1612.

(58) Morris, G. M.; Huey, R.; Lindstrom, W.; Sanner, M. F.; Belew, R. K.; Goodsell, D. S.; Olson, A. J. AutoDock4 and AutoDockTools 4: Automated Docking with Selective Receptor Flexibility. *J. Comput. Chem.* **2009**, *30*, 2785-2791.

(59) Lill, M. A.; Danielson, M. L. Computer-aided Drug Design Platform using PyMOL. *J. Comput. Aided Mol. Des.* **2010**, *25*, 13-19.

(60) Sastry, G. M.; Adzhigirey, M.; Day, T.; Annabhimoju, R.; Sherman, W. Protein and Ligand Preparation: Parameters, Protocols and Influence on Virtual Screening Enrichments. *J. Comput. Aided Mol. Des*. **2013**, *27*, 221-234.

(61) Basarab, G. S.; Manchester, J. I.; Bist, S.; Boriack-Sjodin, P. A.; Dangel, B.; Illingworth, R.; Sherer, B. A.; Sriram, S.; Uria-Nickelsen, M.; Eakin, A. E. Fragment-to-hit-to-lead Discovery of a Novel Pyridylurea Scaffold of ATP Competitive Dual Targeting Type II Topoisomerase Inhibiting Antibacterial Agents. *J. Med. Chem*. **2013**, *56*, 8712-8735.

(62) Friesner, R. A.; Banks, J. L.; Murphy, R. B.; Halgren, T. A.; Klicic, J. J.; Mainz, D. T.; Repasky, M. P.; Knoll, E. H.; Shelley, M.; Perry, J.K.; Shaw, D. E.; Francis, P.; Shenkin, P.

S. Glide: A New Approach for Rapid, Accurate Docking and Scoring 1. Method and Assessment of Docking Accuracy. *J. Med. Chem.* **2004**, *47*, 1739-1749.

(63) Halgren, T. A.; Murphy, R. B.; Friesner, R. A.; Beard, H. S.; Frye, L. L.; Pollard, W. T.; Banks, J. L. Glide: A New Approach for Rapid, Accurate Docking and Scoring 2. Enrichment Factors in Database Screening. *J. Med. Chem.* **2004**, *47*, 1750-1759.

(64) Pettersen, E. F.; Goddard, T. D.; Huang, C. C.; Couch, G. S.; Greenblatt D. M.; Meng E. C.; Ferrin, T. E. UCSF Chimera-A Visualization System for Exploratory Research and Analysis. *J. Comput. Chem.* **2004**, *25*, 1605-1612.

Table of Contents graphic

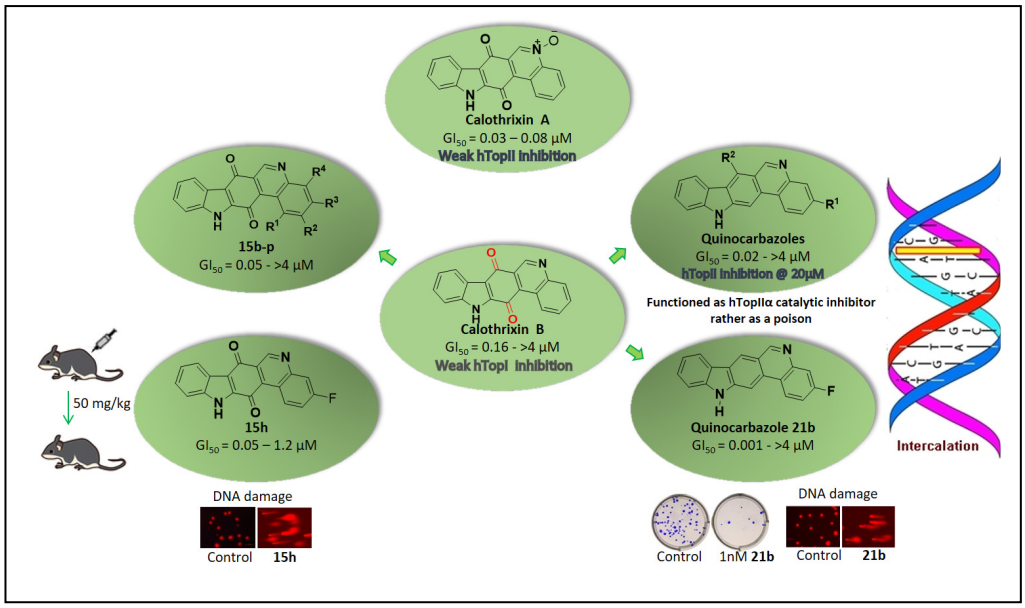

Synthesis and Biological Evaluation of Calothrixins B and their Deoxygenated Analogues

Authors List:

Bose Muthu Ramalingam,[1] Nachiappan Dhatchana Moorthy,[2,4] Somenath Roy Chowdhury,[3] Thiyagarajan Mageshwaran,[1] Elangovan Vellaichamy,[2] Sourav Saha,[3] Karthikeyan Ganesan,[4] B. Navin Rajesh,[3] Saleem Iqbal,[5] Hemanta K. Majumder,[3] Krishnasamy Gunasekaran,[5] Ramamoorthy Siva,[6] and Arasambattu K. Mohanakrishnan[1*]

[1] Department of Organic Chemistry, University of Madras, Chennai 600 025, India

[2] Department of Biochemistry, University of Madras, Chennai 600 025, India

[3] Division of Infectious Diseases & Immunology, Indian Institute of Chemical Biology, 4 Raja S. C. Mullick Road, Jadavpur, Kolkata 700032, India.

[4] Research and Development Centre, Orchid Pharma Ltd, Sholinganallur, Chennai 600 119, India

[5] CAS in Crystallography & Biophysics, University of Madras, Chennai 600 025, India

[6] School of Bio Sciences and Technology, VIT University, Vellore 632 014, India

Graphics File

Chart 1. Calothrixin A (1), Calothrixin B (2) and its Analogues 3-6

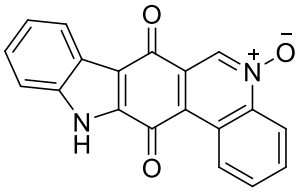

calothrixin A **1**

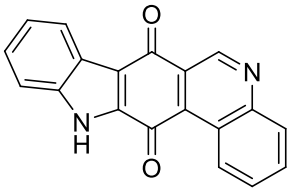

calothrixin B **2**

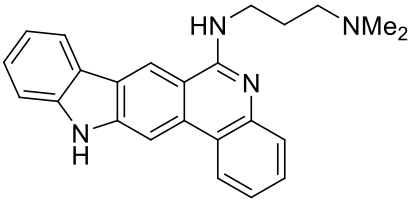

quino[4,3-*b*]carbazole **3**

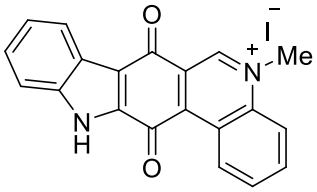

N-methylcalothrixin B **4**

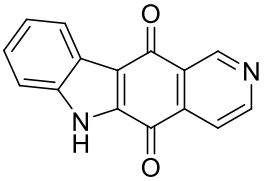

ellipticine quinone **5**

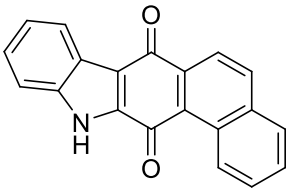

indolophenanthrene-7,10-dione **6**

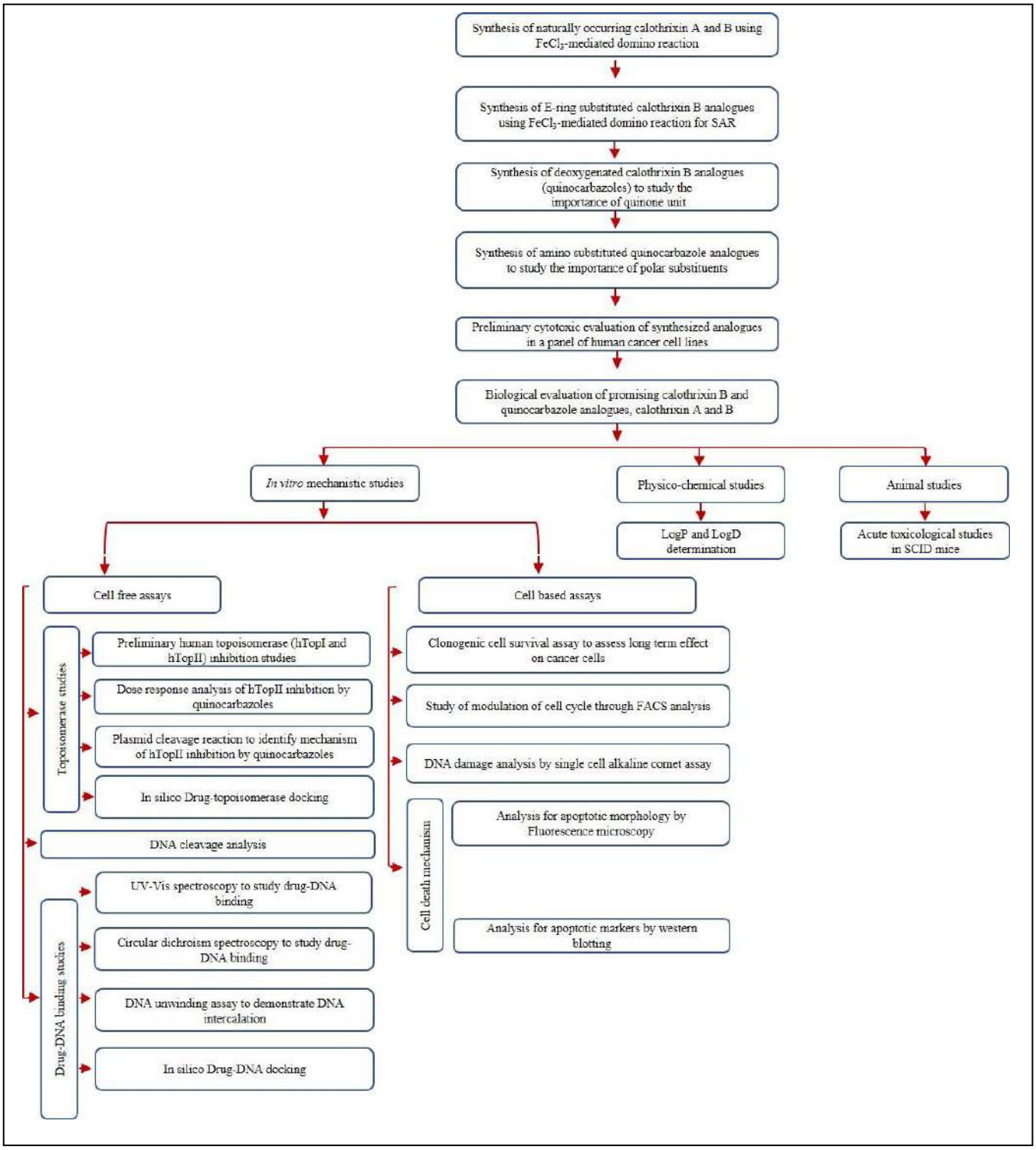

Fig. 1. Schematic representation of synthetic and biological studies carried on calothrixin and its analogues

Scheme 1[a]

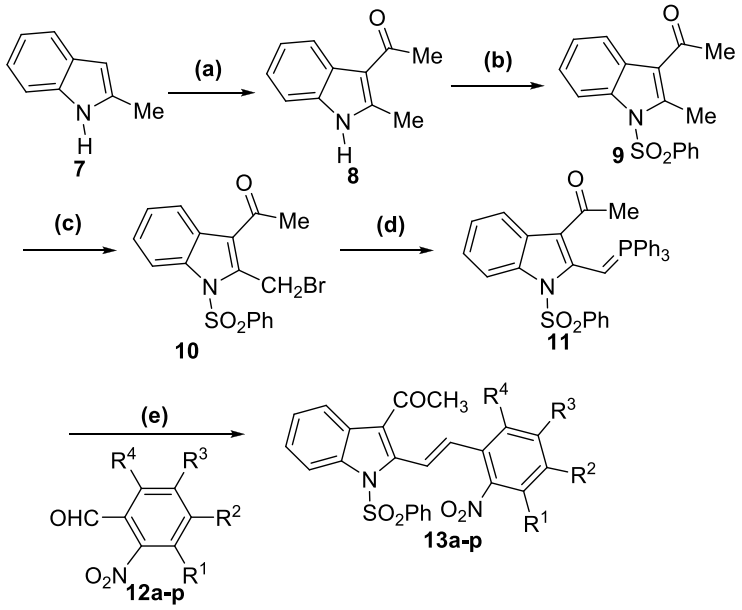

13	R^1	R^2	R^3	R^4	yield (%)
a	H	H	H	H	92
b	OMe	H	H	H	85
c	H	H	OMe	H	92
d	H	OMe	OMe	H	88
e	H	$-OCH_2O-$		H	90
f	H	Br	H	H	90
g	H	Cl	H	H	94
h	H	F	H	H	93
i	H	H	Br	H	90
j	H	H	Cl	H	91
k	H	H	H	Cl	80
l	Cl	H	H	H	89
m	H	F	Br	H	89
n	H	F	Cl	H	90
o	H	Cl	Cl	H	93
p	Cl	H	Cl	H	90

[a]Reagents and conditions : (a) DMA, $POCl_3$; (b) $PhSO_2Cl$, PTC, Benzene, 50% NaOH, rt,1 h; (c) NBS, AIBN, CCl_4, reflux, 3 h; (d) PPh_3, THF, reflux, 2 h followed by K_2CO_3, DCM rt, 12 h; (e) 12a-p, DCM/DCE, reflux, 6-12 h.

Scheme 2[a]

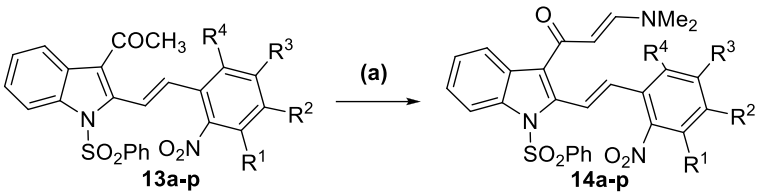

14	R^1	R^2	R^3	R^4	yield (%)
a	H	H	H	H	89[a]
b	OMe	H	H	H	85[a]
c	H	H	OMe	H	90[a]
d	H	OMe	OMe	H	97[b]
e	H	$-OCH_2O-$		H	85[a]
f	H	Br	H	H	96[b]
g	H	Cl	H	H	92[a]
h	H	F	H	H	91[a]
i	H	H	Br	H	92[a]
j	H	H	Cl	H	96[b]
k	H	H	H	Cl	88[a]
l	Cl	H	H	H	91[a]
m	H	F	Br	H	89[a]
n	H	F	Cl	H	88[a]
o	H	Cl	Cl	H	88[a]
p	Cl	H	Cl	H	86[a]

[a]isolated yield, [b]Crude yield of enamine

[a]Reagents and conditions : (a) DMF.DMA, glycocyamine (50 mol %), 100 °C, 3-5 h.

Scheme 3[a]

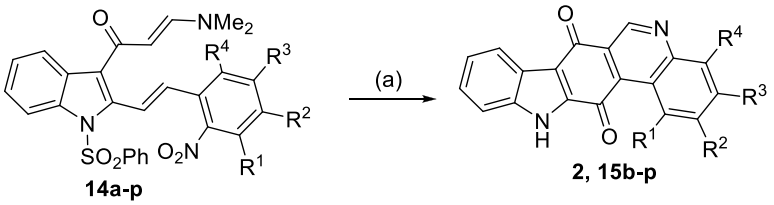

Compound	R^1	R^2	R^3	R^4	yield (%)
2	H	H	H	H	65
15b	H	H	H	OMe	45
15c	H	OMe	H	H	65
15d	H	OMe	OMe	H	57
15e	H	$-OCH_2O-$		H	60
15f	H	H	Br	H	64
15g	H	H	Cl	H	67
15h	H	H	F	H	64
15i	H	Br	H	H	65
15j	H	Cl	H	H	62
15k	Cl	H	H	H	65
15l	H	H	H	Cl	52
15m	H	Br	F	H	63
15n	H	Cl	F	H	62
15o	H	Cl	Cl	H	65
15p	H	Cl	H	Cl	65

[a]Reagents and conditions : (a) 3 equiv $FeCl_3$, DMF, reflux, 3 h.

Scheme 4[a]

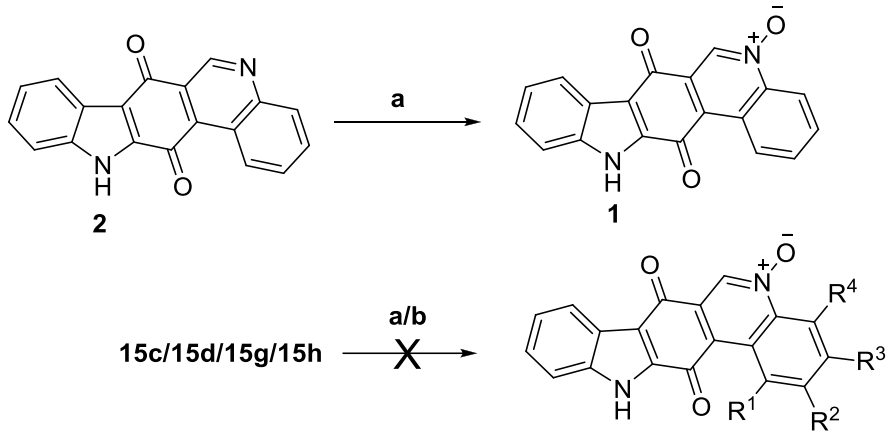

[a]Reagents and conditions : (a) *m*-CPBA, DCM, reflux, 18 h. (b) oxone, acetone, K_2CO_3, rt

Scheme 5[a]

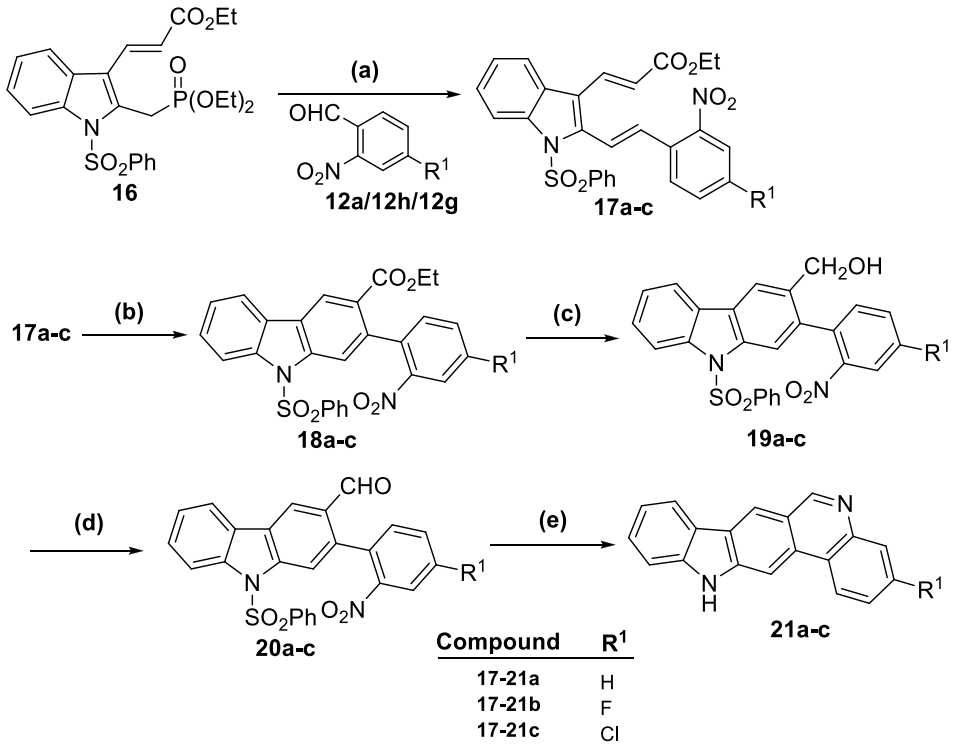

[a]Reagents and conditions : (a) K_2CO_3, DMF, rt, 12 h, 85-88%; (b) 10% Pd-C, xylenes, reflux, 24 h, 80-85%;(c) DIBAL-H, DCM, 0 °C, 30 min; (d) PCC, celite, DCM, rt, 2 h, 77-80% (2 steps); (e) i) Ra-Ni, THF, rt, 3 h; ii) 50% NaOH, DMSO, rt, 6 h, 71-76% (2 steps)

Scheme 6[a]

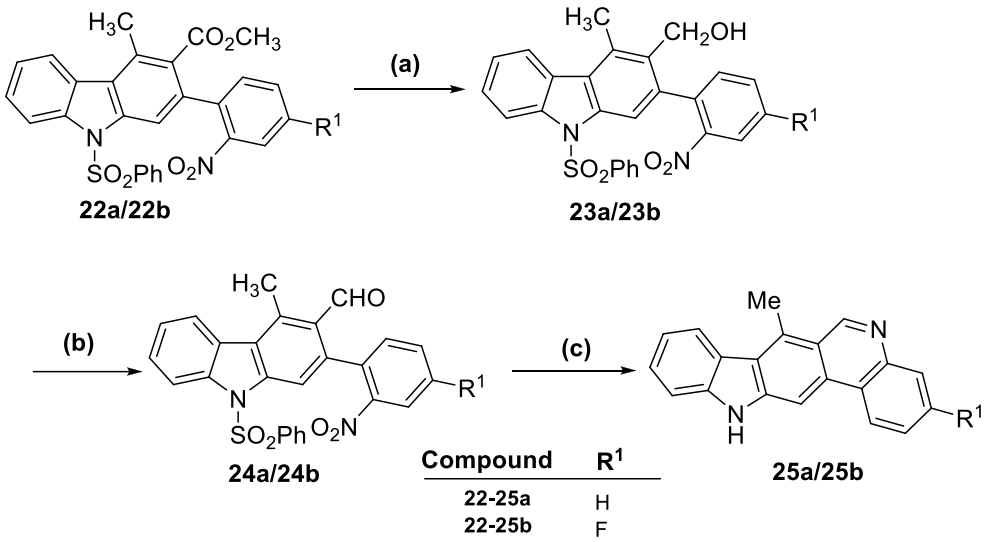

[a]Reagents and conditions : (a) DIBAL-H, DCM, 0 °C, 30 min; (b) PCC, celite, DCM, rt, 2 h, 73-75% (2 steps);(c) i) Ra-Ni, THF, rt, 3 h; ii) 50% NaOH, DMSO, rt, 6 h. 72-75% (2 steps)

Scheme 7[a]

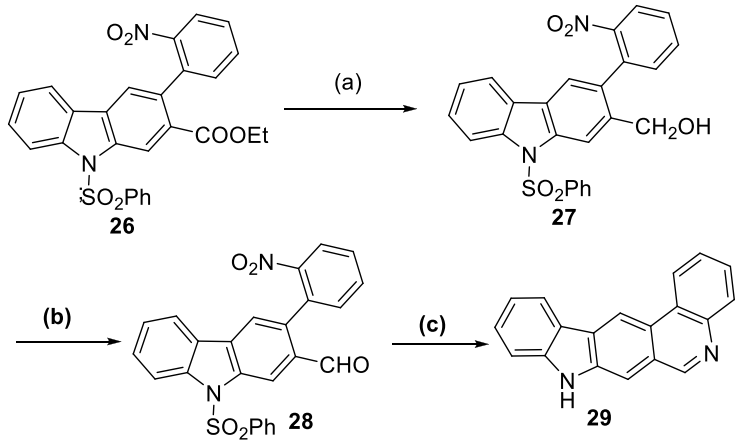

[a]Reagents and conditions : (a) DIBAL-H, DCM, 0 °C, 30 min; (b) PCC, celite, DCM, rt, 2 h, 76% (two steps);(c) i) Ra-Ni, THF, rt, 3 h; ii) 50% NaOH, DMSO, rt, 6 h, 75% (two steps).

Scheme 8[a]

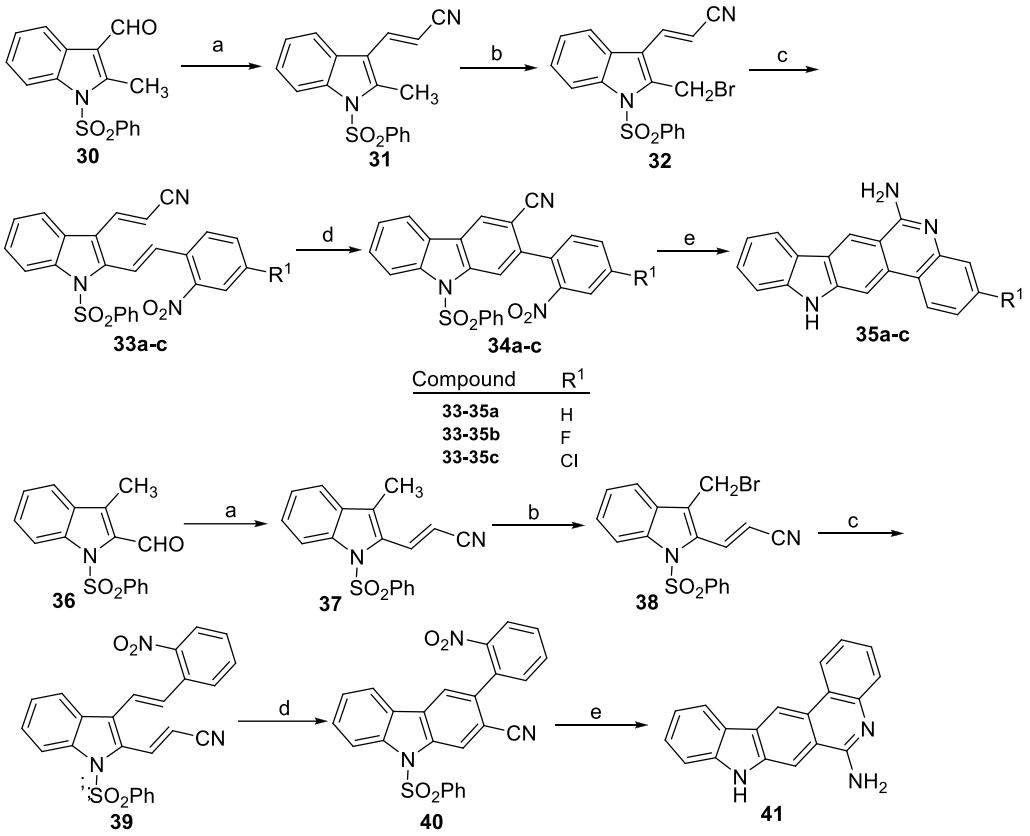

Compound	R^1
33-35a	H
33-35b	F
33-35c	Cl

[a]Reagents and conditions : (a) Ph_3P=CHCN, xylenes, reflux, 8 h, 84-86%;(b) NBS, AIBN, CCl_4, reflux, 45 min, 89-91%; (c) PPh_3, THF, reflux, 3 h, followed by K_2CO_3, DCM rt, 8 h, 74-83%; (d) 10% Pd-C, xylenes, reflux, 24 h, 81-85%; (e) i) Ra-Ni, THF, reflux, 30 min; ii) 50% NaOH, DMSO, rt, 3 h, 74-78% (two steps).

Scheme 9[a]

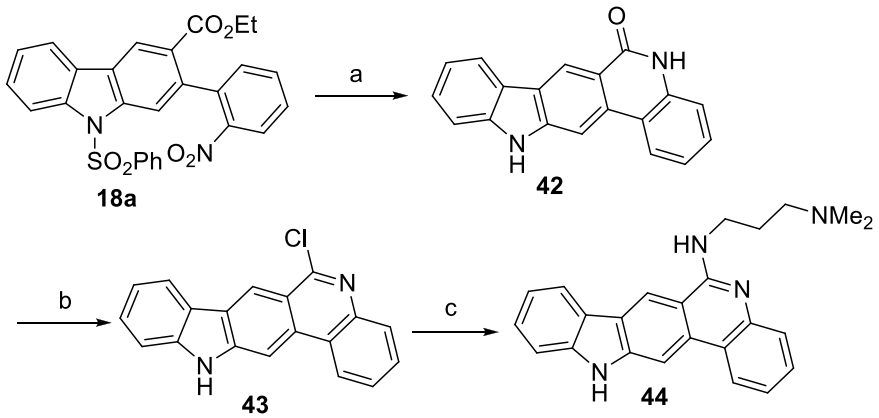

[a]Reagents and conditions : (a) i) Ra-Ni, THF, reflux, 4 h; ii) 50% NaOH, DMSO, rt, 12 h, 78% (two steps); (b) $POCl_3$, reflux, 24 h, 79%; (c) $NH_2(CH_2)_3NMe_2$, reflux, 20 h, 75%.

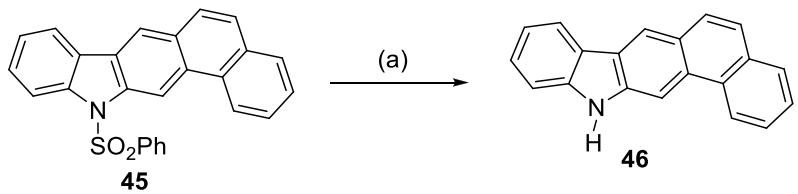

[a]Reagents and conditions : (a) 50% NaOH, DMSO, rt, 6 h, 84%

Table 1. *In vitro* cytotoxicity data for calothrixins **1**, **2** and **15b-p** against nine human tumor cell lines

	GI_{50} Average ± S.D. (μM)[a]																	
Compound	**Jurkat**		**HeLa**		**SiHa**		**MCF7**		**HCT116**		**HCT116 p53-/-**		**MDA-MB 231**		**U251**		**NCI-H460**	
1	0.07	± 0.01	0.08	± 0.00	0.05	± 0.05	0.03	± 0.0	0.11	± 0.05	0.08	± 0.01	0.04	± 0.01	0.08	± 0.01	0.22	± 0.02
2	>4		0.47	± 0.09	3.50	± 0.71	0.26	± 0.01	0.65	± 0.07	2.55	± 0.92	0.16	± 0.02	2.25	± 0.35	>4	
15b	>4		0.39	± 0.20	>4		0.60	± 0.42	0.33	± 0.06	>4		0.31	± 0.01	1.83	± 0.32	>4	
15c	>4		>4		>4		>4		0.63	± 0.11	>4		>4		>4		>4	
15d	>4		>4		>4		0.36	± 0.34	>4		>4		>4		>4		>4	
15e	>4		>4		>4		0.11	± 0.01	>4		>4		>4		>4		>4	
15f	1.50	± 0.57	0.21	± 0.13	>4		0.60	± 0.28	1.50	± 0.42	2.60	± 0.57	1.00	± 0.00	2.00	± 0.42	1.27	± 0.06
15g	3.55	± 0.64	0.07	± 0.02	1.60	± 0.57	0.53	± 0.38	1.50	± 0.28	2.60	± 0.71	0.36	± 0.04	2.83	± 0.29	1.40	± 0.14
15h	1.15	± 0.07	0.05	± 0.02	0.93	± 0.12	0.85	± 0.07	0.83	± 0.06	1.10	± 0.14	0.30	± 0.12	1.20	± 0.22	1.18	± 0.13
15i	1.50	± 0.71	0.29	± 0.05	1.40	± 0.14	0.22	± 0.05	0.70	± 0.00	1.13	± 0.15	0.27	± 0.05	0.60	± 0.14	1.10	± 0.14
15j	1.40	± 0.28	0.50	± 0.14	1.67	± 0.19	0.35	± 0.22	0.42	± 0.17	1.50	± 0.42	0.17	± 0.00	0.50	± 0.00	0.70	± 0.42
15k	>4		>4		>4		0.80	± 0.42	3.50	± 0.71	>4		>4		>4		>4	
15l	>4		>4		>4		>4		>4		>4		>4		>4		>4	
15m	>4		0.27	± 0.11	>4		0.66	± 0.76	>4		>4		0.4	± 0.14	>4		2.25	± 0.78
15n	>4		2.00	± 0.00	>4		1.35	± 0.35	>4		>4		>4		>4		>4	
15o	>4		1.80	± 0.00	>4		>4		>4		>4		1.80	± 0.28	>4		>4	
15p	2.60	± 0.57	0.50	± 0.00	1.80	± 0.00	0.50	± 0.00	1.20	± 0.14	2.00	± 0.00	0.2	± 0.00	1.50	± 0.28	0.73	±0.25
CPT	0.06	± 0.01	0.19	± 0.03	0.55	± 0.00	0.06	± 0.00	0.05	± 0.01	0.195	± 0.01	0.4	± 0.01	0.01	±0.0071	0.0057	±0.0029

[a] Values represents mean from at least two independent experiment

Table 2. *In vitro* cytotoxicity data for quinocarbazoles **21a-c**, **25a, b** and **29**, naphthocarbazole **31** against ten human tumor cell lines

	GI$_{50}$ Average ± S.D. (µM)[a]									
Name	**Jurkat**	**HeLa**	**SiHa**	**MCF7**	**HCT116**	**MDA-MB 231**	**U251**	**NCI-H460**	**HEK293**	**A549**
21a	4.00 ± 0.00	0.41 ± 0.08	>4	>4 ± 0.07	11.5 ± 0.07	>4	>4	5.5 ± 0.70	>4	>4
21b	>4	0.02 ± 0.01	>4	0.02 ± 0.01	6 ± 0.05	0.95 ± 0.07	>4	0.0010 ±0.0002	0.0052 ±0.0021	>4
21c	>4	0.43 ± 0.18	>4	>4 ± 0.23	28 ± 0.23	>4	>4	10 ± 0.00	>4	>4
25a	>4	0.36 ± 0.06	>4	>4 ± 0.00	15 ± 0.00	>4	>4	10.5 ± 0.70	>4	>4
25b	>4	0.05 ± 0.01	>4	0.27 ± 0.02	30 ± 0.12	>4	>4	0.04 ± 0.04	>4	>4
29	>4	1.40 ± 0.14	>4	>4	>50	>4	>4	10 ± 0.05	>4	>4
46	>4	>4	>4	>4	>50	>4	>4	>50	>4	>4

[a] Values represents mean from at least two independent experiments

Table 3. *In vitro* cytotoxicity data for amino quinocarbazoles **35a-c, 41** and **44** against seven human tumor cell lines

	GI$_{50}$ Average ± S.D. (µM)[a]							
Name	**HeLa**	**SiHa**	**MCF7**	**HCT116**	**MDA-MB 231**	**U251**	**NCI-H460**
35a	0.80 ± 0.14	1.05 ± 0.07	1.00 ± 0.14	1.00 ± 0.09	1.00 ± 0.1	1.05 ± 0.09	1.00 ± 0.05
35b	0.01 ± 0.008	1.35 ± 0.21	0.13 ± 0.07	1.20 ± 0.0	1.25 ± 0.35	1.20 ± 0.14	0.14 ± 0.04
35c	0.53 ± 0.10	1.10 ± 0.00	0.95 ± 0.07	1.00 ± 0.0	0.90 ± 0.28	1.20 ± 0.00	1.05 ± 0.07
41	1.40 ± 0.14	1.30 ± 0.28	1.00 ± 0.00	1.05 ± 0.07	1.10 ± 0.00	0.65 ± 0.21	1.05 ± 0.12
44	1.10 ± 0.00	1.15 ± 0.07	2.75 ± 0.35	1.75 ± 0.35	1.00 ± 0.14	1.35 ± 0.21	1.50 ± 0.70

[a] Values represents mean from at least two independent experiments

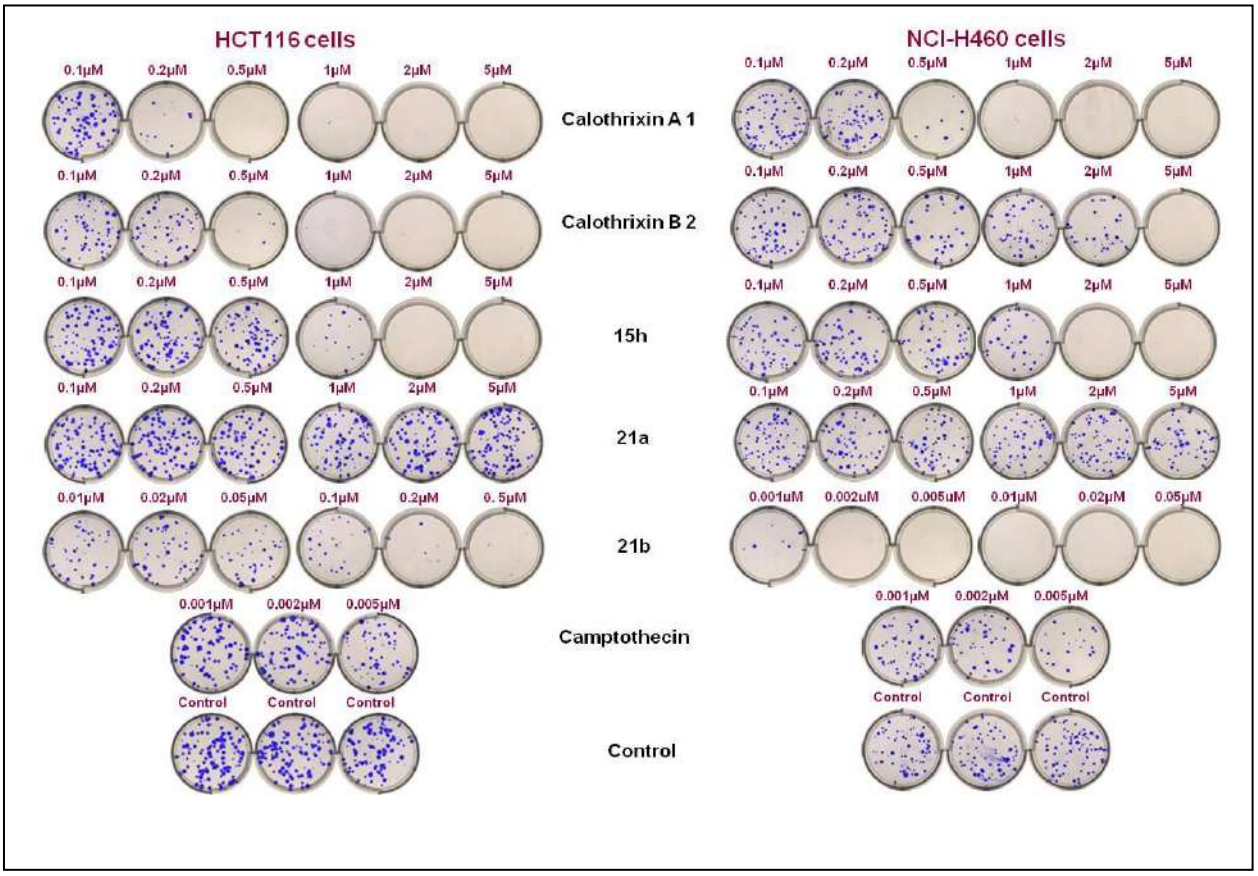

Fig. 2. Effects of calothrixin A**1**, B**2**, **15h** and Quinocarbazoles **21a**, **21b** on the clonogenic growth of colon adenocarcinoma (HCT116) and Lung adenocarcinoma (NCI-H460) cell lines.

Cells were seeded in a six well plate and after over-night adherence, treated with different concentrations (0.1 – 5 μM) of calothrixin A**1**, B**2**, **15h** and quinocarbazoles **21a**, **21b** (HCT116), 0.001 – 0.05 μM of quinocarbazole **21b** in case of NCI-H460 cells, for 48 h. After drug treatment, the cells were washed with Dulbecco's phosphate buffered saline and let grow up to 14 days in drug-free medium. Cell colonies were stained with crystal violet and photographed.

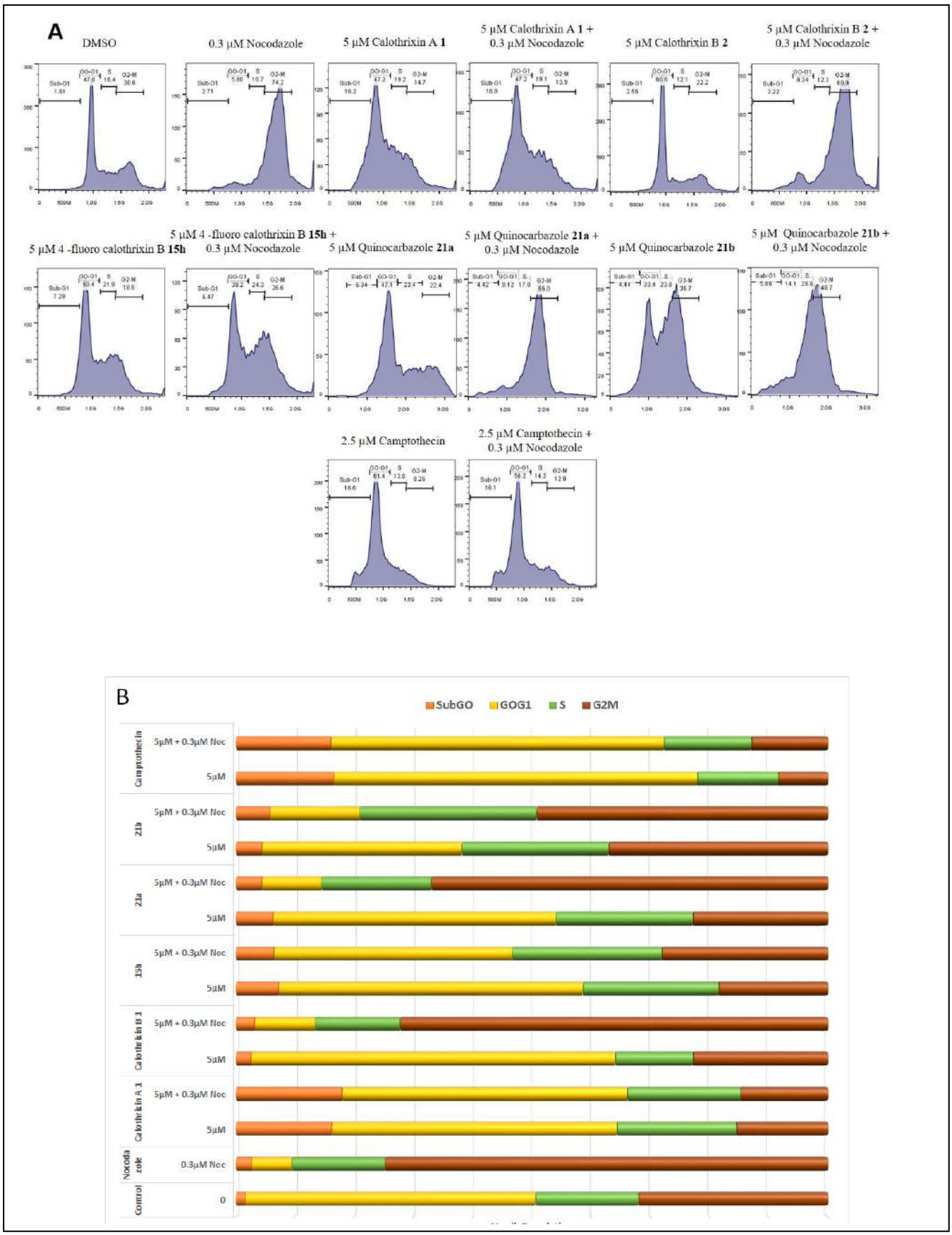
A
DMSO
0.3 μM Nocodazole
5 μM Calothrixin A 1
5 μM Calothrixin A 1 + 0.3 μM Nocodazole
5 μM Calothrixin B 2
5 μM Calothrixin B 2 + 0.3 μM Nocodazole
5 μM 4 -fluoro calothrixin B 15h
5 μM 4 -fluoro calothrixin B 15h + 0.3 μM Nocodazole
5 μM Quinocarbazole 21a
5 μM Quinocarbazole 21a + 0.3 μM Nocodazole
5 μM Quinocarbazole 21b
5 μM Quinocarbazole 21b + 0.3 μM Nocodazole
2.5 μM Camptothecin
2.5 μM Camptothecin + 0.3 μM Nocodazole
B
SubGO
GOG1
S
G2M
Camptothecin
5μM + 0.3μM Noc
5μM
21b
21a
15h
Calothrixin B 1
Calothrixin A 1
Nocodazole
0.3μM Noc
Control
0

Fig. 3. Cell cycle effects of calothrixin and its analogues. Cell cycle perturbation by calothrixins (**1**, **2**, and **15h**) or Quinocarbazoles (**21a** and **21b**) in the presence or absence of nocodazole. HCT116 cells were treated with 5 µM of calothrixin and its analogues for 20 h or 3 h pretreatment with 17 h in the presence of nocodazole (0.3 µM) followed by propidium iodide staining. Population of cells in different phases of cell cycle were analysed by flow cytometry. Figure is representative of other two experiments. (B) Percentages of HCT116 cells in the different phases of the cell cycle

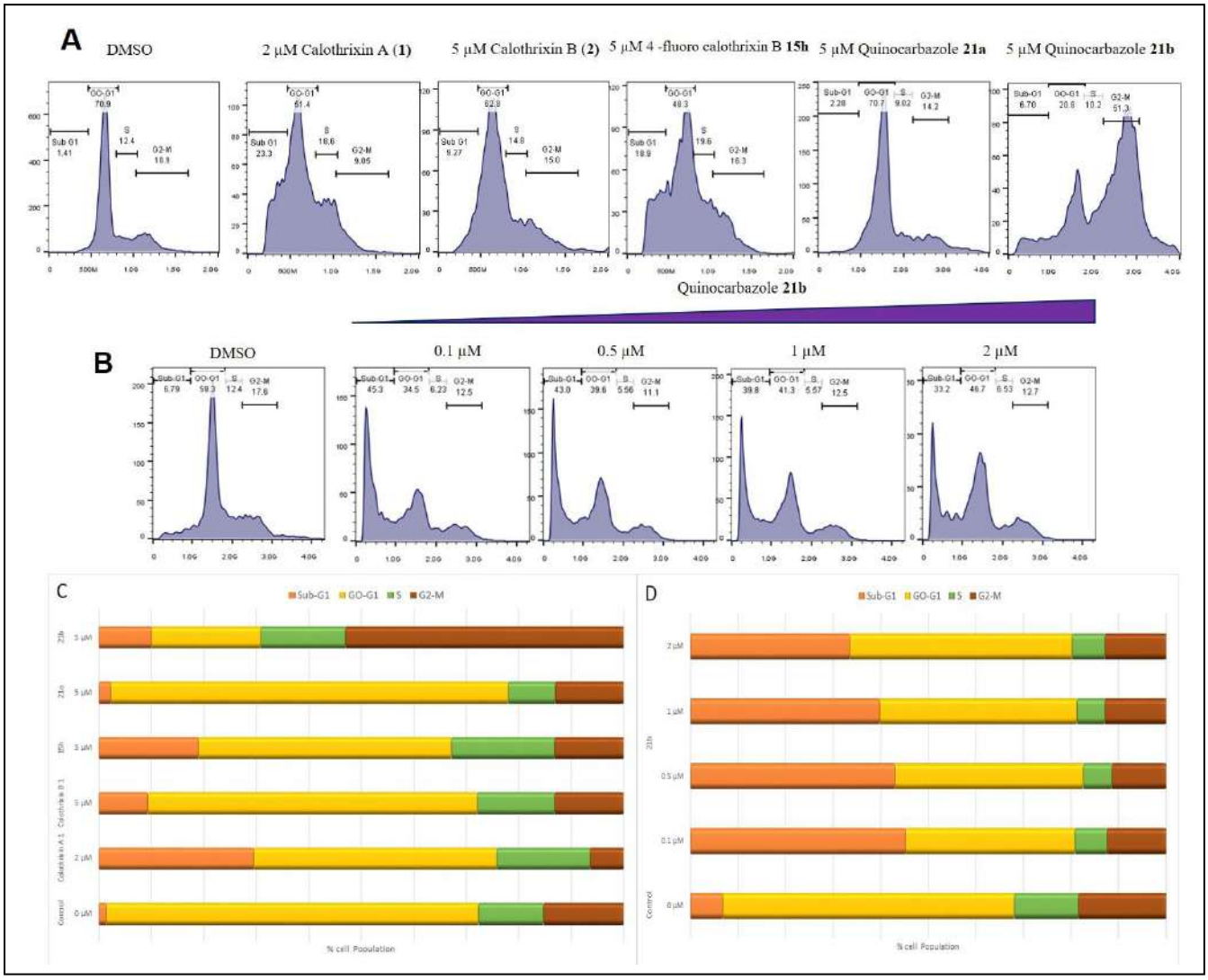

Fig. 4. (A) Cell cycle analysis of human colon HCT116 cells treated with the calothrixins (**1**, **2**, and **15h**) or quinocarbazoles (**21a** and **21b**) for 48 h. (B) Lung NCI-H460 cells treated with increasing concentrations of quinocarbazoles **21b** for 48 h. Figures are representative of other two experiments. (C&D) Percentages of HCT116 (A) or NCI-H460 (B) cells in the different phases of the cell cycle

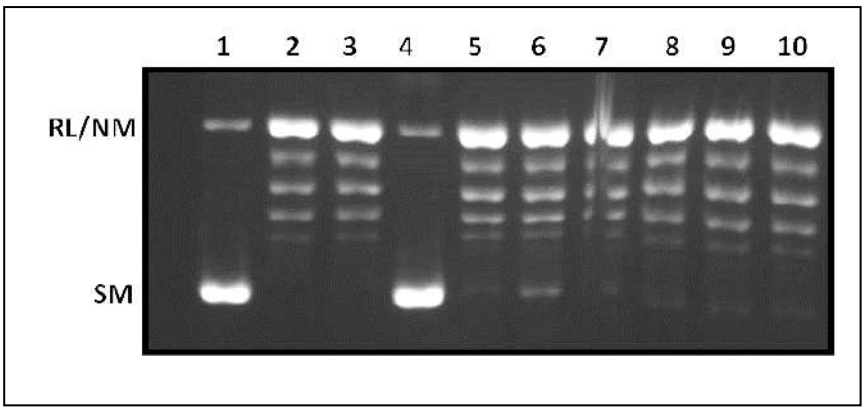

Fig. 5. Effects of calothrixin and quinocarbazole analogues on recombinant human topoisomerase I: Relaxation of negatively supercoiled pBS (SK+) DNA with purified hTopI at a molar ratio of 3:1 in simultaneous assay condition. Lane 1, 90 fmol of pBS (SK+) DNA; Lane 2, same as lane 1, but simultaneously incubated with 30 fmol of hTopI for 30 mins at 37 ºC; Lane 3, same as lane 2 but in presence of 2% v/v DMSO; Lane 4, same as lane 2 but in presence of 25 µM camptothecin as positive control; Lanes 5-10, same as lane 2 but in presence of 200 µM concentration of calothrixin A **1**, calothrixins B **2**, **15h**, quinocarbazoles**21a**, **21b** and **25a**, respectively. Positions of supercoiled monomer (SM) and relaxed and nicked monomer (RL/NM) are indicated.All results depicted were performed three times and representative data are from one set of these experiments.

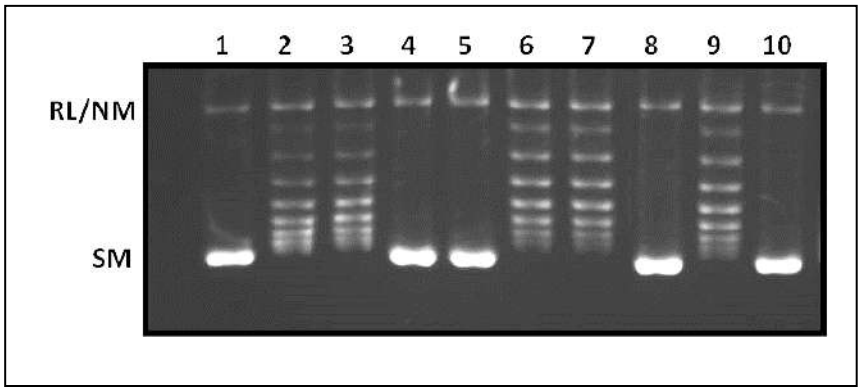

Fig. 6. Effects of calothrixin and quinocarbazole analogues on recombinant human topoisomerase II: Relaxation of negatively supercoiled pBS (SK+) DNA with purified hTopII at a molar ratio of 3:1 in simultaneous assay condition. Lane 1, 90 fmol of pBS (SK+) DNA; Lane 2, same as lane 1, but simultaneously incubated with 30 fmol of hTopII for 30 mins at 37 ºC; Lane 3, same as lane 2 but in presence of 2% v/v DMSO; Lane 4, same as lane 2 but in presence of 25 µM etoposide as positive control; Lanes 5-10, same as lane 2 but in presence of 200 µM concentration of calothrixin A **1**, calothrixins B **2**, **15h**, quinocarbazoles **21a**, **21b** and **25a**, respectively. Positions of supercoiled monomer (SM) and relaxed and nicked monomer (RL/NM) are indicated. All results depicted were performed three times and representative data are from one set of these experiments.

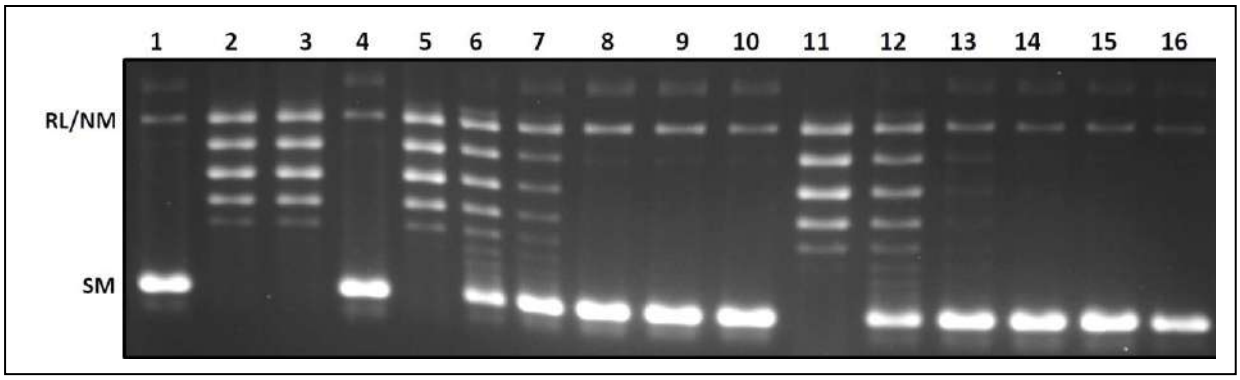

Fig. 7. Dose-dependent inhibition of recombinant human topoisomerase II by quinocarbazole analogues **21a** and **25a**: Relaxation of negatively supercoiled pBS (SK+) DNA with purified hTopII at a molar ratio of 3:1 in simultaneous assay condition. Lane 1, 90 fmol of pBS (SK+) DNA; Lane 2, same as lane 1, but simultaneously incubated with 30 fmol of hTopII for 30 mins at 37 ºC; Lane 3, same as lane 2 but in presence of 2% v/v DMSO; Lane 4, same as lane 2 but in presence of 25 µM etoposide as positive control; Lanes 5-10, same as lane 2 but in presence of increasing concentrations (10, 20, 30, 40, 50, and 60 µM) of quinocarbazole **21a** and Lanes 11-16, same as lane 2 but in presence of increasing concentrations(10, 20, 30, 40, 50, and 60 µM) of quinocarbazole **25a**. Positions of supercoiled monomer (SM) and relaxed and nicked monomer (RL/NM) are indicated. All results depicted were performed three times and representative data are from one set of these experiments

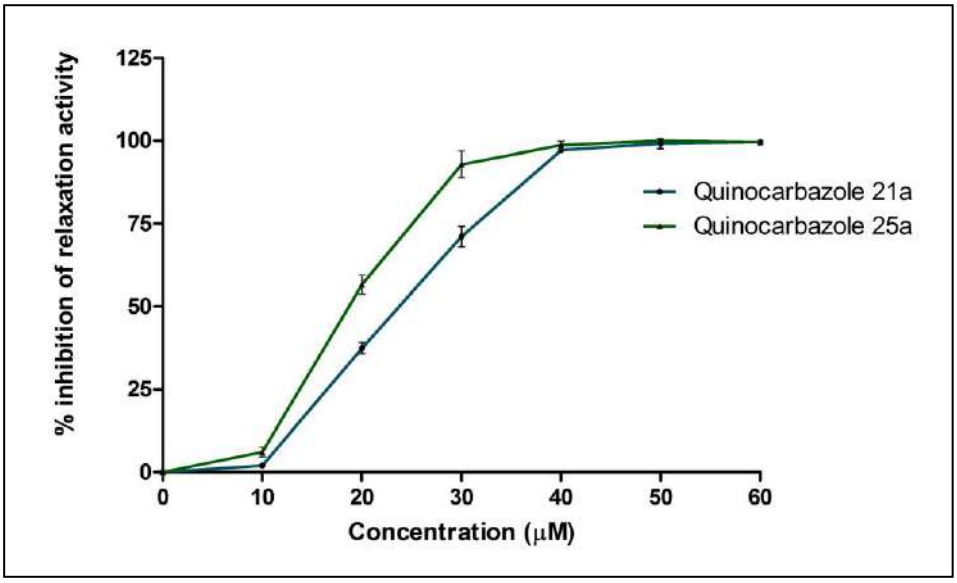

Fig. 8. Quantitative representation of enzyme inhibition as a function of concentrations of quinocarbazoles **21a** and **25a** under standard relaxation condition. Data represent mean value ± S.D. (n = 3).

Table 4. Inhibitory concentration of the compounds on human Topoisomerase II

Name of compound	**IC_{50}**µM± S.D.	**IC_{90}**µM± S.D.
Quinocarbazole **21a**	23.361 ± 0.104	41.514 ± 0.104
Quinocarbazole **25a**	19.086 ± 0.099	28.798 ± 0.099

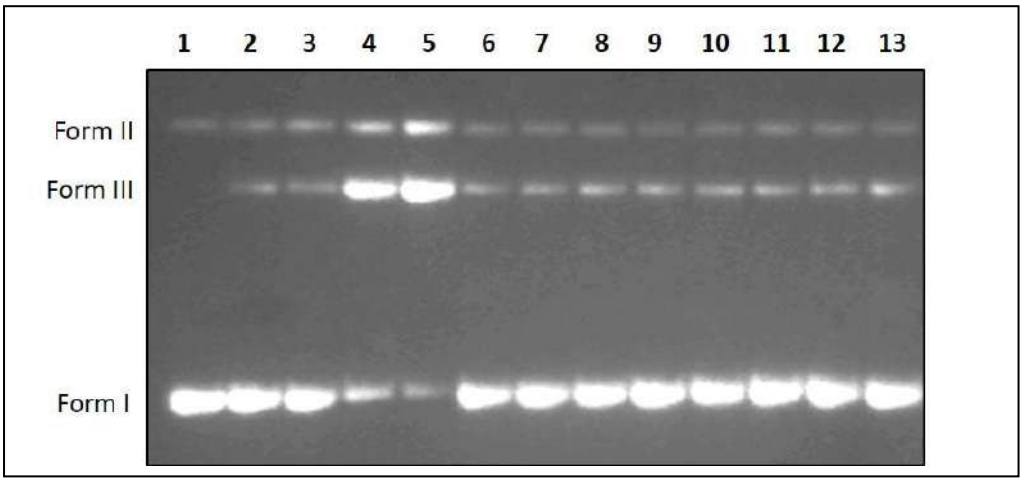

Fig. 9. Inhibition of etoposide-induced cleavage complex formation by quinocarbazole analogues was analyzed by cleavage reaction and agarose gel electrophoresis. Lane 1, negatively supercoiled pRYG DNA; lane 2, pRYG DNA with hTopII alone; lane 3 same as lane 2 but in presence of proteinase k treatment; Lanes 4, 5 same as lane 2 but in presence of increasing concentration (25 and 50µM) of etoposide; Lanes 6-8 and 9-11 same as lane 2 but in presence of increasing concentration (30, 40 and 50µM) of **21a** and **25a**, respectively; lane 12 and 13, hTopPII was incubated with 40 µM of **21a** and **21b**, respectively, followed by the addition of 50 µM of etoposide and pRYG DNA. Form I, closed circular DNA; Form II, nicked circular DNA; Form III, linear DNA. All results depicted were performed three times and representative data are from one set of these experiments.

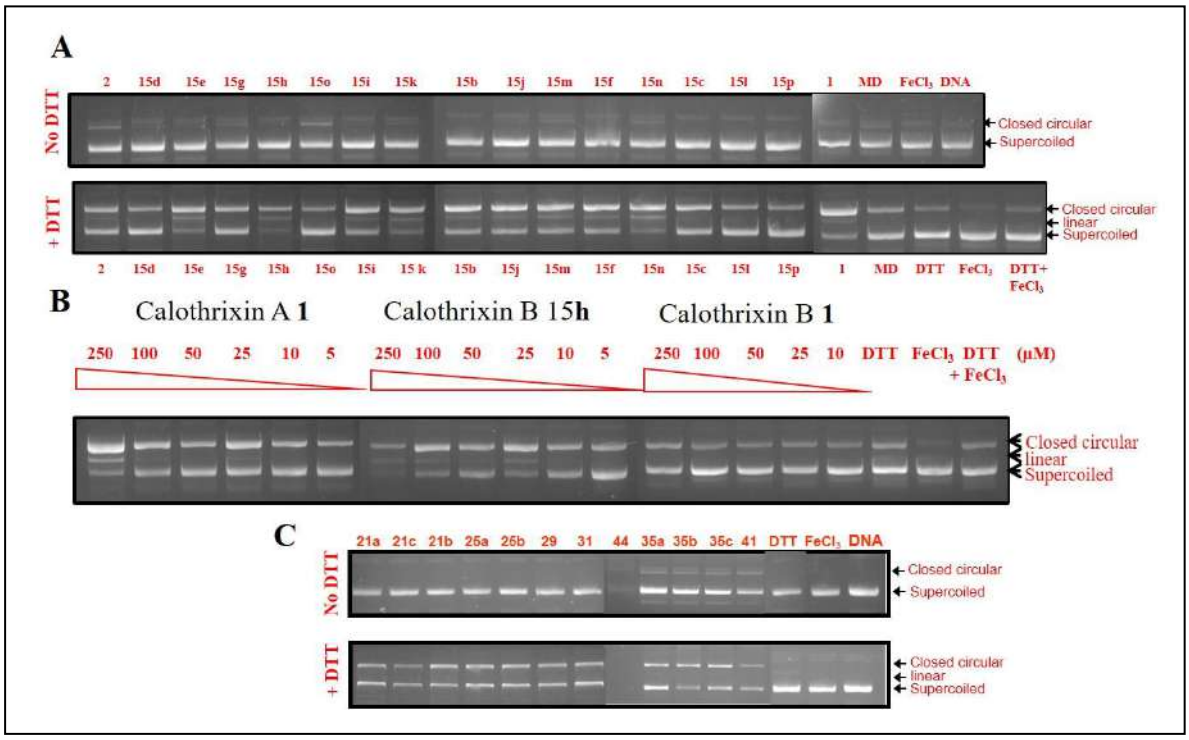

Fig. 10. Cleavage of plasmid DNA by calothrixins and quinocarbazoles in a cell free system.
(A & C) Supercoiled plasmid DNA was incubated for 1 h with 250 µM of calothrixins or quinocarbazoles, 200 µM of ferric chloride in the presence or absence of DTT (200 µM). Plasmid DNA was separated by agarose gel and stained with ethidium bromide. Menadione (250 µM) was used as a positive control. (B) Dose dependent cleavage of plasmid DNA by calothrixins. Different concentrations of calothrixin A (**1**), **15h** and Calothrixin B (**2**) was incubated for 1 h with supercoiled plasmid DNA in the presence of DTT (200 µM) and ferric chloride (200 µM).

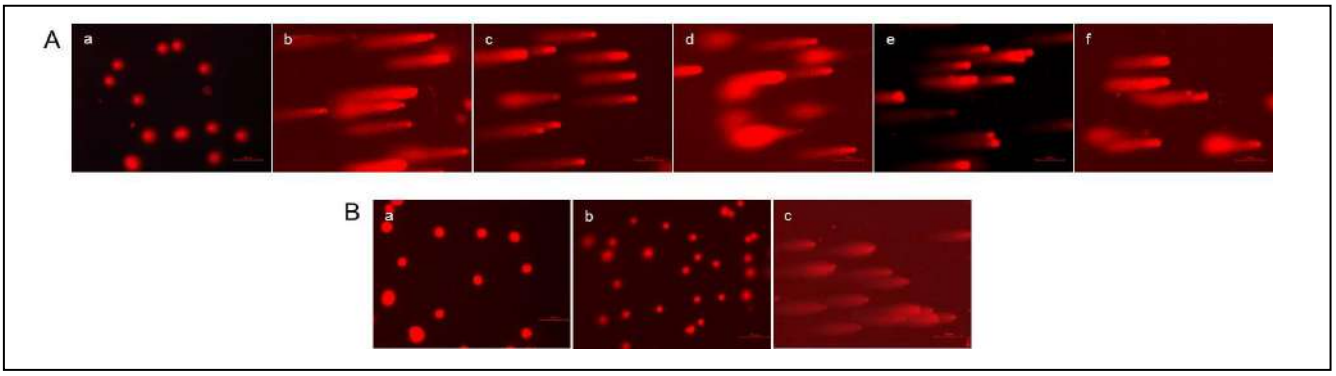

Fig. 11. Single-cell gel electrophoresis data (comet assay) in HCT116 cells (A) or NCI-H460 cells (B). Representative images of HCT116 cells (A) treated for 48 h with 0.5 µM Calothrixin A **1** (b) ; 5 µM Calothrixin B **2** (c) ; 5 µM **15h** (d) ; 5 µM **21a** (e) ; 5 µM **21b** (f) and untreated cells (a) Representative images of NCI-H460 cells (B) treated with 5 µM **21a** (b) ; 0.1 µM **21b** (c) and untreated cells (a)

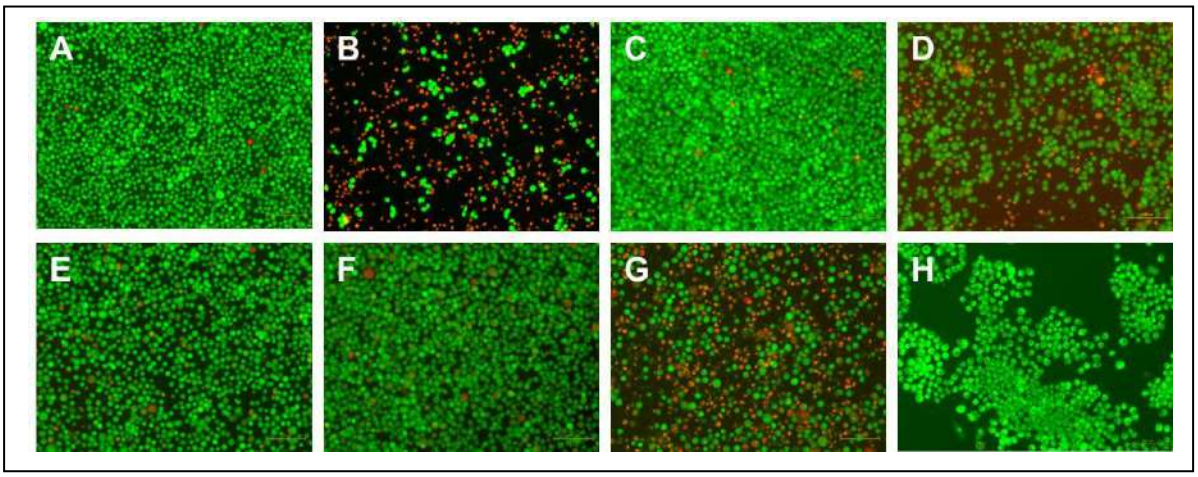

Fig.12. HCT116 cells were stained with acridine orange/propidium iodide after 48 h of treatment with calothrixins/quinocarbazoles. Cells were observed under fluorescence microscope (x100 magnification). Viable cells show green fluorescence. Necrotic and apoptotic cells show orange and yellow fluorescence. (A & E) Untreated HCT116 or NCI-H460 control cells, respectively. Cells were treated with 2 µM of calothrixin A **1** (B) 5 µM of calothrixin B **2** (C), 5 µM of 3-fluorocalothrixin B **15h** (D), 5 µM of quinocarbazole **21a** (F), 0.5 µM of 3-fluoroquinocarbazole **21b** (G), 5 µM of quinocarbazole **25b**.

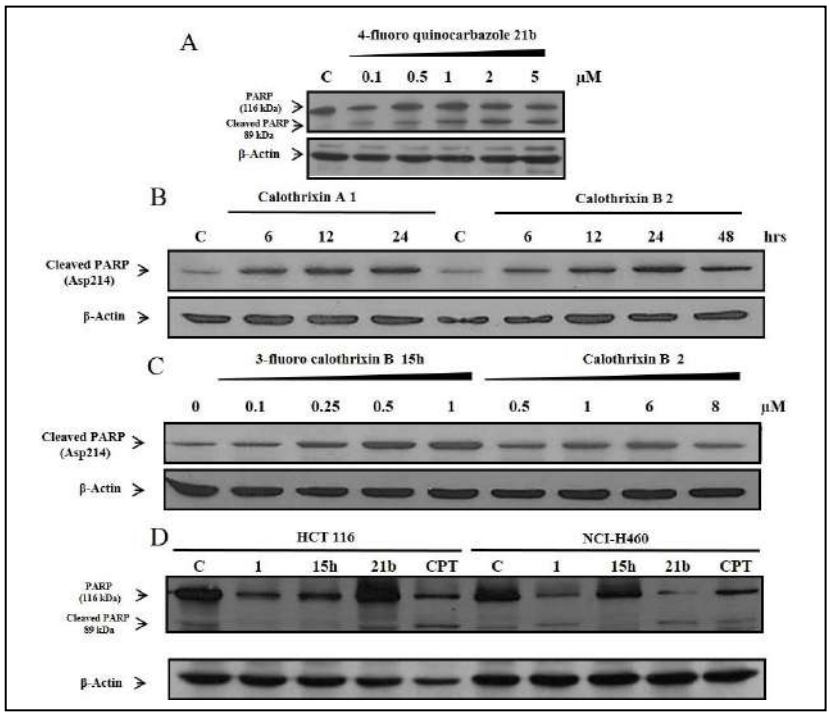

Fig. 13. Induction of apoptosis by calothrixins/quinocarbazoles. Detection of cleaved PARP protein levels by western blotting in the lysates from **A**. NCI-H460 cells treated with increasing concentrations (0.1, 0.5, 1, 2 and 5 µM) of 4-fluoroquinocarbazole **21b** for 48 h **B & C**. HeLa cells treated with calothrixins for different time points (1 µM of calothrixin A **1** for 6, 12, and 24 h ; 10 µM of calothrixin B **2** for 6, 12, 24 and 48 h) and varying concentrations (0.1, 0.25, 0.5 and 1 µM of 3-fluorocalothrixin B **15h** ; 0.5, 1, 6 and 8 µM of calothrixin B **2** for 48 h) **D**. HCT116 or NCI-H460 cells treated with calothrixins/quinocarbazoles (5 µM in case of calothrixin B **2**, compounds **15h** and **21b**; 3 µM of calothrixin A **1,** 0.5 µM of camptothecin) for 48 h. β-Actin staining was used as loading control.

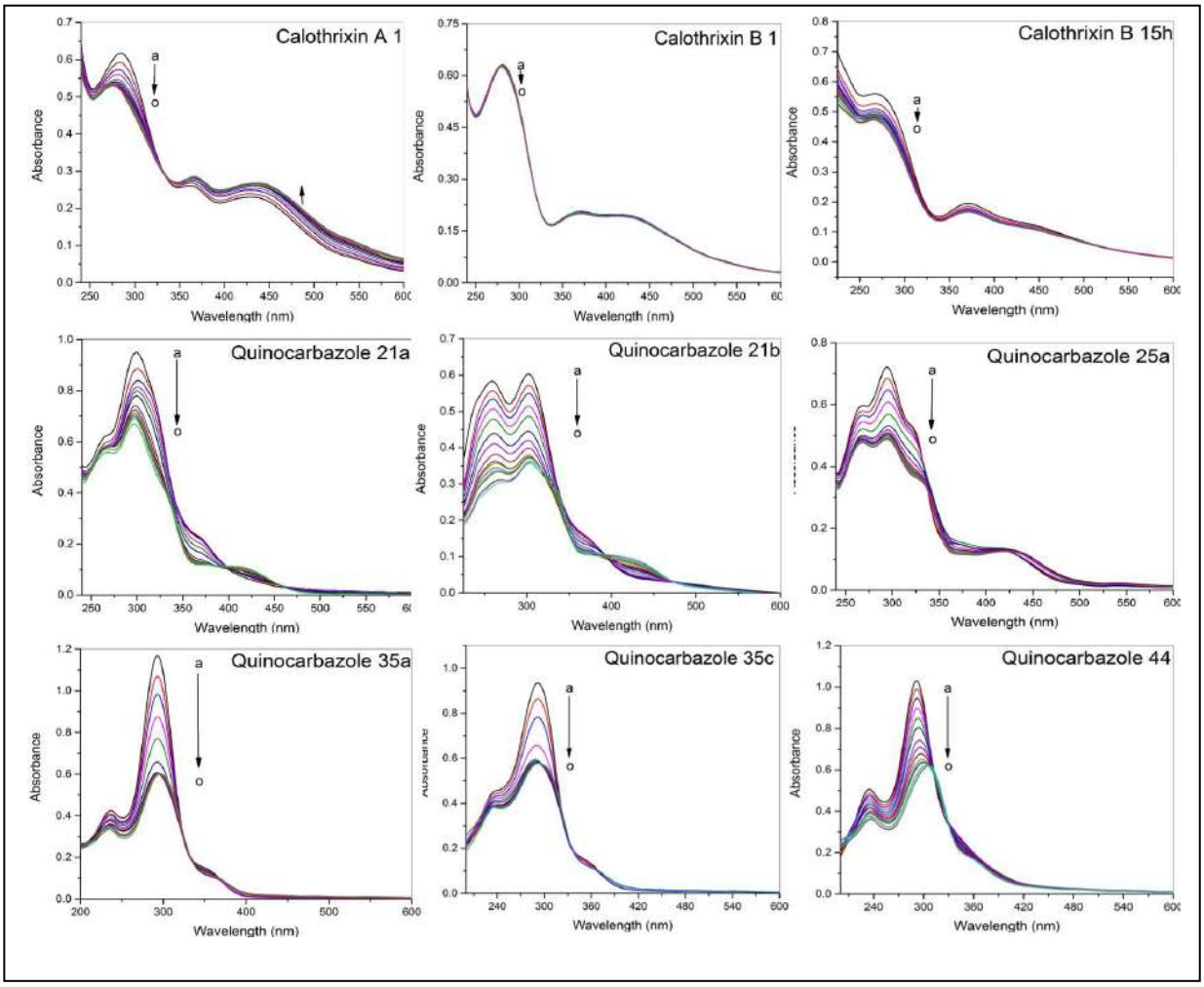

Fig. 14. Effects of increasing concentrations of CT-DNA on the UV-Vis absorption spectra of calothrixins or quinocarbazoles. Conditions: $C_{calothrixins\ or\ quinocarbazoles}$, 3×10^{-5}mol L^{-1}; C_{ctDNA} ($\times10^{-6}$mol L^{-1}); a→o: 0; 2; 5; 10; 15; 20; 25; 30; 35; 40; 45; 50; 60; 80; 100. The arrow shows the intensity changes in increasing CT-DNA concentration

Sl.No.	Compound	Binding constants (K_b in L mol^{-1})
1	**1**	4.77 (± 0.04) x 10^6
2	**2**	No interaction
3	**15h**	5.74 (± 0.12) x 10^6
4	**21a**	1.01 (± 0.07) x 10^5
5	**21b**	1.36 (± 0.13) x 10^5 9.66 (± 0.11) x 10^6
6	**25a**	9.68 (± 0.20) x 10^6
7	**35a**	1.12 (± 0.34) x 10^5
8	**35c**	6.11 (± 0.24) x 10^6
9	**44**	3.70 (± 0.32) x 10^5
10	Ethidium bromide	6.8 (± 0.22) x 10^7

Table 5. Binding constants (K_b in L mol^{-1}) for the interaction of calothrixins or quinocarbazoles with CT-DNA at 298 K

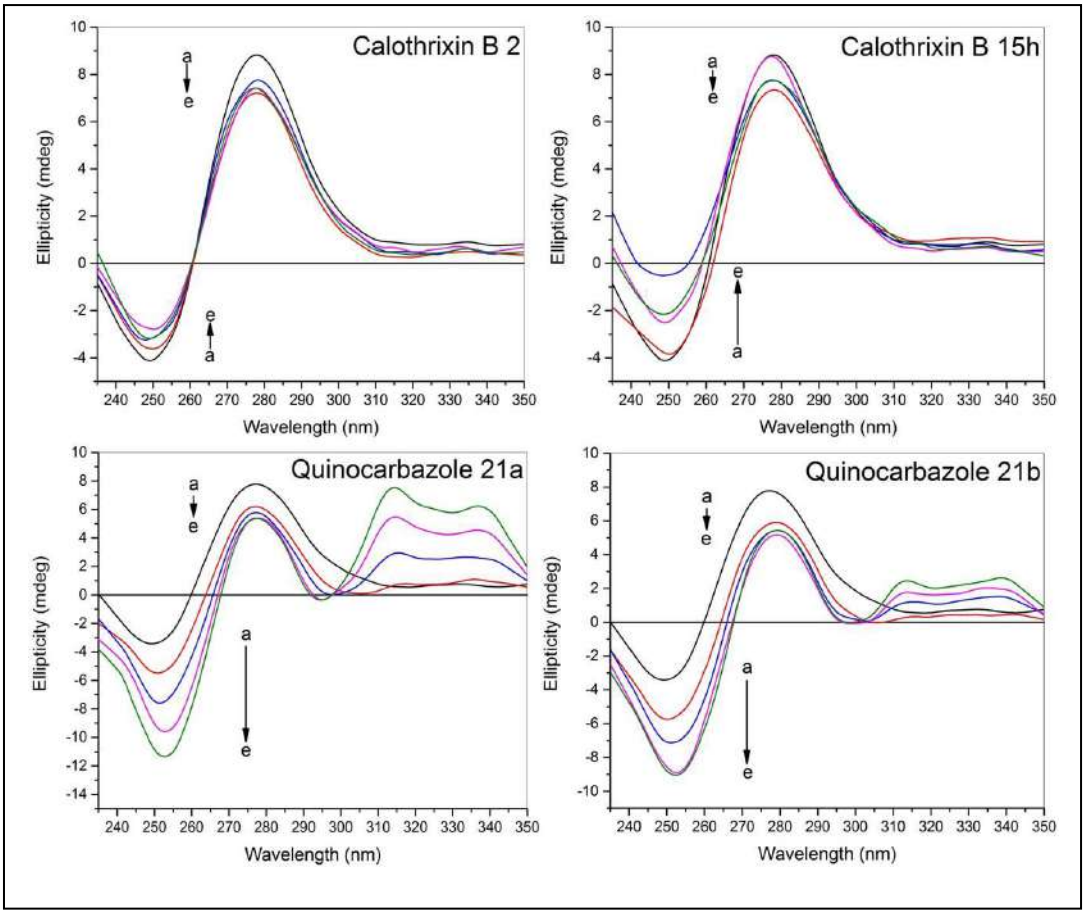

Fig. 15. Circular dichroism spectra of CT-DNA (1×10^{-4}mol L^{-1}) in the presence of increasing amounts of calothrixin or quinocarbazoles. $C_{compounds}$ ($\times 10^{-6}$mol L^{-1}); a→e: 0; 6.6; 13.5; 20; 26.6. The arrow shows the intensity changes in increasing compound concentration.

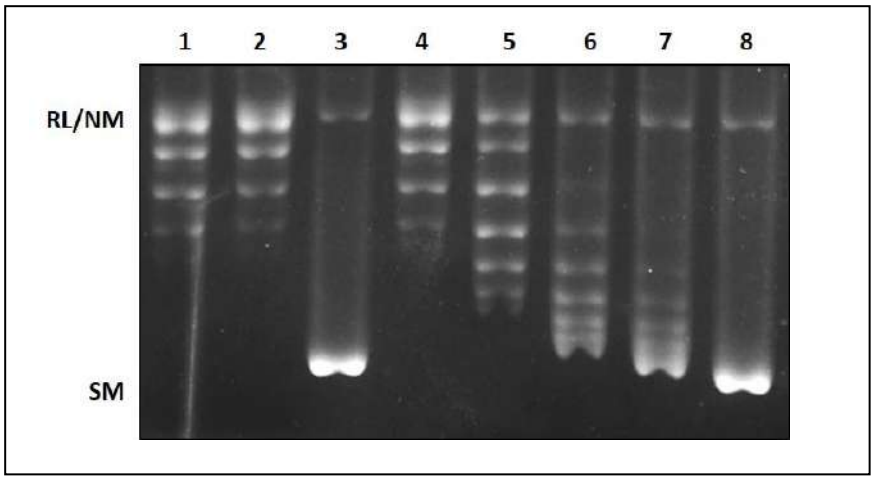

Fig. 16. Analysis of binding mode of quinocarbazole**21b** with DNA by agarose-gel electrophoresis. Lane1, relaxed pBluescript (SK+) plasmid DNA generated by treatment of plasmid DNA with excess hTopI, followed by phenol/chloroform extraction and ethanol precipitation; lane 2, relaxed plasmid DNA with hTopI; lane 3 and 4, same as lane 2 but in presence of 10 μM EtBr or 200 μM Etoposide, respectively; lane 5-8, same as lane 2, but in presence of increasing concentration (60, 70, 80, 90 and 100 μM) of quinocarbazole **21b**. NM, nicked monomer; RL, relaxed monomer; SM, supercoiled monomer.

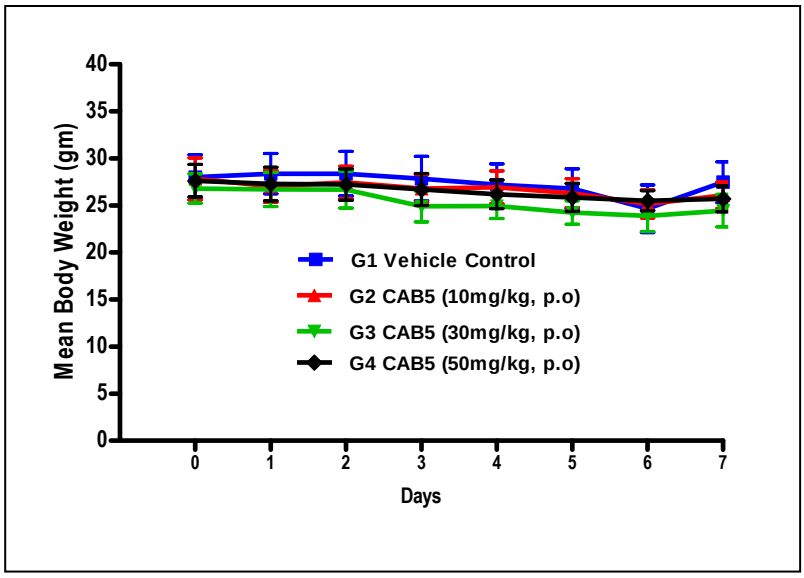

Fig. 17. No significant effect on body weight. Thirty six animals were randomized into four groups. The treated animals were administered compound **15h** at doses of 10, 30, and 50 mg/kg. The animals were dosed po daily for 7 days and were weighed daily for 1 week.

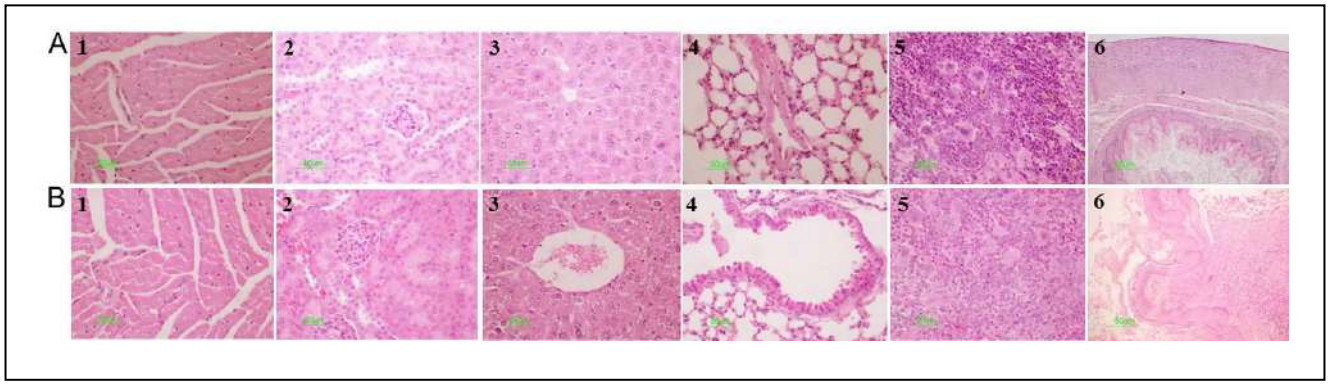

Fig. 18. Histopathological examination of major organs for signs of toxicity. Formalin-fixed heart (1) kidney (2) liver (3) lung (4) spleen (5) and stomach (6) from animals with oral administration of vehicle (**A**) or with 50 mg/kg **15h** (**B**), were embedded in paraffin. Tissue sections were stained with hematoxyline and eosin (H&E). Stained sections were evaluated histopathologically for signs of inflammatory cell infiltration or tissue degeneration. No signs of toxicity in major organs following treatment with 50mg/kg.

Table 6. Evaluation of drug-likeness of selected calothrixin and quinocarbazole analogues with respect to the Lipinski's Rule of Five and experimentally determined logP and logD in an octanol/water system.

Compound	Lipinski's rule of five (highest permitted value) Calculated				Experimental	
	Molecular Weight[a] (500)	HBD[b] (5)	HBA[c] (10)	ClogP[d] (5)	logP[e]	logD[f] at pH7.4
1	314.3	1	5	2.352	1.32	1.02
2	298.3	1	5	2.418	-1.81	-2.11
15h	316.3	1	5	2.651	-1.66	-1.96
21a	268.3	1	1	4.485	-1.25	-1.55
21b	286.3	1	1	4.754	1.91	1.61

[a] Molecular weights were calculated for nonionized calothrixin or quinocarbazole analogues. [b] Calculated number of hydrogen bond donor (HBD) groups. [c] Calculated number of hydrogen bond acceptor (HBA) groups. [d] Calculated octanol-water partition coefficient ClogP of the neutral species of the compounds. [e] Experimentally determined logP values in an octanol/water system. [f] Experimentally determined logD values in an octanol/buffer system at physiological pH of 7.4. All predictions were calculated using the Schrodinger QikProp application included in the Schrodinger's Maestrosoftware v9.1.